Microfluid Nanofluid (2012) 12:841–886
DOI 10.1007/s10404-012-0940-8

REVIEW PAPER

Numerical modeling of multiphase flows in microfluidics and micro process engineering: a review of methods and applications

Martin Wörner

Received: 8 June 2011 / Accepted: 11 July 2011 / Published online: 10 March 2012

Abstract This article presents a comprehensive review of numerical methods and models for interface resolving simulations of multiphase flows in microfluidics and micro process engineering. The focus of the paper is on continuum methods where it covers the three common approaches in the sharp interface limit, namely the volume-of-fluid method with interface reconstruction, the level set method and the front tracking method, as well as methods with finite interface thickness such as color-function based methods and the phase-field method. Variants of the mesoscopic lattice Boltzmann method for two-fluid flows are also discussed, as well as various hybrid approaches. The mathematical foundation of each method is given and its specific advantages and limitations are highlighted. For continuum methods, the coupling of the interface evolution equation with the single-field Navier–Stokes equations and related issues are discussed. Methods and models for surface tension forces, contact lines, heat and mass transfer and phase change are presented. In the second part of this article applications of the methods in microfluidics and micro process engineering are reviewed, including flow hydrodynamics (separated and segmented flow, bubble and drop formation, breakup and coalescence), heat and mass transfer (with and without chemical reactions), mixing and dispersion, Marangoni flows and surfactants, and boiling.

Keywords Microfluidics · Micro process engineering · Multiphase flow · Interfacial flow · Numerical methods · Direct numerical simulation

M. Wörner (✉)
Karlsruhe Institute of Technology (KIT), Institute for Nuclear and Energy Technologies, Hermann-von-Helmholtz-Platz 1, 76344 Eggenstein-Leopoldshafen, Germany
e-mail: martin.woerner@kit.edu

1 Introduction

1.1 Microfluidics and micro process engineering

Microfluidic devices such as microreactors (Ehrfeld et al. 2000), micro heat exchangers (Schubert et al. 2001) and lab-on-a-chip modules (Geschke et al. 2008) are characterized by systems where at least one of the dimensions is below a few millimeters. Frequently, this means rectangular channels with cross-sectional dimensions on the order of tens or hundreds of microns. They find applications in a number of different fields which range from chemistry (Doku et al. 2005) and chemical engineering (Hessel et al. 2004; Dietrich 2009) to biology (Gomez 2008) and medicine (Saliterman 2006). In micro process engineering (Hessel et al. 2009), they are for example used or potentially attractive for the production of fine and specialty chemicals, the generation of highly mono-disperse emulsions, high-throughput catalyst screening and combinatorial material science. In the life sciences, applications range from pharmaceutical research to diagnostic testing and DNA manipulation (Lion et al. 2006). Very often these applications involve the flow of multiple fluid phases.

In recent years, several books (Karniadakis et al. 2005; Tabeling 2005; Nguyen and Wereley 2006; Bruus 2008; Kockmann 2008; Dietrich 2009) and review papers have been published which deal with different aspects of microdevices and microfluidics (Whitesides 2006). Squires and Quake (2005) give a comprehensive review of the variety of physical phenomena that occur in microfluidic devices and discuss the dimensionless numbers that indicate the relative importance of the competing forces. For *multiphase* microfluidic flows, there exist rather general reviews (Zhao and Middelberg 2011) as well as more specific ones. A discussion of phenomena

occurring at interfaces can be found in Atencia and Beebe (2005), and an overview on electrokinetics, mixing and dispersion in multiphase flows for lab-on-a-chip applications in Stone et al. (2004). Comprehensive reviews on multiphase microfluidics for chemical and material synthesis and micro process engineering are given by Günther and Jensen (2006) and Günther and Kreutzer (2009), respectively. A review on microchemical systems for continuous-flow synthesis is provided by Hartman and Jensen (2009), and a review on microstructured reactors for multiphase reactions by Kashid and Kiwi-Minsker (2009). A review with special focus on actuation and manipulation methods of multiphase flow in micro- and nanochannels is given by Shui et al. (2007). Huebner et al. (2008) review methods for generating, controlling and manipulating droplets and discuss novel applications in the biological and physical sciences where systems with microdroplets make a significant impact. Reviews on microfluidics and microdroplets in chemistry are given by Abou-Hassan et al. (2010) and Theberge et al. (2010).

As systems are reduced in size, phenomena such as viscosity, diffusion, surface tension and contact lines become ever more important and may, at the microscale, dominate over gravitational and inertial effects which are often dominant in macroscopic flows. Though the flow in microdevices is in general laminar ($Re < 2000$) this does not imply that inertia can always be neglected (Di Carlo 2009). In many cases, the Reynolds number (Re) is larger than one so that neglecting inertia using the (linear) Stokes equations is not appropriate. Also the influence of geometry is significant since for a given pressure drop the flow rate through a capillary changes with the fourth power of the radius in laminar flow (Stone and Kim 2001). Therefore, since viscosity, inertia and surface tension forces are all important often the numerical solution of the full (nonlinear) Navier–Stokes (NS) equations is required. Representing and tracking an interface with complicated shape and dynamics that can develop large deformations, singularities, and topological changes within three-dimensional (3D) confined geometries is a numerical challenge.

While numerical methods and models for general multiphase flows are the topic of several books (Prosperetti and Tryggvason 2007; Tryggvason et al. 2011; Groß and Reusken 2011) and review papers (Scardovelli and Zaleski 1999; Lakehal 2002; Lakehal et al. 2002), there exist only few reviews that are specifically devoted to microdevices. Cristini and Tan (2004) gave a review on theoretical and numerical studies and methods for droplet formation, breakup, and coalescence in flows relevant to the design of microchannels for droplet generation and manipulation. Erickson (2005) presented an overview of tools, techniques and applications for modeling and numerical prototyping of labs-on-chip. Also in books (Hessel et al. 2004; Karniadakis et al. 2005; Bruus 2008; Kockmann 2008) or book chapters (Fletcher et al. 2009) numerical and modeling aspects for interfacial multiphase flow simulations in microdevices are covered rather briefly and a comprehensive in depth review is missing. This article aims to close this gap.

1.2 Classification of methods for two-phase flows

In gas–liquid and immiscible liquid–liquid flow, the phases are separated by an interface. The interface is deformable and the two-fluid flow may undergo topological changes due to breakup and coalescence. Macroscopic two-fluid flows in chemical engineering are often *turbulent* and the phase distribution is characterized by a large number of disperse elements (with a wide size distribution) and a free surface (e. g. in stirred tanks, bubble columns or air-lift reactors). The length scales of the problem that have to be resolved in a direct numerical simulation ranges then from the diameter of the stirred tank or bubble column down to the radius of curvature of the smallest bubbles. This spans at least four orders of magnitude. Full 3D time-dependent interface resolving numerical simulations over sufficiently long problem time to reach statistically relevant data are therefore impossible, and will it be for the foreseeable future. For this reason, simulation methods are usually used for such problems which do not resolve details of the interface. In the Euler–Euler (E–E) approach, an averaging procedure (i.e. time, volume, or ensemble averaging) is used to obtain so-called interpenetrating field equations which are valid in the entire domain (Ishii 1975; Drew and Passman 1999; Ishii and Hibiki 2006). The E–E method (or two-fluid model) can be applied in principle to any two-phase flow pattern. The second widely used method for computation of macroscopic two-phase flows is the Euler–Lagrange (E–L) method (Crowe et al. 1998). The method is restricted to disperse flows and is based on the point particle approach where the flow around individual disperse elements of presumed shape is not resolved by the grid. Both, the E–E and E–L methods rely on physical models for the interfacial transfer of momentum, heat, and mass. These models are often based on the theoretical or experimental results obtained for single “isolated” bubbles or drops far from walls. For macroscopic applications, interface resolving simulations are used only in very special cases.

In mini- and microscale, the flow is predominantly laminar and the number of bubbles or drops in disperse flows is computationally manageable. The disperse elements are proximate to walls and there is significant interaction between the individual bubbles or drops (e.g. in emulsification processes) so that physical models obtained for isolated fluid particles cannot be used. For this reason,

the E–E and L–E method do not play a significant role for computation of two-fluid flows in small dimensions. In microchannels, the phases are well separated and it is hard to predict or assume the shape of disperse elements in advance, so that interface resolving numerical simulations are instead the method of choice.

1.3 Scope and outline of this review

The present review is structured in two parts. In the first part, the various numerical methods and models that are available for simulation of interfacial two-fluid flows are presented and discussed. This includes the lattice Boltzmann, volume-of-fluid, level set, front tracking and phase-field methods and their variants. In the second part, applications of these methods in microfluidics and micro process engineering are reviewed. These are structured in separated and segmented flow, bubble and drop formation, breakup and coalescence, heat and mass transfer (with and without chemical reaction), mixing and dispersion, Marangoni flows and surfactants, and boiling.

Though the intention of this review is to cover a wide range of methods and applications, there are nevertheless also some issues that are disregarded. In general, computational methods for free surface/two-phase flows can be categorized into three groups: meshless methods, moving grid methods, and fixed grid methods. In meshless methods (such as smoothed particle hydrodynamics and dissipative particle dynamics), a finite set of discrete points are used to represent the fluid motion (Heyes et al. 2004). Though there is an increasing interest in these methods, they have only limited application in microfluidics so far and are thus not considered here. Fluid flows in small-scale systems are driven by applied pressure difference, electric fields, capillary forces owing to wetting of surfaces, and gradients in interfacial tension. In this review we focus on pressure driven and capillary driven flows, but do not discuss flows driven by electric fields. For most applications considered in the second part of this review, the mean free path λ is much smaller than the characteristic length scale L of the flow. Typically, the Knudsen number $Kn \equiv \lambda/L$ vanishes or is below 0.001 so that the flow can be treated as continuum, and the Navier–Stokes equations apply (Gad-el-Hak 1999). Velocities are small in general so that compressibility effects are negligible. Further, we restrict this review to gas–liquid and immiscible liquid–liquid flows where the shape of the interface is not prescribed but part of the solution. Applications for particulate flows in microchannels (such as particle separation and filtration and flow cytometry of cells and chromosomes) are not considered and the interested reader is referred to Di Carlo et al. (2007) and Di Carlo (2009).

2 Methods and models

Theory and modeling methods can be conveniently classified into four groups, depending on the length and time scales to which they imply (Gubbins and Moore 2010): (a) the "*electronic*" scale of description, in which matter is regarded as made up of fundamental particles (electrons, protons, etc.) and is described by quantum mechanics; (b) the *atomistic* level of description, in which matter is made up of atoms, whose behavior obeys the laws of statistical mechanics; (c) the *mesoscale* level, in which matter is regarded as composed of blobs of matter, each containing a number of atoms; and (d) the *continuum* level, in which matter is regarded as a continuum, and the well-known macroscopic laws (equations of continuity and momentum conservation, constitutive equations such as Fourier's law, etc.) apply. In this review, we will only very briefly cover atomistic methods such as molecular dynamics (MD) and the direct simulation Monte Carlo method (DSMC), but will focus on the lattice Boltzmann method as an example for mesoscale methods and on continuum methods based on the Navier–Stokes (NS) equations.

2.1 Atomistic methods

At the atomistic level of description, matter is composed of atoms or molecules and obeys statistical mechanics. The equations of statistical mechanics can be solved numerically by either the MD or DSMC method. While in MD individual particles are considered which move under their own intermolecular forces and follow Newton's second law, in DSMC particle groups are considered and their moves are completely stochastic. Fluid properties, such as the flow velocity or density field, can be calculated as averages over the trajectories of the particles. Both MD and DSMC constitute a powerful and growing set of techniques for fluid dynamic simulations; see e.g. the review by Kadau et al. (2010). These methods are, however, computationally expensive, and the computational effort increases linearly with the number of particles and the physical time scale simulated. While recently the first trillion atom simulation was performed on the BlueGene/L system (Germann and Kadau 2008), due to limits of computational capacity these simulations are currently restricted to the description of length scales of the order of microns and time scales of the order of microseconds. Thus, for engineering applications of fluid mechanics there is, in the foreseeable future, no alternative to a mesoscale or continuum description.

2.2 Lattice Boltzmann (LB) method

In recent years, the lattice Boltzmann method has evolved into a promising method of computational fluid dynamics (CFD), see e.g. Succi (2001) and Aidun and Clausen (2010) for details. The fundamental idea is to construct simplified kinetic models that incorporate the essential physics of microscopic processes. Macroscopic hydrodynamic behaviors, such as interface dynamics, naturally emerge as a result of this kinetics. According to Verhaeghe et al. (2009), the LB approach is a simple explicit algorithm which can be derived from the linearized Boltzmann equation and is often associated with a square (in 2D) or cubic (in 3D) lattice on which the discretized particle distribution function $f_i(\mathbf{r}_j, t_n) \equiv f(\mathbf{r}_j, \mathbf{c}_i, t_n)$ evolves. The particle velocity space is discretized into a symmetric discrete velocity set $\{\mathbf{c}_i\} = -\{\mathbf{c}_i\}$. The grid size and the time step are chosen in such a way that in discrete time $t_n \equiv \delta_t \mathbb{N}_0 = \delta_t\{0, 1, 2, \ldots\}$ fictious particles represented by $\{f_i\}$ move synchronously from one grid point $\mathbf{r}_j$ to one of its neighbors $\mathbf{r}_j + \mathbf{c}_i\delta_t$ according to their discrete velocities. In the most general form, the lattice Boltzmann equation can be written as

$$\mathbf{f}(\mathbf{r}_j + \mathbf{c}\delta_t, t + \delta_t) = \mathbf{f}(\mathbf{r}_j, t) + \mathbf{\Omega}\big[\mathbf{f}(\mathbf{r}_j, t)\big] + \mathbf{F}(\mathbf{r}_j, t) \tag{1}$$

where $\mathbf{\Omega}$ is the collision term and $\mathbf{F}$ the external forcing, and bold-face symbols denote $(Q+1)$-tuple vectors for a model of $(Q+1)$ discrete velocities, e.g.

$$\mathbf{f}(\mathbf{r}_j + \mathbf{c}\delta_t, t + \delta_t) = (f_0(\mathbf{r}_j, t_n + \delta_t), \ldots, f_Q(\mathbf{r}_j + \mathbf{c}_Q\delta_t, t_n + \delta_t))^{\mathrm{T}} \tag{2}$$

where T denotes the transpose operator. In practice, a LB time step involves a propagation or streaming substep, where fictious particles (given by the distribution function) move to their neighboring sites, and a collision substep, where they collide with fictious particles coming in from the other directions and the distribution functions are changed by the effects of interparticle collisions (which account for example for intermolecular forces). Commonly used lattices in two and three dimensions are the D2Q7 ($D = 2$, $Q = 7$), D2Q9, D2Q13 and D3Q15, D3Q19, D3Q27 models, respectively. Macroscopic quantities such as the density and the fluid velocity are obtained by taking suitable moments of the distribution function

$$\rho = \sum_{i=1}^{Q} f_i, \quad \mathbf{u} = \frac{1}{\rho}\sum_{i=1}^{Q} f_i\mathbf{c}_i, \tag{3}$$

Within the LB framework, there exist different approaches for immiscible multiphase flows (Chen and Doolen 1998; Succi 2001; Nourgaliev et al. 2003; Aidun and Clausen 2010). One approach is the color gradient method which contains two sets of LB populations, one for each phase (Gunstensen et al. 1991). Interfaces are implicitly defined by the fluid fraction isosurface where the content of the two fluids is equal. To prevent the two fluids from mixing with each other, a so-called recoloring step is applied which acts as anti-diffusion. Another method is that of Shan and Chen (1993), which also uses a distribution function for each chemical component and defines an interaction potential to ensure phase separation. The third widely used method is the free energy approach which relies on a second set of populations which describes the fluid fraction by an order parameter (Swift et al. 1996). While the early versions of LB methods for multiphase flows were based on fictitious interactions or heuristic ideas, Luo and Girimaji (2003) rigorously derived a two-fluid LB model from kinetic theory. Also, early models were, for reasons of numerical stability, limited to small values of the density and viscosity ratio. Since then, there is an ongoing effort to improve the stability of the LB method for two-phase flows with high density ratio (Inamuro et al. 2004; Lee and Lin 2005; Zheng et al. 2006; Yan and Zu 2007; Cheng et al. 2010). Surface tension can be incorporated in LB schemes by a number of different methods, which will not be reviewed here. The interested reader is referred to Lishchuk et al. (2003) and Jia et al. (2008), where also the status of the Shan–Chen and the free-energy model is critically reviewed.

A popular way to simplify the collision integral is the lattice Bhatnagar-Gross-Krook (LBGK) model which expresses it as a simple relaxation term with time scale τ towards a suitable equilibrium (Bhatnagar et al. 1954). The LBGK model has, however, some drawbacks which are related to the dependence of the boundary conditions on the viscosity, see Verhaeghe et al. (2009); furthermore, its applicability is restricted to unity Prandtl and Schmidt numbers (Luo and Girimaji 2003). Therefore, there is a tendency to employ multiple relaxation time models, especially in the context of LB methods for multiphase flows (Pooley et al. 2008).

The main advantages often attributed to the LB method as compared to continuum methods are the ease of implementation (since the nonlinear Navier–Stokes equations are replaced by the semi-linear Boltzmann equation), the simplicity in simulating domains with complex geometry, and the ease of parallelization (since only local operations are performed); for a critical scrutiny of these advantages see Nourgaliev et al. (2003). For multiphase flows, LB models have advantages over conventional methods because they do not track interfaces, but can maintain sufficiently sharp interfaces without significant effort. Chao et al. (2011) e.g. performed long time simulations of flows with density ratio up to $O(100)$ where the interface thickness is maintained within five to six lattices.

A disadvantage of LB methods is that macroscopic fluid properties and transport coefficients cannot be prescribed as input parameters (as in continuum methods). In the LB method, the macroscopic behavior of the fluid system, such as the dynamics of the density, velocity, and temperature fields, the equation of state, the viscosity and the coefficient of surface tension, are all consequences of the microscopic or mesoscopic dynamics of the distribution function. Thus, simulating a fluid system with a given set of thermophysical properties (density, viscosity, diffusivity, surface tension,…) requires adjustments of the microscopic parameters, which constitute the input parameters in the LB method. A further disadvantage is that due to the kinetic nature of the LB method, hydrodynamic boundary conditions are difficult to satisfy on a grid point exactly. Also the lack of strict mass conservation is an issue with some interpolation methods (Rohde et al. 2006) and wall boundary condition formulations (Bao et al. 2008). To improve mass conservation, Chao et al. (2011) applied a global mass correction procedure which required, however, substantial additional CPU time.

2.3 Continuum methods

For most fluids, the scale of tens or hundreds of micrometer is well suited to the standard continuum description of transport processes, even though surface forces play a more important role than in macroscopic applications (Stone and Kim 2001). Continuum methods for computation of two-fluid flows are based on macroscopic conservation laws for mass, momentum and energy. They rely on the coupling of a method for description of the phase evolution (which often expresses the conservation of phase specific mass) with a solver for the momentum equation (e.g. the Navier–Stokes equation) and the energy equation. Here, we are interested in the full non-linear problem and do, therefore, not consider methods that are limited to Stokes flow, such as the boundary integral method (Pozrikidis 2001). In the following, we discuss first various methods for description of the interface evolution and then consider the coupling of these algorithms with equations describing the transport of momentum, species mass, and energy. Detailed information about these balance equations can be found in various text books, see for example Bird et al. (2007).

2.3.1 Description of the interface evolution

In the classical view, an interface is the thin boundary layer that separates two distinct phases of matter (each of which may be a solid, or a liquid or a gas) and that has properties distinct from the bulk material on either side. Continuum methods can be classified in approaches where the interface thickness is zero (sharp interface) or finite (diffusive interface). In sharp interface methods, the physical interface is a functional interface of zero thickness and physical quantities such as density and viscosity are discontinuous at the interface. Mathematically, such an interface is a $(D-1)$ dimensional object in a D dimensional space. In diffuse interface methods, the interface has a finite thickness and physical quantities vary continuously across the interface. However, the numerical interface thickness in diffuse interface methods is usually much larger than the actual physical thickness which is for liquid–fluid interfaces typically a few nanometers (Lyklema 1991; Yang and Li 1996). In the following, we first describe methods with formally zero interface thickness and then methods where the interface thickness is finite, either for numerical or physical (modeling) reasons. Here, we limit the presentation to flows without phase change but will discuss respective extensions in Sect. 2.3.4. For clarity, we illustrate in Fig. 1 main features of the various methods that are covered in the sequel of this section.

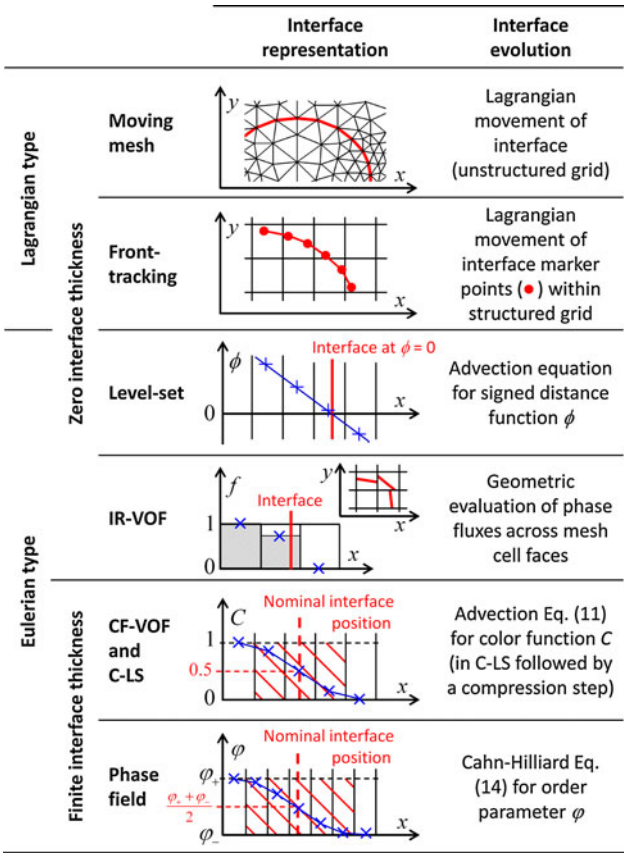

Fig. 1 Illustration of the different continuum methods for describing the evolution of deforming interfaces in Sect. 2.3.1. For methods with zero interface thickness the interface position is indicated by a solid red line. For methods with finite interface thickness, the nominal interface position is indicated by a dashed red line. The interface thickness (as indicated by the red hatched area) is typically 2–3 mesh cells for the CF-VOF and C-LS methods and is larger (up to 10 mesh cells) for the PF method

2.3.1.1 Methods with zero interface thickness (sharp interface methods) Numerical methods for interfaces of zero thickness can be divided into two main groups depending on the type of the grid. In the first group, moving unstructured grids are used (Huang and Russell 2011) and the interface is treated as a boundary. The interface is represented by a set of cell edges (in 2D) or cell faces (in 3D); this allows a precise representation of interfacial jumps in the physical variables on the zero-thickness interface without any smoothing. Such methods are often based on the arbitrary Lagrangian–Eulerian (ALE) formulation (Hirt et al. 1974), where the interface is resolved by a moving mesh (Welch 1995; Hu et al. 2001; Quan and Schmidt 2007; Ganesan and Tobiska 2008). Local mesh adaptations including mesh coarsening and mesh refining can be performed for both the interior and the interface elements to maintain good mesh quality, to achieve enough mesh resolution, to capture the changing curvature, and to obtain computational efficiency. However, handling topological transitions of fluid particles such as coalescence, breakup or pinch-off requires rather complex algorithms (Quan et al. 2009).

In this review, the focus is on the second group of methods. In these the momentum equation is solved on a structured grid and an interface representation and advection algorithm is required to define its motion across the computational domain. These methods may be divided into two classes. In *front-capturing methods*, the interface is implicitly embedded in a scalar field function defined on a fixed Eulerian mesh, such as a Cartesian grid. The second category is given by Lagrangian *front-tracking methods*, in which the interface is explicitly represented by Lagrangian particles ("markers") and its dynamics is tracked by the motion of these particles. Among the front-capturing methods are the volume-of-fluid (VOF) and level set (LS) method which are, at least in their simplest version, relatively simple to implement. An early Lagrangian method is the Marker in Cell (MAC) method of Harlow and Welch (1965), where a fixed number of discrete Lagrangian particles are advected by the local flow. The distribution of these particles identifies the regions occupied by a certain fluid. Modern Lagrangian techniques emerged with the front-tracking (FT) method (Unverdi and Tryggvason 1992; Tryggvason et al. 2001) which uses surface markers. FT methods can give a more precise evolution of a deforming interface, but they may be relatively complex, with their need to book-keep logical connections among surface elements. In the following, we discuss these methods in the order of their historical appearance, i.e. the VOF, LS and FT method.

In the sharp interface limit, one can define two phase indicator or characteristic functions X_+ and $X_- = 1 - X_+$ with value 1 in one phase and 0 in the other phase. When there is no phase change then the value $X_\pm$ of a fluid particle is constant along its trajectory (i.e. Lagrange invariant). Then, the following so-called topological equation holds and can be used to describe the interface evolution

$$\frac{\mathrm{D}X_\pm}{\mathrm{D}t} = \frac{\partial X_\pm}{\partial t} + \mathbf{u}\cdot\nabla X_\pm = 0 \tag{4}$$

Here, the flow field $\mathbf{u}(\mathbf{x},t)$ is obtained by solution of the momentum equation, see Sect. 2.3.2. Since the density of each fluid is assumed constant it is $\mathrm{D}\rho_\pm/\mathrm{D}t = 0$, which is equivalent to Eq. (4). This means that the mass conservation of the two phases (which is synonymous with volume conservation for incompressible fluids) can be represented by the combination of the topological equation for one phase (here we take the +phase) with the condition for a divergence free velocity field

$$\nabla\cdot\mathbf{u} = 0 \tag{5}$$

Interface reconstruction volume-of-fluid (IR-VOF) method In interface reconstruction (IR) VOF methods, the convective term in Eq. (4) is, by combination with Eq. (5), written in conservative form and integrated over the volume V_{mc} of a mesh cell with boundary ∂V_{mc}. Application of the Gauss divergence theorem and division by V_{mc} yields

$$\frac{\partial f_+}{\partial t} + \frac{1}{V_{\mathrm{mc}}}\oiint_{\partial V_{\mathrm{mc}}} (\hat{\mathbf{n}}_{\partial V_{\mathrm{mc}}}\cdot\mathbf{u})X_+\mathrm{d}S = 0 \tag{6}$$

Here,

$$f_+ \equiv \frac{1}{V_{\mathrm{mc}}}\iiint_{V_{\mathrm{mc}}} X_+\mathrm{d}V \quad \text{with} \quad 0\le f_+\le 1 \tag{7}$$

is the volume fraction of phase + in the mesh cell and $\hat{\mathbf{n}}_{\partial V_{\mathrm{mc}}}$ is the unit normal vector on ∂V_{mc} (pointing outward of the mesh cell). For a hexahedral mesh cell e.g., the closed surface integral over ∂V_{mc} consists of six contributions, one for each face of the mesh cell. The evaluation of these surface integrals requires the knowledge of the velocity and phase distribution at the mesh cell faces. The velocity is approximated by the face centered mean value, which is obtained by solution of the momentum equation (e.g. on a staggered grid). The distribution of X_+ within the mesh cell (and on its faces) is obtained by an interface reconstruction procedure (see below). Equation (6) is integrated in time by a so-called advection step where the volume flux of phase + across all mesh cell faces is evaluated in a geometrical manner, see below. Since the volume of fluid that is fluxed across a certain mesh cell face appears in the donating mesh cell as sink term and in the accepting one as source term of the same magnitude, all volume fluxes across mesh cell faces in the entire

computational domain should sum up to zero (at least in principle, see below). This inherent volume (and mass) conservation property is the main advantage of IR-VOF methods.

A mesh cell with $0 < f_+ < 1$ is called a *cut cell*. For geometrical representation of the interface in a cut cell different concepts are used, namely piecewise constant, piecewise linear, and piecewise parabolic interface segments. In the earliest work on the VOF method, the interface orientation was always aligned with one side of a rectangular mesh cell. Examples for this *piecewise constant* approach are the simple line interface calculation (SLIC) method of Noh and Woodward (1976) and the stair-stepped interface representation of Hirt and Nichols (1981). Today, SLIC methods are seldom used though there are some recent efforts to improve the method (Yokoi 2007). State-of the art are so-called *piecewise linear* interface calculation (PLIC) methods. In PLIC methods, the interface is represented by a line (in 2D) or a plane (in 3D). The orientation of the plane within a cut cell is obtained by reconstructing its unit normal vector C (pointing into phase +) from the discrete values of f_+ in the neighborhood of each mesh cell. Once $\hat{\mathbf{n}}_+$ is known, the position of the plane within the cut cell is determined from the condition that the interface divides the cut cell in two parts, so that the correct value of f_+ is obtained. For this task, analytical relations are available for orthogonal hexahedral (Scardovelli and Zaleski 2000), triangular (Yang et al. 2006) and tetrahedral grids (Lv et al. 2010).

An early PLIC reconstruction algorithms for the VOF method is that of Youngs (1982), see also Rudman (1997), in which a finite-difference gradient approximation of the volume fraction is used to compute the interface normal vector by relation $\hat{\mathbf{n}}_+ = \nabla f_+ / |\nabla f_+|$. While the method of Youngs is still widely used (e.g. in the FLUENT code) since then a large number of different PLIC methods have been proposed. For a historical perspective (with status up to 2002) on the vast literature on VOF reconstruction algorithms we refer to Rudman (1997), Rider and Kothe (1998) and Benson (2002). Still, there is an ever ongoing development of new and improved methods, see e.g. Pilliod and Puckett (2004) and Aulisa et al. (2007). A drawback of the piecewise linear approach is that planar segments in neighboring cut cells are (in general) not continuous so that at the common face of two neighboring cut cells there is a jump of the interface position, see sketch in Fig. 1. More recently, *piecewise parabolic* interface calculation (PPIC) schemes (Price et al. 1998; Renardy and Renardy 2002; Diwakar et al. 2009) and piecewise cubic spline interface reconstruction schemes (Ginzburg and Wittum 2001; López et al. 2004) have been proposed; however, only the method of Renardy and Renardy (2002) is formulated in 3D. In some of these methods the interface is still discontinuous at the mesh cell boundaries. Diwakar et al. (2009) developed a method where the interfaces and their first derivative are continuous at cell boundaries. In practice, however, this method as well as spline-based methods tends to produce small interface oscillations or wavy interfaces in some cases. So it is not clear yet if these higher order methods are in practice really superior to PLIC methods.

Due to the complexity of the interface reconstruction step, the PLIC-VOF method is traditionally used on a fixed rectangular (in 2D) or hexahedral (in 3D) Cartesian grid. However, there are efforts to extend the method to non-orthogonal curvilinear meshes (Jang et al. 2008). Also interface reconstruction schemes for multimaterial flows (i.e. for flows where more than two immiscible phases may exist in one mesh cell) are under development for generalized polyhedral meshes (Ahn and Shashkov 2007).

Once the interface is reconstructed, the advection step can be performed, where the volume fluxes of phase + across all mesh cell faces are evaluated geometrically. We illustrate this for the 2D case where the domain occupied by each phase is a polygon. The flux of phase + across one mesh cell face within a time step Δt is then evaluated by virtual movement of the corners of this polygon by a distance $\Delta L = u_\perp \Delta t$, where $u_\perp$ is the velocity component normal to the mesh cell face. Advection schemes can be classified in two different categories (Rider and Kothe 1998): operator split schemes, which consist of a sequence of one-dimensional advection steps, and multidimensional (unsplit) schemes. In a split method, the fluxes along one coordinate direction are computed and the volume fractions f_+^n (where the superscript n indicates the time step) are updated to an intermediate level f_+^*. The interface is then reconstructed from the intermediate f_+^* data and the fluxes along the second direction are calculated, yielding the intermediate data f_+^{**}. By a third reconstruction and advection step (in three dimensions) finally the values f_+^{n+1} for the new discrete time level are obtained. In contrast, in unsplit methods there is only one reconstruction step and one advection step per time step (Pilliod and Puckett 2004). While unsplit methods thus require less CPU time per time step, they have the disadvantage that the same liquid volume in a mesh cell may be fluxed twice or three times (Rider and Kothe 1998). This can result in mesh cells where the consistency property $0 \le f_+^{n+1} \le 1$ is not satisfied. While values $f_+ < 0$ can simply be set to 0, setting values $f_+ > 1$ to 1 will yield a mass loss. As a remedy, often the small surplus $\delta f_+ = f_+ - 1 > 0$ from such mesh cells is redistributed (i.e. added) to a neighboring cut cell where $0 < f_+ < 1 - \delta f_+$. For the two-dimensional case, unsplit schemes for cell boundary flux integration have been proposed that minimize the problem or need no local redistribution algorithm at all (Harvie and Fletcher 2000, 2001).

The problem of overfilling of cells is, however, more severe for operator split methods. After the first one-dimensional advection step volume fractions greater than unity may result which create a problem in the second advection step, as cells in the interior of the fluid may then attain values less than unity. To overcome this problem Rudman (1997) made allowance for the effective change in volume of a cell during each one-dimensional advection step. Also a stretching of the velocity field (which is not divergence free in one dimension) can produce notable overshoots in the intermediate volume fractions, see Weymouth and Yue (2010). To fix this problem, the latter authors developed an operator split advection scheme which ensures complete mass conservation by accounting in a proper way for the dilatation term. Also Aulisa et al. (2007) proposed a split advection algorithm in three dimensions which conserves mass exactly for a divergence free velocity field, thus allowing computations to machine precision. In spite of the recent improvements of split methods, the general trend is toward unsplit methods (López et al. 2004; Liovic et al. 2006; Cervone et al. 2009). However, both split and unsplit methods for geometric flux computation require sufficiently small time steps (Courant numbers) in order to be stable and accurate.

A rather novel conceptual extension of the VOF method is the moment-of-fluid (MOF) method (Ahn and Shashkov 2009). The MOF method can be thought of as a generalization of the IR-VOF method. In the MOF method, the material volume (0th moment) as well as the centroid (ratio of the 1st moment and the 0th moment) are advected and the interface is reconstructed based on the updated moment data (reference volume and reference centroid). In the MOF method, the computed interface is chosen to match the reference volume exactly and to provide the best possible approximation to the reference centroid of the material. Using the centroid information, the volume-tracking with dynamic interfaces can be performed much more accurately. Furthermore, the interface in a particular mesh cell can be reconstructed independently from its neighboring cells (Ahn and Shashkov 2009).

Level set (LS) method The level set (LS) method was introduced by Osher and Sethian (1988) as a general technique to capture a moving interface. It has subsequently been applied to two-phase flows (Sussman et al. 1994; Sethian and Smereka 2003) as well as in many other fields (Osher and Fedkiw 2003; Sethian 1999b). The basic idea of the LS method is to represent the interface by the zero level set of a smooth scalar function $\phi(\mathbf{x}) : \mathbb{R}^D \rightarrow \mathbb{R}$, $\Gamma = \{x : \phi(\mathbf{x}) = 0\}$. Thus, the position of the interface is only known implicitly through the nodal values of ϕ. In order to extract the position of the interface, an interpolation (e.g. first or second order) of the ϕ data on the grid points must be performed. One often mentioned advantage of the LS method is its ability to handle topological changes and complex interfacial shapes in a simplified way.

In practice, the level set function ϕ is initialized as the signed distance from the interface. For description of the interface evolution the phase indicator function in Eq. (4) is replaced by ϕ. This LS equation is solved with high-order numerical discretization schemes in time and space, e.g. third-order total variation diminishing (TVD) Runge–Kutta schemes and third or fifth order Hamilton–Jacobi (HJ) weighted essentially non-oscillatory (WENO) schemes. Under evolution in time ϕ does not retain the property of a signed distance function and may develop steep and very small gradients. This results not only in inaccurate calculation of the interface normal vector and curvature (see "Models for surface tension" in Sect. 2.3.2.3) but also in severe errors regarding mass conservation. For improved mass conservation of LS methods it is essential that ϕ stays a smooth function throughout the entire simulation. In order to achieve this, a reinitialization step is introduced, where the LS function is transformed into a scalar field that satisfies the properties of a signed distance function and has the same zero level set. This reinitialization of ϕ is done in regular time intervals, often after each time step, but less frequent reinitializations (e.g. after every 10th time step) are also common. For this reinitialization essentially two different methods are used in literature. Fast marching methods (Sethian 1996, 1999a) solve the Eikonal equation $|\nabla\phi| = 1$ by computing the signed distance value for points in the computational domain or in a narrow band near the interface (Adalsteinsson and Sethian 1995). A more efficient and popular approach is to use a partial differential equation to reinitialize the LS function. Sussman et al. (1994, 1999) proposed to solve the following transient problem to steady state

$$\begin{aligned} \frac{\partial\phi}{\partial\tau} &= \mathrm{sgn}(\phi_0)(1 - |\nabla\phi|) \\ \phi(\mathbf{x}, \tau = 0) &= \phi_0(\mathbf{x}) \end{aligned} \tag{8}$$

Here, τ is the virtual time for reinitialization, ϕ_0 is the LS function at any computational instant, and $\mathrm{sgn}(x)$ is a smoothed signum function which Sussman et al. (1994) approximated numerically as

$$\mathrm{sgn}(\phi_0) = \frac{\phi_0}{\sqrt{\phi_0^2 + L_\varepsilon^2}} \tag{9}$$

Here, L_ε is a small length scale to avoid dividing by zero, usually chosen as the mesh size. Equation (8) has the formal property that ϕ remains unchanged at the interface and converges to $|\nabla\phi| = 1$ (i.e. the actual distance function) away from the interface. Russo and Smereka (2000) showed that the discretized version of Eq. (8) can displace

the zero level set and may lead to substantial errors due to the reinitialization; as a remedy they proposed a fix for the redistance step discretization of Sussman et al. (1994). Recently, Hartmann et al. (2008, 2010a, b) presented two new improved formulations of the methods of Sussman et al. (1994) and Russo and Smereka (2000) for differential equation-based constrained reinitialization of the LS method. Different temporal discretization schemes for solution of Eq. (8) were investigated by Min (2010). However, even with a frequent reinitialization step the LS method tends in long time simulations to shrink convex iso-surfaces, i.e. it leads to mass loss. To correct this mass loss, global (Chang et al. 1996; Lakehal et al. 2002; Smolianski 2005; Spelt 2005; Yap et al. 2006; Groß et al. 2006; Son and Dhir 2007; Zhang et al. 2010) as well as local (Ausas et al. 2011) mass correction steps have been proposed to explicitly enforce mass conservation.

Front-tracking (FT) method In his immersed boundary (IB) method for calculation of blood flow in the heart, Peskin (1977, 2002) introduced the concept to explicitly represent the boundary by a discrete data structure, which is updated continuously to track its movement. The immersed interface (II) method extends this concept to moving interfaces. Unverdi and Tryggvason (1992) applied this idea in their front-tracking (FT) method in order to simulate the motion of bubbles in a surrounding fluid. In the FT method, interfacial locations are tracked by a set of Lagrangian marker points. A marker point lying on the interface at position $\mathbf{x}_\mathrm{p}$ is advected by the flow according to

$$\frac{\mathrm{d}\mathbf{x}_\mathrm{p}}{\mathrm{d}t} = \mathbf{u}_\mathrm{p} \tag{10}$$

The velocity $\mathbf{u}_\mathrm{p}$ at position $\mathbf{x}_\mathrm{p}$ is determined from the velocity field on the Eulerian grid by interpolation. In order to keep the interface adequately resolved throughout the simulation a remeshing procedure is performed, where marker points may be added or removed.

In Tryggvasons FT method, the interface is defined explicitly by means of a set of logically connected marker particles (Unverdi and Tryggvason 1992; Tryggvason et al. 2001). Consequently, multiple interfaces can easily be represented in a single mesh cell and droplet or bubble collision without coalescence is naturally simulated. However, the FT method cannot be used to handle topological changes without explicit treatment of the connection and splitting of the interface data structure. Thus, to merge interfaces, special effort needs to be made. Nobari and Tryggvason (1996) and Nobari et al. (1996) studied the collision of two droplets and removed (at a prescribed time when the droplets are close enough) interface elements that are very close and nearly parallel, and reconnected the rest of the elements to form a single interface. To simplify the treatment of topological changes in 3D multiphase flows, FT methods without logical connectivity of the interface points have been proposed. Examples are the point-set method (Torres and Brackbill 2000) and the level contour reconstruction method (Shin and Juric 2002, 2009). As compared with VOF and LS techniques, which are ubiquitous in the multiphase CFD community, FT codes have been developed only by a few groups so far, though their number is increasing (de Sousa et al. 2004; Hao and Prosperetti 2004; Muradoglu and Kayaalp 2006; Dijkhuizen et al. 2010).

2.3.1.2 Methods with finite interface thickness We now discuss three methods where the interface thickness is finite. In the color function VOF method and the conservative level set method this finite thickness arises from numerical reasons, whereas in the phase-field method (which is a special kind of diffuse interface method) it stems from physical modeling.

Color function volume-of-fluid (CF-VOF) method The disadvantage of IR-VOF methods is the complexity of the interface reconstruction, especially in 3D. For a simplified computational treatment, VOF methods without interface reconstruction have been developed. These rely on a (smooth) color function C which can be considered as an approximation for the volume fraction function in the classical IR-VOF method. Accordingly, C takes a value of one in one phase (here phase +) and zero in the second phase, while the interface location is associated with the contour $C = 0.5$. Replacing the phase indicator function $X_\pm$ in Eq. (4) by the color function C and taking into account Eq. (5) yields

$$\frac{\partial C}{\partial t} + \nabla \cdot (\mathbf{u}C) = 0 \tag{11}$$

This equation is solved by difference schemes. The essential problem is that upwind schemes are diffusive and immediately smear out the interfaces, while downwind schemes maintain a sharp interface but are unstable, and central or higher-order schemes do not preserve the monotonicity and boundedness of the solution. The challenge is thus to design a suitable combination of up- and downwind fluxes that eliminates both the diffusiveness of the upwind scheme and the instability of the downwind scheme, so that the smearing is limited to an acceptable amount and the interface has a constant and uniform thickness regardless of the flow field.

Early versions of such schemes are the donor–acceptor method of Hirt and Nichols (1981) and Rudman's (1997) scheme which is based on the multidimensional flux-corrected transport (FCT) algorithm of Zalesak (1979). A FCT scheme is also used by Bonometti and Magnaudet

(2007) to solve in their JADIM code the color-function equation in non-conservative form by three successive one-dimensional steps. In regions of strong strain and shear, they prevent the front from spreading in time by a specific strategy in which the velocity at nodes crossed by the interface is modified to keep the thickness of the transition region constant (about three mesh cells). In addition the C field is modified every 50 time steps to guarantee that the global mass of each fluid is constant. Another CF-VOF method is the high resolution interface capturing (HRIC) scheme (Muzaferija and Peric 1999), which uses a nonlinear blend of upwind and downwind cell-face values, based on the spatial distribution of C, the local Courant number, and the angle between the normal to the interface and the cell-face surface vector. Bounded downwind differencing schemes, such as the compressive interface-capturing scheme for arbitrary meshes (CICSAM) (Ubbink and Issa 1999), which switches between different high resolution schemes, or THINC (tangent of hyperbola for interface-capturing) (Xiao et al. 2005) achieve a sufficiently sharp profile of C by introducing a controlled amount of numerical dispersion in the vicinity of the interface. In the method of Yabe et al. (2001) a tangent function is used to transform the color function to a smoothed profile. The latter is then advected using the constrained interpolation profile (CIP) scheme; finally the smoothed function is inverted to give a sharper profile.

Another strategy is adopted in the CF-VOF method of OpenFOAM (Weller 2006). The code uses the MULES (multidimensional universal limiter with explicit solution) algorithm develop by OpenCFD Ltd. to solve the equation

$$\frac{\partial C}{\partial t} + \nabla \cdot (\mathbf{u}C) + \nabla \cdot (C(1-C)\mathbf{U}_\mathrm{r}) = 0 \quad \text{with} \quad \mathbf{U}_\mathrm{r} = c_\mathrm{r}|\mathbf{u}|\frac{\nabla C}{|\nabla C|} \tag{12}$$

Compared with Eq. (11), an artificial compression term is added to counteract the effect of numerical diffusion. The compression term acts only in the interfacial region. For the constant c_r a value in the range $1 \le c_\mathrm{r} \le 4$ is recommended in order to ensure a sharp interface and limit the color function field to values between 0 and 1.

Conservative level set (C-LS) method Olsson and Kreiss (2005) developed a method which combines elements from the CF-VOF and LS method and denoted it as *conservative* level set method. Instead of the signed distance function usually used to define the interface, this method uses a regularized indicator function C. Similar to the CF-VOF method, C takes the value of 0 in one fluid and the value 1 in the other fluid, while the 0.5 level defines the interface. The method consists of two steps. In the first step, the conservative Eq. (11) is solved with a high resolution scheme. In the second (reinitialization) step, an equation that acts as an artificial compression is solved until steady state is reached

$$\frac{\partial C}{\partial \tau} + \nabla \cdot [C(1-C)\hat{\mathbf{n}}_+] = \varepsilon_\tau \nabla \cdot (\nabla C) \tag{13}$$

where $\hat{\mathbf{n}}_+ = \nabla C/|\nabla C|$. The artificial compression flux eliminates the numerical diffusion of the volume fraction, which appears due to numerical discretization of the advection term in Eq. (11). In Eq. (13), the small amount of "viscosity" ε_τ is added to avoid discontinuities. This value is taken as low as possible to get the interface smeared over a minimal number of mesh cells. A typical value is $\varepsilon_\tau = \Delta x/2$. Too small values of ε_τ compared with the grid size Δx result in over- or undershoots of the volume fraction. Since ε_τ is proportional to the grid size, the method does not solve the same equation on different grids. In a follow-up paper, the right hand side (RHS) of Eq. (13) is replaced by a different formulation which restricts diffusion in the reinitialization step in the direction normal to the interface in order to achieve better convergence (Olsson et al. 2007).

Strubelj et al. (2009) implemented this method in a two-fluid model for free surface flows where a separate momentum equation is solved for each phase and the contribution of surface tension is split. They used a time step $\Delta\tau = \Delta x/32$ and reported that one iteration is sufficient to significantly reduce the numerical diffusion. While the conservative LS method smears the interface over several cells (typically 3–4), this amount of smearing remains constant during the simulation and does not depend on the number of mesh cells used for discretization of the whole domain. A smaller grid size reduces the thickness of the smeared interface and also improves the volume conservation.

Phase-field (PF) method In diffuse interface (DI) methods, the infinitely thin boundary of separation between two immiscible fluids in the sharp interface limit is replaced by a transition region of small but finite width, across which physical properties vary steeply but continuously. The DI treatment can be motivated physically/thermodynamically (e.g. to account for long range van der Walls-type forces) or numerically as a regularization of the sharp interface limit (Sun and Beckermann 2007). Anderson et al. (1998) mention three main advantages of DI methods. First, from a computational point of view, modeling of fluid interfaces as having finite thickness greatly simplifies the handling of topological changes of the interfaces, which can merge or breakup while no extra coding is required. Second, the composition field has physical meanings not only on the interface but also in the bulk phase. Therefore, this method can be applied to many physical states such as miscible,

immiscible, and partially miscible ones. Third, the method is able to simulate contact line motion as the contact-line stress singularity in the immediate vicinity of the contact line is removed (Seppecher 1996). The most significant advantage in the present context is, however, that explicit tracking of the interface is unnecessary and all governing equations can be solved over the entire computational domain without any a priori knowledge of the location of the interfaces.

Phase-field (PF) models can be considered as a particular type of DI models that are based on fluid free energy. In the present context, we are interested in PF methods for the flow of two incompressible, immiscible phases with different density (Lowengrub and Truskinovsky 1998; Jacqmin 1999; Boyer 2002; Badalassi et al. 2003; Yue et al. 2004; Takada et al. 2006) (for three phase flows see Kim and Lowengrub (2005)). The basic idea is to introduce a conserved order parameter or phase-field, φ, to characterize the two different phases. This order parameter changes rapidly but smoothly in the thin interfacial region and is mostly uniform in the bulk phases, where it takes distinct values φ_+ and φ_-, respectively. The interfacial location is defined by the contour level $(\varphi_+ + \varphi_-)/2$. The interface dynamics is modeled by an evolution equation for φ, the Cahn–Hilliard equation

$$\frac{\partial \varphi}{\partial t} + (\mathbf{u}\cdot\nabla)\varphi = \nabla\cdot\left(M\nabla\mu_\varphi\right) \tag{14}$$

Here, $M(\varphi)$ is a diffusion parameter, called the mobility. The chemical potential, μ_φ, is the rate of change of free energy (which consists of a bulk and an interface contribution) with respect to φ and is given by

$$\mu_\varphi = \frac{\mathrm{d}\psi}{\mathrm{d}\varphi} - \varepsilon_\varphi^2\nabla^2\varphi \tag{15}$$

For the bulk energy density $\psi(\varphi)$ different formulations are used in the literature which depend on the choice for $\varphi_\pm$. Commonly used forms are e.g. $\psi = \varphi^2(1-\varphi^2)/4$ for $\varphi_+ = 1$, $\varphi_- = 0$ and $\psi = (\varphi+0.5)^2(\varphi-0.5)^2$ for $\varphi_\pm = \pm 0.5$ (Jacqmin 1999). With Eq. (15), the Cahn–Hilliard Eq. (14) involves fourth-order derivatives with respect to φ. This makes its numerical treatment more complex as compared to the NS equation which involves only second-order derivatives. The parameter ε_φ in Eq. (15) is a capillary width indicative of the thickness of the diffuse interface. The Cahn number $Cn \equiv \varepsilon_\varphi/L_\mathrm{c}$ relates ε_φ to a characteristic macroscopic length L_c.

An important issue in the PF method is the resolution of the interface thickness. Jacqmin (1999) used $\varphi_\pm = \pm 0.5$ and defined ε_φ to be the distance from $\varphi = -0.45$ to $\varphi = 0.45$ (90% of the variation of φ). He and Kasagi (2008) claimed that the PF method allows the accurate calculation of two-phase flows on fixed grids with interfaces only two cells wide when $\varepsilon_\varphi = \Delta x$ is used. Zhou et al. (2010) achieved grid convergence when the grid size in the interfacial region is less than or equal to ε_φ. Yue et al. (2004, 2006), however, reported an interface thickness of approximately $7.5\varepsilon_\varphi$ so that about 10 grid points are required to resolve it. Ding et al. (2007) developed a DI method with the volume fraction as an order parameter and applied it to several two-phase flow test cases with large density ratio. The authors found that the method can accurately conserve global mass but requires rather many grid points to achieve a smooth variation of dependent variables in a sufficient narrow interfacial region.

The issue of mass conservation of the PF method was studied in detail by Yue et al. (2007) for the case of a single drop in a quiescent fluid. While the phase-field variable was globally conserved, the drop could shrink spontaneously as φ shifted from its expected values in the bulk phases. The mass loss of the drop was proportional to both, the ratio between the domain and drop volume, and the Cahn number $Cn = \varepsilon_\varphi/R_0$, where R_0 is the radius of the drop. The mass loss became negligible if Cn was small enough; recommended values are below 0.01. Furthermore, it was found that there exists a critical drop radius R_c for a given computational domain size and value of ε_φ so that drops smaller than R_c eventually disappear.

2.3.2 Momentum equation and interfacial phenomena

2.3.2.1 Navier–Stokes (NS) equation We consider the flow of two immiscible incompressible Newtonian fluids in a domain $\Omega \subset \mathbb{R}^3$ which is split by an interface Γ into two distinct parts Ω_+ and Ω_-. In each of the subdomains, the density and viscosity are assumed to be piecewise constant with values (ρ_+, ρ_-) and (μ_+, μ_-), respectively. The conservation equations for mass and momentum valid in each subdomain $\Omega_\pm = \Omega_\pm(t)$ are

$$\begin{aligned} &\nabla\cdot\mathbf{u}_\pm = 0,\\ &\frac{\partial\rho_\pm\mathbf{u}_\pm}{\partial t} + \nabla\cdot(\rho_\pm\mathbf{u}_\pm\otimes\mathbf{u}_\pm) = \nabla\cdot\mathbb{S}_\pm + \rho_\pm\mathbf{g} \end{aligned} \tag{16}$$

The stress and deformation tensors are given by

$$\mathbb{S}_\pm = -p_\pm\mathbb{I} + 2\mu_\pm\mathbb{D}_\pm, \quad \mathbb{D}_\pm = \frac{1}{2}\left(\nabla\mathbf{u}_\pm + (\nabla\mathbf{u}_\pm)^\mathrm{T}\right) \tag{17}$$

where $\mathbb{I}$ denotes the identity tensor. At the interface $\Gamma = \Gamma(t)$ (which is assumed to have no mass and no interfacial viscosity) the following jump conditions hold (Drew 1983)

$$\begin{aligned} &[\![\rho(\mathbf{u}-\mathbf{u}_\Gamma)]\!]_\Gamma\cdot\hat{\mathbf{n}}_\Gamma = 0,\\ &[\![\rho\mathbf{u}\otimes(\mathbf{u}-\mathbf{u}_\Gamma) - \mathbb{S}]\!]_\Gamma\cdot\hat{\mathbf{n}}_\Gamma = \sigma\kappa\hat{\mathbf{n}}_\Gamma + \nabla_\Gamma\sigma \end{aligned} \tag{18}$$

Here, $\mathbf{u}_\Gamma$ is the velocity of the interface, σ is the coefficient of interfacial tension, $\kappa = -\nabla_\Gamma\cdot\hat{\mathbf{n}}_\Gamma$ is the signed interface

curvature (twice the mean curvature), and $\nabla_\Gamma = (\mathbb{I} - \hat{\mathbf{n}}_\Gamma \otimes \hat{\mathbf{n}}_\Gamma) \cdot \nabla$ is the surface gradient operator. The symbol $\hat{\mathbf{n}}_\Gamma$ denotes the unit normal vector to the interface with a fixed but arbitrary orientation (e.g. pointing into Ω_+). The notation $[\![\,]\!]_\Gamma$ represents the jump of physical quantities across the interface (in direction of $\hat{\mathbf{n}}_\Gamma$). When there is neither phase change nor tangential slip at the interface the jump conditions simplify to the form

$$[\![\mathbf{u}]\!]_\Gamma = 0, \quad [\![-\mathbb{S}]\!]_\Gamma \cdot \hat{\mathbf{n}}_\Gamma = \sigma\kappa\hat{\mathbf{n}}_\Gamma + \nabla_\Gamma\sigma \tag{19}$$

The local Navier–Stokes equation in each phase and the jump conditions at the interface can be combined into the following *single-field* equations which are valid in the entire computational domain

$$\nabla \cdot \mathbf{u} = 0, \quad \frac{\partial \rho \mathbf{u}}{\partial t} + \nabla \cdot (\rho \mathbf{u} \otimes \mathbf{u}) = -\nabla p + \nabla \cdot \mu\left(\nabla \mathbf{u} + (\nabla \mathbf{u})^{\mathrm{T}}\right) + \rho \mathbf{g} + \mathbf{f}_\sigma \tag{20}$$

Here, $\rho = \rho(\mathbf{x}, t)$ and $\mu = \mu(\mathbf{x}, t)$ are piecewise constant in each phase but discontinuous at the interface. The surface tension force is localized at the interface by means of a Dirac delta function δ_Γ with support on Γ

$$\mathbf{f}_\sigma = (\sigma\kappa\hat{\mathbf{n}}_\Gamma + \nabla_\Gamma\sigma)\delta_\Gamma \tag{21}$$

The solution of the single-field Navier–Stokes Eq. (20) requires knowledge of the instantaneous phase distribution which is provided by solving an interface evolution equation by one of the methods discussed in Sect. 2.3.1. The information about the phase distribution is needed to determine the density and viscosity fields and to compute the surface tension term according to Eq. (21); both issues are discussed in the following sections. In Fig. 2, we illustrate the intrinsic coupling between the single-field momentum equation, the interface evolution equation, and the instantaneous phase distribution graphically.

2.3.2.2 Treatment of fluid properties at the interface In the single-field (or one-fluid) approach for two-phase flow, the fluids in both phases are mathematically treated as one single fluid with varying physical properties. In IR-VOF methods the density and viscosity then depend on $f_+(\mathbf{x}, t)$ and are commonly computed by the relations

$$\rho_\mathrm{m} = f_+\rho_+ + f_-\rho_-, \qquad \mu_\mathrm{m} = f_+\mu_+ + f_-\mu_- \tag{22}$$

where $f_- \equiv 1 - f_+$. For the viscosity instead of the arithmetic mean also the harmonic mean

$$\frac{1}{\mu_\mathrm{h}} = \frac{f_+}{\mu_+} + \frac{f_-}{\mu_-} \tag{23}$$

is widely used. Thus, the fluid properties are computed as averages suitably weighted by the volume fraction.

The fact that the volume fraction Eq. (6) is averaged over the mesh cell volume V_mc while the NS Eq. (20) is local, motivated Wörner et al. (2001) to derive the following consistent volume-averaged (VA) set of equations

$$\frac{\partial f_+}{\partial t} + \nabla \cdot (f_+\mathbf{u}_\mathrm{m}) = -\nabla \cdot \left(f_+f_-\frac{\rho_-}{\rho_\mathrm{m}}\mathbf{u}_\mathrm{r}\right) \tag{24}$$

$$\nabla \cdot \mathbf{u}_\mathrm{m} = \nabla \cdot \left(f_+f_-\frac{\rho_+ - \rho_-}{\rho_\mathrm{m}}\mathbf{u}_\mathrm{r}\right) \tag{25}$$

$$\frac{\partial \rho \mathbf{u}_\mathrm{m}}{\partial t} + \nabla \cdot (\rho_\mathrm{m}\mathbf{u}_\mathrm{m} \otimes \mathbf{u}_\mathrm{m} + \mathbb{D}_\mathrm{r}) = -\nabla p_\mathrm{m} + \nabla \cdot \left[\mu_\mathrm{m}\left(\nabla \mathbf{u}_\mathrm{m} + (\nabla \mathbf{u}_\mathrm{m})^{\mathrm{T}}\right) + \mathbb{T}_\mathrm{r}\right] + \rho_\mathrm{m}\mathbf{g} + \mathbf{f}_\sigma \tag{26}$$

The barycentric (or center-of-mass) velocity, $\mathbf{u}_\mathrm{m}$, and the mean relative velocity of the phases within the averaging volume, $\mathbf{u}_\mathrm{r}$, are given by

$$\mathbf{u}_\mathrm{m} \equiv \frac{f_+\rho_+\langle\mathbf{u}\rangle_+ + f_-\rho_-\langle\mathbf{u}\rangle_-}{\rho_\mathrm{m}}, \quad \mathbf{u}_\mathrm{r} \equiv \langle\mathbf{u}\rangle_+ - \langle\mathbf{u}\rangle_- \tag{27}$$

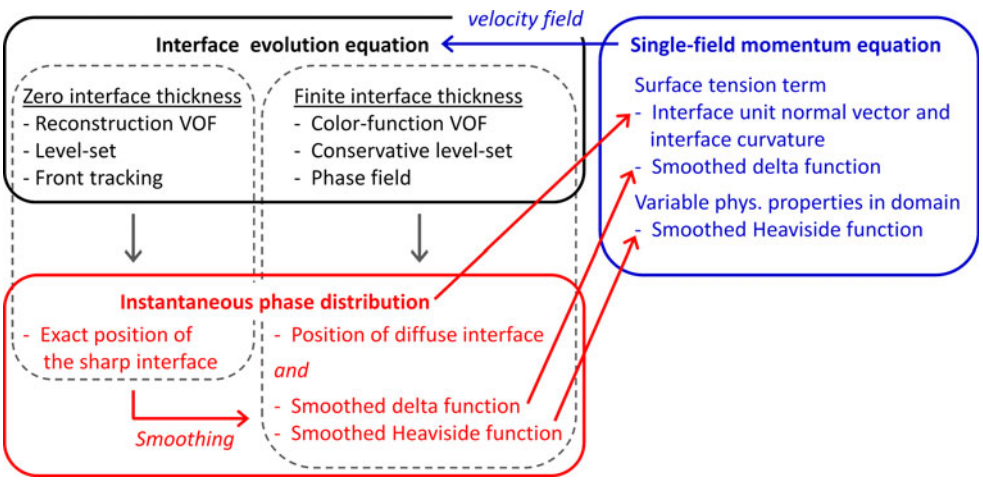

Fig. 2 Illustration of the intrinsic coupling between single-field momentum equation, interface evolution equation and instantaneous phase distribution. The *arrows* indicate the transfer of information

where

$$\langle \mathbf{u} \rangle_{\pm} \equiv \frac{1}{f_{\pm} V_{\mathrm{mc}}} \iiint_{V_{\mathrm{mc}}} X_{\pm} \mathbf{u} \mathrm{d}V \tag{28}$$

The definitions of further terms, appearing in the volume averaged NS Eq. (26) are

$$p_{\mathrm{m}} \equiv \frac{1}{V_{\mathrm{mc}}} \iiint_{V_{\mathrm{mc}}} p \mathrm{d}V \tag{29}$$

$$\mathbb{D}_{\mathrm{r}} \equiv f_{+} f_{-} \frac{\rho_{+} \rho_{-}}{\rho_{\mathrm{m}}} \mathbf{u}_{\mathrm{r}} \otimes \mathbf{u}_{\mathrm{r}} \tag{30}$$

$$\begin{aligned} \mathbb{T}_{\mathrm{r}} \equiv\ & f_{+} \mu_{+} \left\{ \nabla \left(\frac{f_{-} \rho_{-} \mathbf{u}_{\mathrm{r}}}{\rho_{\mathrm{m}}} \right) + \left[\nabla \left(\frac{f_{-} \rho_{-} \mathbf{u}_{\mathrm{r}}}{\rho_{\mathrm{m}}} \right) \right]^{\mathrm{T}} \right\} \\ & - f_{-} \mu_{-} \left\{ \nabla \left(\frac{f_{+} \rho_{+} \mathbf{u}_{\mathrm{r}}}{\rho_{\mathrm{m}}} \right) + \left[\nabla \left(\frac{f_{+} \rho_{+} \mathbf{u}_{\mathrm{r}}}{\rho_{\mathrm{m}}} \right) \right]^{\mathrm{T}} \right\} \end{aligned} \tag{31}$$

The terms on the RHS of Eqs. (24) and (25) as well as the tensors $\mathbb{D}_{\mathrm{r}}$ and $\mathbb{T}_{\mathrm{r}}$ are non-zero only at the interface (where $0 < f_{+} < 1$) but vanish in both bulk phases. Furthermore, all these terms depend on $\mathbf{u}_{\mathrm{r}}$. Due to the continuity of the velocity on both sides of the interface (cf. Eq. (19), the relative velocity $\mathbf{u}_{\mathrm{r}}$ vanishes as the mesh cell volume V_{mc} shrinks to zero. In this limit, all terms involving $\mathbf{u}_{\mathrm{r}}$ vanish and the VA Eqs. (24)–(26) essentially reduce to the local Eqs. (6) and (20). Though this set of VA VOF equations has not been used in practical computations so far, it is interesting to remark that the term on the RHS of Eq. (24) serves as anti-diffusion and is very similar to the empirically motivated artificial compression term in OpenFOAM, cf. Eq. (12), and to the term in the compression step of the C-LS method, cf. Eq. (13).

For finite difference (FD) based methods the discontinuity of the material properties at the interface can have a substantial (unfavorable) effect on the stability of the numerical scheme. To avoid a sudden jump in the material properties, a common approach in LS methods is to define a zone of thickness $2\varepsilon_{\phi}$ in the vicinity of the interface and to smooth the discontinuous density and viscosity over this thickness (Sussman and Fatemi 1999; Tornberg and Engquist 2000; van der Pijl et al. 2005). For this purpose, f_{+} in Eq. (22) is replaced by a smooth increasing function H_{ε} which approximates the Heaviside function as ε_{ϕ} goes to zero. For H_{ε} different formulations can be found in the literature; widely-used is (Sussman et al. 1999)

$$H_{\varepsilon}(\phi) = \begin{cases} 0 & \text{if} \quad \phi < -\varepsilon_{\phi} \\ \frac{\phi + \varepsilon_{\phi}}{2\varepsilon_{\phi}} + \frac{1}{2\pi} \sin\left(\frac{\pi \phi}{\varepsilon_{\phi}} \right) & \text{if} \quad |\phi| \leq \varepsilon_{\phi} \\ 1 & \text{if} \quad \phi > \varepsilon_{\phi} \end{cases} \tag{32}$$

Often, the "half-thickness" of the interface is taken as $\varepsilon_{\phi} = 1.5\Delta x$. We remark that in some recent LS methods the viscosity is smoothed but not the density (Coyajee and Boersma 2009; Gibou et al. 2007). Also there are methods that do not perform a smoothing of the density and viscosity at all but fully account for the discontinuous character of these properties at the interface (Marchandise and Remacle 2006).

In the FT method (Unverdi and Tryggvason 1992; Tryggvason et al. 2001), a material indicator function $I(\mathbf{x})$ is determined from the known position of the interface by solution of a Poisson equation. This indicator function serves as a smoothed Heaviside function and is used to smooth the otherwise discontinuous fluid properties across the interface in order to increase the numerical stability.

Fedkiw et al. (1999) introduced the ghost fluid (GF) method to treat contact discontinuities in the case of multiphase compressible flows with no phase change and utilized it for a wide range of applications. The underlying idea is to extrapolate the values of discontinuous variables across the fluid interface. This allows reducing smearing of discontinuous variables such as density or other material properties when solving the governing equations. For interfacial flows, the GF method is often combined with the LS method (e.g. Kang et al. (2000)) and less often with the FT method (e.g. Terashima and Tryggvason (2009)).

The above discussion indicates that the zero-thickness sharp interface of the IR-VOF, LS and FT method is usually not retained in the Navier–Stokes equation. Instead the fluid properties are (either in the context of finite volume discretization or for reasons of numerical stability) smoothed in the vicinity of the interface which is effectively smeared over typically 2–3 mesh cells. During the approach of two interfaces, local phenomena such as film draining are therefore not handled accurately when the interfaces come closer than 1–2 mesh cells. In IR-VOF and LS methods, the interfaces are often assumed to have merged if the distance between them becomes less than one grid spacing (Mukherjee and Dhir 2004), cf. Sect. 3.1.3.3. Due to this and the smearing of the fluid properties in the Navier–Stokes equations the IR-VOF and LS methods are in some references (but not here) classified as belonging to diffuse interface methods.

In methods with finite interface thickness, the smoothed representation of the phase indicator function serves as smoothed Heaviside function. Thus, in the CF-VOF method and the C-LS method the fluid properties are computed by replacing in Eq. (22) the volume-fraction f_{+} by the color function C. Accordingly, in the PF method a suitable formulation of the order parameter is used so that the correct values of the density and viscosity are recovered in both bulk phases. In the case $\varepsilon_{\varphi} \to 0$ (i.e. $Cn \to 0$) the PF method converges to the sharp interface limit and the classical Navier–Stokes equations and pressure jump conditions are recovered (Anderson et al. 1998; Jacqmin

1999). Zhou et al. (2010) showed in their 3D computations of the retraction of an elongated drop (of undeformed radius R_0) on a substrate that the PF model converges to the sharp interface limit when $Cn = \varepsilon_\varphi/R_0 \leq 0.05$, whereas in 2D simulations the more stringent criterion $Cn \leq 0.01$ is found (Yue et al. 2006). For the diffuse interface LB method, Amaya-Bower and Lee (2010) report that Cn has very little to no effect on both the terminal velocity and shape of a single bubble rising due to buoyancy, as long as the interface thickness is high enough to apply the technique of Lee (2009) to reduce the spurious currents.

2.3.2.3 Interfacial tension Accurate representation of interfacial forces such as surface tension and contact lines is a challenging problem, especially for methods with fixed grid representation. In the following we give an overview of different approaches for modeling of surface tension forces, discuss the problem of spurious currents associated with the numerical implementation of these models, consider issues related to the variation of surface tension due to the presence of surfactants (i.e. molecules which adsorb to a fluid interface), and present models for contact lines and wetting.

Models for surface tension Brackbill et al. (1992) transformed in their continuum surface force (CSF) model the surface force $\mathbf{f}_\sigma$ as given by Eq. (21) into a localized body force which is distributed within a transition region of finite thickness at the interface. For this purpose, the delta function δ_Γ is replaced by a regularized delta function δ_ε. In LS methods, the discrete Dirac delta function is given by

$$\delta_\varepsilon(\phi) = \begin{cases} \frac{1}{\varepsilon_\phi} f_\varepsilon(\phi/\varepsilon_\phi), & |\phi| \leq \varepsilon_\phi \\ 0, & |\phi| > \varepsilon_\phi \end{cases} \tag{33}$$

Here, f_ε is a kernel function and $\varepsilon_\phi = m\Delta x$, where m is a positive number that determines the support of f_ε. For the kernel function different formulations are used in literature, which are of linear, cosine or polynomial type, see e.g. Hysing (2006) and Raessi et al. (2009). A smeared delta function consistent with the smeared Heaviside function of Eq. (32) is Peskin's (1977) delta function

$$\delta_\varepsilon(\phi) = \frac{\mathrm{d}H_\varepsilon(\phi)}{\mathrm{d}\phi} = \begin{cases} \frac{1}{2\varepsilon_\phi} + \frac{1}{2\varepsilon_\phi}\cos\left(\frac{\pi\phi}{\varepsilon_\phi}\right), & |\phi| \leq \varepsilon_\phi \\ 0, & |\phi| > \varepsilon_\phi \end{cases} \tag{34}$$

In general, the choice of δ_ε and its discretization has a significant impact on the results (Raessi et al. 2009). A regularization often used in VOF methods, is to replace the product $\delta_\Gamma \hat{\mathbf{n}}_\Gamma$ by the gradient of a spatially smoothed or unsmoothed volume fraction.

In the CSF model, the interface normal vector and interface curvature are computed as

$$\hat{\mathbf{n}} = \frac{\nabla c}{|\nabla c|}, \quad \kappa = -\nabla \cdot \hat{\mathbf{n}} = -\nabla \cdot \left(\frac{\nabla c}{|\nabla c|}\right) \tag{35}$$

Here, the meaning of c depends on the method. In the LS method, c is replaced by the distance function ϕ. Since ϕ is smooth and continuous across the interface, its gradient can be evaluated rather accurately by higher order finite differences. However, for evaluating the curvature special care has to be taken when two interfaces are in close contact (Macklin and Lowengrub 2006). In CF-VOF methods, c in Eq. (35) is the color function. For PLIC-VOF methods the choice $C = f_+$ seems natural. However, the discontinuous character of f_+ at the interface makes it difficult to accurately evaluate the first and second derivatives, which leads to inaccurate interface normal vectors and curvatures. One possibility for improvement is to smooth the f_+ field before computing its gradient. For estimating the curvature from the f_+ field, various approaches exist in PLIC-VOF methods which are based on least-squares-fit, height functions, convolution techniques or reconstructed distance functions, see e.g. (Pilliod and Puckett 2004; Renardy and Renardy 2002; Cummins et al. 2005; Francois et al. 2006) and references therein. In recent publications, a trend to curvature estimates from height functions can be observed because this method is rather simple to implement and provides superior results (Cummins et al. 2005; Francois and Swartz 2010; Lopez and Hernandez 2010). However, any method for curvature estimation relies on an adequate resolution of the interface and problems occur when the curvature becomes comparable with the mesh size. Raessi et al. (2007) showed that the accuracy of curvatures calculated from the VOF function deteriorates with mesh refinement, and that there is a constant error associated with curvatures calculated from the LS function in a coupled LS and VOF method. The authors proposed a new methodology for calculating interface normal vectors and curvatures, in which the normal vectors are advected along with the interface, and the curvatures are calculated directly from the advected normals (Raessi et al. 2007, 2010).

The CSF method is explicit, so that the time step size is limited by a respective time step criterion to ensure numerical stability (Brackbill et al. 1992; Galusinski and Vigneaux 2008). To mitigate this time step restriction, Hysing (2006) proposed a semi-implicit CSF model for finite element (FE) simulations. Recently, this model was modified for finite volume (FV) methods and it was found that the time step restriction due to surface tension can be exceeded by at least a factor of five, without destabilizing the numerical solution (Raessi et al. 2009). Overall, the CSF model is widely used especially in combination with VOF and LS methods, but also finds occasional application

in the LB (Wu et al. 2008a, b) and PF (He and Kasagi 2008) methods.

Lafaurie et al. (1994) proposed the continuous surface stress (CSS) model where the surface tension force is modeled as the divergence of a surface stress tensor which acts tangential to the interface

$$\mathbf{f}_\sigma = \nabla \cdot [(\mathbb{I} - \hat{\mathbf{n}}_\Gamma \otimes \hat{\mathbf{n}}_\Gamma)\sigma\delta_\varepsilon] \tag{36}$$

The advantage of the CSS model over the CSF model is its conservative nature, which ensures that for closed interfaces the net surface tension force is zero. The CSS model is used e.g. in Gueyffier et al. (1999), Renardy et al. (2001, 2002) and Bothe et al. (2009a; 2009b).

With a smoothed (continuous) viscosity and for $\sigma = \text{const.}$ the stress jump condition in Eq. (19) reduces to $[\![p]\!] = \sigma\kappa$. Then, the GF method can be used to explicitly implement this pressure jump in the discretization of the pressure gradient in order to account in an implicit way for the surface tension force (Liu et al. 2000).

In the volume-averaged VOF method (Wörner et al. 2001; Sabisch et al. 2001) surface tension is given by $\mathbf{f}_\sigma = \sigma\kappa a_i\hat{\mathbf{n}}$. Here, $a_\mathrm{i} = A_\mathrm{i}/V_\mathrm{mc}$ is the local interfacial area concentration, i.e. the ratio between the interfacial area A_i within the mesh cell (which is in PLIC-VOF methods given by the area of the planar polygon representing the interface) and the mesh cell volume. This model restricts the surface tension force to those mesh cells, that actually contain a part of the interface. Essentially, it replaces δ_Γ by the local interfacial area concentration a_i, which can be interpreted as a smoothed delta function, see also Gada and Sharma (2009). Shepel and Smith (2009) performed simulations with the LS method and compared the performance of this interfacial area concentration surface tension model and a modification of it with that of CSF models based on a regularized Dirac delta function. The authors found that the modified interfacial area concentration model gives superior results for film-like interfaces.

In the FT approach, the surface tension force is calculated directly on the Lagrangian interface grid by evaluation of line integrals (Unverdi and Tryggvason 1992; Popinet and Zaleski 1999; Tryggvason et al. 2001; Shin and Juric 2002). This force is then distributed onto the fixed Eulerian grid using Peskin's (1977, 2002) immersed boundary method. In Tornberg and Engquist (2000) a weak formulation of the 2D NS equation is presented where the surface tension force is included through line integrals along the interfaces, and where the segments of the interface are defined from the LS function. This avoids explicit discretization of the delta function.

For the numerical treatment of the surface tension force in the weak formulation of FE methods, an approach proposed by Dziuk (1991) and successfully applied by Bänsch (2001) became very popular recently. The curvature in the surface integral is replaced by the Laplace–Beltrami operator so that integration by parts allows reducing one order of differentiation associated with the curvature. This formulation is used e.g. in Groß et al. (2006), Groß and Reusken (2007) and Ganesan and Tobiska (2009a) and has also been combined with the CSF method (Hysing 2006).

In diffuse interface methods for incompressible immiscible flows various formulations for the surface tension force are used in the literature, see e.g. Kim (2005) and references therein. In general, the surface tension force depends on the chemical potential and is modeled either with the proportionality $\mathbf{f}_\sigma \propto -\varphi\nabla\mu_\varphi$ (Jacqmin 1999; Jacqmin 2000; He and Kasagi 2008) or $\mathbf{f}_\sigma \propto \mu_\varphi\nabla\varphi$ (Badalassi et al. 2003).

Spurious currents A common problem encountered by all above surface tension models is the appearance of artificial vortex-like flows in the neighborhood of the interface, which are commonly referred to as spurious or artificial currents or parasitic flow (Lafaurie et al. 1994). While spurious currents also occur for flowing liquids, they are best explained for the case of a static neutrally buoyant spherical bubble or drop. Physically, both fluids are at rest and the difference in pressure inside and outside the bubble/drop is given by the Young–Laplace equation. The numerical solution of the NS equations yields, however, in general a velocity field where both fluids are *not* at rest. Instead artificial velocities occur in the neighborhood of the

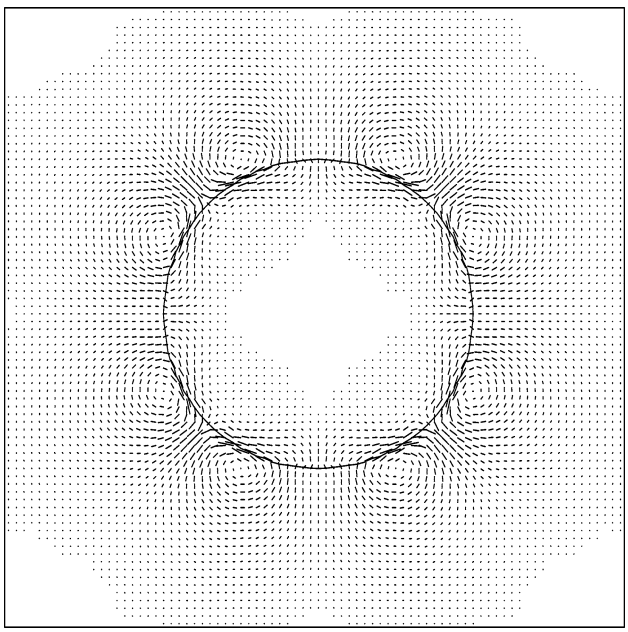

Fig. 3 Spurious currents for a static (neutrally buoyant) two-dimensional bubble. Figure from Sabisch (2000)

interface, see Fig. 3. The origin of this numerical artifact is twofold: spurious currents occur when the implementations of the surface tension and pressure gradient forces do not balance on the discrete level (Renardy and Renardy 2002) and/or when the curvature of the interface is not accurately computed. The amplitude of spurious currents depends on surface tension, viscosity, density ratio, and spatial and temporal discretization; it increases with decreasing ratio $\mu/\alpha \propto Ca$, where $Ca \equiv \mu U/\sigma$ is the capillary number based on a characteristic velocity U. At worst, the spurious currents can be strong enough to dominate the solution.

There exist a large number of papers which deal with spurious currents in the CSF and CSS method and how to reduce them, see e.g. Popinet and Zaleski (1999), Renardy and Renardy (2002), Aulisa et al. (2006), Harvie et al. (2006b) and (for a historical perspective) Fuster et al. (2009). Tong and Wang (2007) proposed a so-called pressure boundary method which utilizes a capillary pressure gradient term in the Navier–Stokes to account for surface tension, see also Wang and Tong (2010). Shirani et al. (2005) multiplied the surface tension force as given by the CSF and CSS models by a factor that represents the fraction of area of a cell face in contact with the heavier fluid. Groß and Reusken (2007) proposed an extended (discontinuous) pressure FE space which greatly reduces spurious currents when combined with the Laplace-Beltrami technique.

Spurious currents are, however, not only a problem in sharp interface continuum methods (VOF, LS, FT), but also exist in LB methods (Lishchuk et al. 2003; Dupin et al. 2006; Pooley and Furtado 2008; Lee 2009) where they can be reduced e.g. by employing multiple relaxation time algorithms (Pooley et al. 2008), and in the PF method (Kim 2005; De Menech 2006). Jamet et al. (2002) developed a second-gradient method which is a special kind of DI method where the fluids are compressible. Their method can completely eliminate spurious currents; the essential requirement to achieve this is energy conservation. He and Kasagi (2008) performed PF computations of a stationary axisymmetric gas bubble in quiescent water and compared the performance of the CSF and a chemical potential model where $\mathbf{f}_\sigma \propto -\varphi\nabla\mu_\varphi$. With the CSF method they obtained significant spurious currents. Due to the exact conservation of surface tension energy and kinetic energy, the chemical potential formulation of surface tension in the frame of the PF method can reduce the spurious currents to the level of the truncation error. While the parasitic flow is thus very small, the authors note, however, spurious oscillations in the position of the interface. Namely, the interface moves forward and backward with an oscillation amplitude of about one-third of the mesh size.

An important step forward towards the elimination of spurious currents for sharp interface models was the paper by Francois et al. (2006). The authors devised an algorithm based on the CSF model combined with the GF method for a PLIC-VOF method which achieves a (to within round-off) exact balance of surface tension and pressure gradient forces when interfacial curvatures are known accurately. Based on this work, the CSF variant implemented in the Gerris code (http://gfs.sourceforge.net) of Popinet (2009) is the first that demonstrated recovery of an exact equilibrium solution for this simple test case up to machine accuracy.

Marangoni effects and surfactants Gradients in surface tension commonly arise for one of two reasons: a non-uniform temperature or a non-uniform distribution of a surface active substance (SAS) or surfactant at the interface. By Eq. (21) surface tension gradients enter in the form of the Marangoni stress $\Delta_\Gamma\sigma$ into the NS equations and so-called Marangoni flows may arise, which can drastically change the interfacial and wetting behavior. To relate σ to the local interface temperature or surfactant concentration a constitutive equation of state (EOS) is required. Often, a linear relationship is assumed while for surfactants a non-linear Langmuir equation of state is also commonly used.

For thermal Marangoni flows, the local value of σ at the interface can be computed from the local temperature which is obtained by solution of the energy equation. In this sense, the computational treatment of thermal Marangoni flows is much simpler than of solutal ones. There, surfactants may be accumulated and transported along the interface which requires the implementation of a special conservation law on the interface. In the following we therefore concentrate on numerical methods for surfactant induced Marangoni flows. For numerical investigations of thermal Marangoni flows with a LS method the interested reader is referred to Haj-Hariri et al. (1997) and Zhao et al. (2010), with a FT method to Nas and Tryggvason (2003), and with a VOF method to Ma and Bothe (2011).

Surfactants may be insoluble or soluble. In the former case the surfactant exists only at the interface. Its transport along the interface is described by an equation which accounts for surface fluid velocity, surface diffusion and local stretching or contraction of the interface (Stone 1990). For a soluble surfactant in addition desorption and adsorption with the bulk phases may occur. Their net effect is accounted for by a source term in the surfactant interfacial transport equation. In addition an advection–diffusion equation for the surfactant concentration in one or both of the bulk phases is solved. Surfactants may also be produced in situ by chemical reactions in the interfacial region. An overview of experimental, analytical and numerical studies on the effect of

surfactants on fluidic interfaces can be found in Alke and Bothe (2009).

In numerical studies of surfactant transport often the boundary integral (BI) method is used and Stokes flow is considered, see e.g. Booty and Siegel (2010) and Feigl et al. (2007). The latter authors modified a 3D BI method which calculates the deformation of drops with clean interfaces to include the motion of insoluble surfactants on the interface and studied its effect on droplet formation in shear flow. A moving mesh FE method for computation of free surface flows with insoluble surfactants was developed by Ganesan and Tobiska (2009a).

Only few numerical methods have been proposed so far which solve the full NS equations in both phases with soluble or insoluble surfactant. Among them are PLIC-VOF methods for an insoluble SAS with a linear EOS (Renardy et al. 2002; Drumright-Clarke and Renardy 2004) and an arbitrary EOS (James and Lowengrub 2004). In the latter method the surfactant mass and interfacial area are computed separately and the SAS concentration is obtained from their ratio. Davidson and Harvie (2007) incorporated the method of James and Lowengrub (2004) into the VOF algorithm of Rudman (1998) and investigated transient axisymmetric deformations of a drop rising in a liquid. Alke and Bothe (2009) developed a PLIC-VOF method where an extended surface transport theorem is used for describing the interfacial flux of a soluble surfactant and an iso-surface of the VOF-variable is used as a connected approximation of the interface. The method is implemented in FLUENT and an air bubble rising in a quiescent surfactant solution is studied. The first LS based method for computation of 2D interfacial flows with insoluble surfactant is presented by Xu et al. (2006). Recently, Lakshmanan and Ehrhardt (2010) combined the C-LS method of Olsson and Kreiss (2005) with a surface transport equation for the surfactant. The resulting continuum SAS concentration is zero everywhere but on the interface, where it has a peak of width 2ε in agreement with the smoothing of the color function. To avoid dispersion of this peak, an artificial compression step (which is similar to the color function compression step) is applied to the surfactant concentration field. Lee and Pozrikidis (2006) developed a method which combines the immerse interface (respectively FT) method for solution of the 2D NS equation (by a FD scheme) with the solution of the interface surfactant transport equation by a FV scheme. Zhang et al. (2006) developed an axisymmetric FT method for gas–liquid flows with insoluble or soluble surfactant. For the soluble surfactant the sublayer is not resolved but the adsorption scheme is designed such that the total mass of the surfactant is well conserved. Muradoglu and Tryggvason (2008) proposed a FT method for computation of interfacial flows with surfactants which is very flexible in the sense that an almost arbitrary EOS for the surfactant can be used while the SAS may be soluble in one or two phases with different concentrations. Ceniceros (2003) coupled the FT method with the LS method and studied the effects of surfactants on capillary waves. Van der Sman and van der Graaf (2006) developed a 2D free energy LB model for surfactant adsorption on droplet interfaces. The emulsion/surfactant system is described with two order parameters, indicating the oil/water interface and the surfactant volume fraction, respectively. The model relies on three distribution functions (one for each order parameter and one for the NS equation).

Moving contact lines Droplets and bubbles in contact with a solid surface are ubiquitous in microfluidic devices. Their motion is strongly affected by the wettability of the substrates and the dynamics of the contact line. A review of recent theoretical, experimental and numerical progress in the description of moving contact line dynamics is given by Bonn et al. (2009); it covers approaches based on the sharp interface limit, DI methods and MD simulations. A review of wetting phenomena in microfluidics is provided by Ralston et al. (2008). Here we focus on concepts for modeling contact lines in engineering applications.

The contact line (triple line) denotes the intersection of the interface between two immiscible fluids with the solid wall. The macroscopic angle at which the interface meets the solid is called the contact angle. The static (equilibrium) contact angle θ_s is ideally a unique property of the material system and its value is determined by the microscopic interactions across the three interfaces. In practice, a hysteresis often arises depending on how the interface is formed. The advancing and receding angles θ_A and θ_R are the largest and smallest contact angles achievable before the wetting line begins to move in the direction of the continuous and disperse phase, respectively. The contact angle observed experimentally for a contact line that is moving relative to the solid surface is called the dynamic contact angle θ_d. Unlike the static contact angle, the dynamic contact angle is not a material property and many correlations relating it with the contact line speed or the capillary number have been proposed in the literature (Dussan 1979). For an overview see e.g. Saha and Mitra (2009a), where eight different theoretical dynamic contact line models are tested in CFD computations. In numerical computations the dynamic contact angle is often set to vary linearly between the prescribed receding and advancing angles if the instantaneous contact line velocity u_{cl} is within a given range $\pm u_{cl,max}$. Beyond this range, the contact angle is assigned by the value of θ_R or θ_A, depending on the sign of the contact line velocity (Francois and Shyy 2003; Huang et al. 2004; Chen et al. 2009a). For $u_{cl,max} = 0$ this model reduces to that of Fukai et al. (1995).

A classical problem in continuum hydrodynamics is the incompatibility between the moving contact line and the no-slip boundary condition, as the latter leads to a force singularity at the contact line (Huh and Scriven 1971; Dussan 1979; Cox 1986; Qian et al. 2006). The respective non-physical divergent stress stems from the fact that continuum fluid mechanics breaks down at molecular distances from the contact line. A common remedy to the problem is to replace the no-slip condition on the solid surface by the Navier boundary condition

$$u = L_S \frac{\partial u}{\partial n} \tag{37}$$

with a slip length L_S, so that for $L_S > 0$ the contact line can move. For $L_S = 0$ and $L_S = \propto$ Eq. (37) reduces to the no-slip and free-slip boundary condition, respectively. In most applications, the physical slip length is much smaller than any realistic mesh size for numerical simulation. Renardy et al. (2001) introduced an artificial slip length with magnitude in the order of the grid size. Slip leads to a decrease of the viscous force which resists the motion of the contact line so that its velocity speeds up. Finite volume codes integrate over the mesh cell adjacent to the wall which results in an apparent finite interface velocity at the wall (Renardy et al. 2001; Rosengarten et al. 2006).

Methods which prescribe a static contact angle have difficulties in describing flows dominated by capillary forces. Typically such flows are driven by a deviation of the contact angle from the static angle. A suitable numerical procedure is therefore to use the mismatch between the dynamic and static (equilibrium) contact angle to obtain a movement of the contact line. This approach is used in the VOF (Renardy et al. 2001) and the LS (Liu et al. 2005; Naraynan and Lakehal 2006) context as well as in ALE moving mesh methods (Ganesan and Tobiska 2009b). Renardy et al. (2001) reconstructed the interface normal vector close to the contact line in such a way that the contact angle takes the prescribed value. Recently, Fang et al. (2008) proposed a 3D contact line hysteresis model for the PLIC-VOF method. In their approach, the local contact angle becomes a function of the local contact line velocity. The latter is calculated from the displacement of the contact line between consecutive time steps, while no-slip boundary conditions are used at all walls. Dupont and Legendre (2010) presented a CF-VOF method for computation of static contact lines (including hysteresis) and moving ones. The method is implemented in 2D and relies on imposing the apparent contact angle by suitable values of the color function in ghost cells at the wall.

CFD results are often mesh dependent when a no-slip or Navier-slip condition is imposed along the solid boundary and a fixed contact angle is imposed on the contact line. Schönfeld and Hardt (2009) addressed this issue and introduced a macroscopic slip range in combination with a localized body force close to the contact line. The authors considered the capillary rise between parallel plates and demonstrated that their approach gives almost mesh independent results; however, it requires the usage of a fitted pre-factor. Afkhami et al. (2009) considered a mesh dependent dynamic contact angle model and showed mesh independent results for two cases, the withdrawal of a plate and the spreading of a drop. Afkhami and Bussmann (2009) presented a height function based method which yields accurate estimates of curvature and surface tension at a contact line and converges with mesh refinement.

Brackbill et al. (1992) described a method where the contact angle is implemented in the code not as a boundary condition, but within the surface tension model in the solver. In cells adjacent to the walls they compute the interface normal vector $\hat{\mathbf{n}}$ from the contact angle as

$$\hat{\mathbf{n}} = \hat{\mathbf{n}}_w \cos\theta + \hat{\mathbf{t}}_w \sin\theta \tag{38}$$

Here, $\hat{\mathbf{n}}_w$ and $\hat{\mathbf{t}}_w$ are the unit vectors normal and tangential to the wall. From this "rotated" interface normal vector then the interface curvature near the wall is computed as usual by relation $\kappa = -\nabla \cdot \hat{\mathbf{n}}$. A similar approach for modeling moving contact lines in the VOF method is presented in Sikalo et al. (2005), where the local dynamic contact angle depends on the instantaneous advancing/receding contact-line velocity.

For the LS method, different approaches have been proposed to account for contact line motion (Spelt 2005; Smith et al. 2005; Zahedi et al. 2009). Spelt (2005) modified the LS method of Sussman et al. (1999) to account for moving contact lines and contact line hysteresis. In his method the slip length is an input parameter and reasonably accurate results are obtained when the grid spacing is approximately equal to the slip length. The contact line law is enforced by prescribing the value of the LS function at ghost cells. Ding and Spelt (2007) used this method to compute the spreading of an axisymmetric droplet and obtained results in good agreement with those of the DI method of Jacqmin (1999). Zahedi et al. (2009) extended the C-LS method of Olsson and Kreiss (2005) to describe contact line dynamics. The contact line movement is driven by enforcing the equilibrium contact angle at the solid boundary. A modified reinitialization procedure provides a diffusive mechanism for contact line motion without explicit reconstruction of the interface.

In the context of FT methods, we mention two approaches for contact line motion. Huang et al. (2004) modeled the moving contact line by a slip condition. The value of the dynamic contact angle is determined by a linear model and local forces are introduced at the moving contact lines, which are based on a relationship between the moving contact line angle and contact line speed.

Muradoglu and Tasoglu (2010) developed a FT method for computational modeling of impact and spreading of droplets on a solid wall. In their method the contact angle is specified dynamically and it is assumed that the drop interface connects to the wall when the distance between both gets shorter than a prescribed threshold value. The authors found that this threshold distance has little influence on the computational results as long as it is equal or larger than two mesh cells. A method for computing the FT material indicator function near the contact line is given by Khenner (2004). Jacqmin (2000) developed a PF method to compute contact line dynamics where the interface can move either through convection or through diffusion driven by chemical potential gradients. When the angle of the interface differs from the static angle the contact line moves by a diffusive process on a fast time scale in a small region at the solid boundary so that the contact angle is adjusted to the static value. The fact that the interface can move by diffusive processes eliminates the need for modeling fluid slip. The drawback of the model is that the interface must be highly resolved to achieve accuracy.

2.3.3 Heat and mass transfer across the interface

The transport equation for a solute chemical species with molar concentration $c_\pm$ in subdomains $\Omega_\pm(t)$ is

$$\frac{\partial c_\pm}{\partial t} + \mathbf{u}_\pm \cdot \nabla c_\pm = \nabla \cdot (D_\pm \nabla c_\pm), \quad \mathbf{x} \in \Omega_\pm(t) \tag{39}$$

with the coupling conditions at the interface $\Gamma(t)$

$$[\![D\nabla c]\!]_\Gamma \cdot \hat{\mathbf{n}}_\Gamma = 0, \quad c_+ = Hc_- \tag{40}$$

Here $D_\pm$ are the diffusivities and $H \geq 0$ is the distribution coefficient (i.e. the dimensionless Henry law constant or Henry number). In case of chemically reacting flows, Eq. (39) is extended by respective source and sink terms, see e.g. Bothe (2009). The equations describing heat transfer (without phase change) are obtained by replacing in Eqs. (39) and (40) the concentration by the temperature and the species diffusivity by the thermal diffusivity, and by setting $H = 1$. In the case of mass transfer, the value of H is in general different from one and can take very small or very large values depending on the actual system. The respective discontinuity of the concentration at the interface complicates computations of interfacial mass transfer as compared with interfacial heat transfer.

The first numerical simulations of heat and mass transfer from deforming rising drops and bubbles with the VOF method were, therefore, restricted to $H = 1$ where the concentration field is continuous (Ohta and Suzuki 1996; Davidson and Rudman 2002). In the general case $H \neq 1$ the discontinuity of $c_\pm$ at the interface is difficult to treat within a single-field approach. Petera and Weatherley (2001) transformed, therefore, the discontinuous physical concentrations field into a continuous numerical one. A suitable transformation is e.g. $\tilde{c} = c_+$ in Ω_+ and $\tilde{c} = Hc_-$ in Ω_-. For $\tilde{c}$ then a single-field concentration equation can be solved. However, the continuity of mass flux across the interface, cf. Eq. (40), yields a source/sink term in the transport equations for $\tilde{c} \equiv f_+ c_+ + (1 - f_+)Hc_-$ so that it is not a conserved quantity (Onea et al. 2009). This transformation technique has been combined with a moving mesh FE method (Petera and Weatherley 2001), with the PLIC-VOF method (Bothe et al. 2004; 2009b; Onea et al. 2009) and with the LS method (Yang and Mao 2005). This approach is, however, only meaningful when H is a constant which represents a significant limitation. In reality, H depends on pressure and temperature and thus may vary along the interface. Haroun et al. (2010b) did not transform the concentration fields but derived a single-field transport equation for $\bar{c} \equiv f_+ c_+ + (1 - f_+)c_-$ which contains an additional term that exists only close to the interface; the concentration equation is solved in combination with a CF-VOF method. Recently, Bothe et al. (2009a, 2011) developed a so-called two scalar method which solves Eq. (39) in each phase separately. While the diffusive fluxes in each bulk phase are computed by a standard central difference scheme, the convective transport of the species is treated by the PLIC algorithm, analogous to the convective transport of f. Due to this, a very good conservation of the species mass is achieved and the method is suited for reactive mass transfer. Kenig et al. (2011) solved two species equations in the entire computational domain (one for each phase). They incorporated the interfacial coupling conditions of Eq. (40) directly into the species equations by representing them as source terms localized at the interface.

2.3.4 Phase change

The numerical computation of interfacial flows with phase change (i.e. evaporation, boiling or condensation) is complicated by the fact that unlike in Eq. (19) the velocity on both sides of the interface is not continuous. Instead, a jump in normal velocity occurs which is related to the mass flux due to phase change across the interface. This leads to additional terms not only in the interfacial jump conditions but also in the continuity, NS and energy equations. Here, we do not list these modifications but refer to the references below.

The first attempt toward the development of advanced numerical method for flows with phase change can be attributed to Welch (1995) who used a moving triangular

grid for 2D simulations of film boiling. Later, Welch and Wilson (2000) introduced a VOF approach for fluid flows with phase change. Hardt and Wondra (2008) proposed an evaporation model that relies on a continuum-field representation of the source terms in the mass conservation equation which allows implementing almost arbitrary evaporation laws (instead of the common assumption of an isothermal interface). The model is largely independent of the specific interface tracking scheme but is implemented and tested for the PLIC-VOF method. In order to simulate evaporating droplets, Schlottke and Weigand (2008) developed a PLIC-VOF method which involves two VOF variables, one for the liquid phase and one for the vapor phase. The vapor phase is assumed to be insoluble inside the liquid phase but there is diffusion in the gaseous phase.

Son and Dhir (1998) and Son et al. (1999) were among the first who modified the LS method to account for phase change. They assumed that the vapor phase is at saturation temperature and solved the energy equation in temperature formulation for the liquid phase. In the latter reference, they considered the axisymmetric growth and departure of a single vapor bubble during nucleate pool boiling, and accounted in their model for the effect of microlayer evaporation. LS methods for incompressible NS equations with phase change are also presented by Tanguy et al. (2007) and Gibou et al. (2007) and are applied to vaporization of a water droplet moving in air and to film boiling, respectively. In the latter study, depending on the grid size either periodic bubble pinch off (coarse grid) or growing mushroom-shaped structures are found (fine grid). Many LS methods for boiling use the GF approach to impose the jump conditions at the interface (Gibou et al. 2007; Tanguy et al. 2007; Son and Dhir 2007). A coupled LS and VOF method (see Sect. 2.4.1) for simulation of bubble growth in film boiling was developed by Tomar et al. (2005). For phase-change heat transfer in turbulent interfacial flows Lakehal and Labois (2011) developed a large-eddy and interface simulation methodology (LEIS) which is based on the LS approach.

Juric and Tryggvason (1998) developed a FT method for the simulation of boiling flows. Their approach is based on the single-field formulation and relies on a delta function formulation to impose interfacial source terms. They apply the method to 2D studies of liquid–vapor phase change in film boiling. In a follow-up paper the scope is extended to 3D film boiling with multiple interacting bubbles and merging and breakup of interfaces (Shin and Juric 2002). A diffuse interface method for numerical simulation of liquid–vapor flows with phase change and moving contact lines (denoted as second gradient method) is presented by Jamet et al. (2001).

2.3.5 *Boundary conditions and wall roughness*

The numerical solution of the governing equations requires the specification of boundary conditions at the borders of the computational domain. In microfluidics, inlet and outlet conditions at the open boundaries of the domain do not pose a severe problem, because the flow is in general laminar. Therefore, at the inlet the laminar velocity profile may be specified while at the outlet unsteady convective conditions may be used for example (Ferziger and Peric 2002). We note that in microchannel flows the usual homogeneous Neumann boundary condition of vanishing directional derivative in the normal direction of velocity (together with a prescribed pressure at the outlet) may severely distort exiting vortices (Bothe 2009).

At solid walls the use of no-slip boundary conditions is appropriate for Knudsen numbers below 0.001 (Gad-el-Hak 1999). For larger values of Kn a first notable departure from continuum behavior occurs with the creation of a slip layer at the wall. In the slip regime ($0.001 < Kn < 0.1$), the Knudsen layer is small, and the bulk of the flow can be treated as a continuum fluid with a slip model, cf. Eq. (37), accounting for the effect of the Knudsen layer (Aidun and Clausen 2010). In contrast to gases, the slippage of liquids over solid surfaces is still in a debate (Lauga et al. 2007). Tabeling (2009, 2010) states that the estimate of slippage for hydrophobic surfaces tends to reach a consensus among the experimentalists but still the amplitude of the effect—measured in terms of the slip length—lies one order of magnitude above numerical estimates from atomistic simulations. Experiments with water indicate typical slip length in the range between 10 and 30 nm for hydrophobic walls while for hydrophilic walls the order of magnitude for the slip length is of the order of a nanometer. The impact of slip on systems with typical dimensions larger than tens of microns will therefore likely be limited so that the use of the no-slip boundary condition at the solid–liquid interface seems appropriate (Lauga et al. 2007).

In classical fluid mechanics, the wall roughness is typically considered negligible for laminar flow. However, with decreasing channel size and increasing relative roughness, as it applies in microdevices, the wall roughness increases in importance. A recent review on roughness effects on single phase laminar internal flows in microdevices is provided by Kandlikar (2008). To the author's knowledge, there exist yet no investigations dealing with roughness effects in two-fluid flow. Therefore, in the following paragraph some recent papers dealing numerically with roughness effects in single-phase flow are discussed. We remark that for accurate computation of such flows a layer of mesh cells representing a structured grid are necessary as unstructured grids are not suitable close to walls (Hirsch 2007). In advanced general purpose CFD codes

adequate meshes for capturing boundary layers can be generated by so-called "mesh inflation".

Early numerical studies investigated the influence of roughness elements on pressure drop and heat transfer in a simplified way by modeling the roughness by a set of randomly generated peaks and valleys of specified form along the otherwise smooth surface (Croce and D'Agaro 2005). More realistic 3D surfaces with random roughness can be obtained by a method recently proposed by Xiong and Chung (2010). The importance of the wall roughness for fluid friction was demonstrated by Silva et al. (2008). The authors performed μPIV measurements for a single phase laminar flow ($Re \leq 50$) in a microchannel (with hydraulic diameter of 637 μm) that possessed rough walls (roughness height equal to 1.6% of the hydraulic diameter) and a very irregular cross-section shape. They compared Poiseuille numbers obtained from experimental velocity profiles against those obtained from CFD predictions for the same operating conditions but with hydrodynamically smooth walls. The results showed that the non-consideration of the wall roughness in the CFD calculations yields an underestimation of the friction factor of 11% for the conditions under study. Herwig et al. (2010) investigated the influence of wall roughness on friction in laminar single phase pipe flow for different roughness elements. They computed the entropy production in the flow and found an appreciable influence of wall roughness. The authors pointed out the need for a reasonable choice of the wall location as well the roughness parameter. 3D numerical investigation of laminar flow in a rectangular channel with irregular roughness were performed by Chen et al. (2009b). The authors used the Weierstrass–Mandelbrot function in conjunction with fractal geometry to model and characterize the multiscale self-affine roughness. They showed that surfaces with the larger fractal dimensions (i.e. more frequent variations in the surface profile) result in a significant larger incremental pressure loss, even if the relative roughness is the same. Mohammadi et al. (2011) studied stationary flows of second-order fluids in rough microchannels by a spectral method. The algorithm models irregular roughness geometry using the Fourier expansions and enforces the flow boundary conditions on the rough wall by means of the immersed boundary method.

2.4 Specific issues

2.4.1 Hybrid methods

In the literature, many hybrid methods are proposed which aim to combine the advantages of different approaches while avoiding their limitations. For sharp interface models the coupling of LS and PLIC-VOF techniques into the CLSVOF method became very popular (Sussman and Puckett 2000; Son and Hur 2002; Sussman 2003; van der Pijl et al. 2005; Yang et al. 2006; Tong and Wang 2007; Sussman et al. 2007; Coyajee and Boersma 2009; Wang et al. 2009a; Lv et al. 2010; Sun and Tao 2010). The main motivation for this coupling is to combine the better mass conservation properties of the VOF method with the more accurate computation of interface normal vectors and interface curvature of the LS method. Thus, after advection of ϕ and f_+ from time step n to $n+1$, the piecewise linear interface is reconstructed from f_+^{n+1} using the interface normal vectors calculated from ϕ^{n+1}. Then ϕ^{n+1} is reinitialized by calculating the distance between any cell center and the PLIC-VOF interface.

Problematic in the LS method are regions where the curvature of the interface is not well resolved by the grid. When the LS function is advected, the sharp edges are usually smoothed out and mass loss occurs. To circumvent this problem Enright et al. (2002, 2005) proposed the particle LS method, in which mass-less marker particles seeded near the interface are used to correct (i.e. redistance) the LS function in the underresolved regions. This particle correction procedure takes place when a particle is advected from one side to the other side of the interface, see also Wang et al. (2009b). Another hybrid method is the level contour reconstruction method (Shin and Juric 2002, 2009) which combines the characteristics of both the FT and LS methods. Ceniceros (2003) described the evolution of the interface by a FT method while a LS distance function is used for smoothing the density and viscosity close to the interface. Other hybrid methods combine elements from FT with marker particles and PLIC-VOF (Aulisa et al. 2003; López et al. 2005).

There exist several approaches where the LB method is coupled with the LS method. In these methods the LS function is used to distinguish the components and a single LB equation is solved. Mehravaran and Hannani (2008) incorporated the surface tension term in the LB method as source which is localized near the interface and zero elsewhere. A different approach was made by Thömmes et al. (2009). Their method uses special boundary conditions at the interface between the two phases which realize the macroscopic jump conditions on the kinetic level and incorporate surface tension into the model. Lallemand et al. (2007) combined the LB method with elements from the FT approach. The latter is used to explicitly track the interface by a set of marker particles. The interface curvature is computed from adjacent markers and is then used to determine the surface tension force and to distribute it to nearby Eulerian grid points.

As final remark on hybrid methods we note that for single phase flows hybrid continuum and molecular

dynamics methods (Nie et al. 2004) as well as hybrid atomistic-continuum methods (Werder et al. 2005) are under development.

2.4.2 *Refined and adaptive grids*

For numerical simulation of fluid flow problems with moving interfaces, in general high grid resolution is needed for adequate computation of the interface curvature and solution of the governing equations. However, there are often also large portions of the domain where high levels of refinement are not needed. Using a highly refined mesh in these regions represents a waste of computational effort. An efficient manner for such problems is the use of *adaptive* methods which refine the mesh locally only where needed. In this subsection we give a short overview on adaptive grid refinement techniques and refer to Losasso et al. (2006) and Compère et al. (2008) for a broader discussion (mainly in the context of the LS method). For rectangular structured grids two options are widely used. Block-structured grid methods allow increasing the resolution with multiple levels of refinement on nested blocks located near regions where the scales cannot be resolved by the coarse grid. They are used in the VOF method (Ginzburg and Wittum 2001), the LS method (Sussman et al. 1999; Min and Gibou 2007), the CLSVOF method (Kadioglu and Sussman 2008) and the PF method (Ceniceros and Roma 2007; Ceniceros et al. 2010). The second class is constituted by tree-based methods. They are more general and more efficient than block-structured grids in that each discretization element can be refined independently from the others, so that additional mesh cells can be added only where it is required. In tree-based methods, hierarchical grids are generated by recursive subdivision of a simple geometric shape. 2D rectangular and 3D hexahedral or tetrahedral grids can be generated recursively by the quadtree and octree algorithms, where a 2D/3D mesh cell is subdivided in four/eight equal-sized subcells. Adaptive multilevel quadtree/octree methods have been combined with the LS method (Strain 1999; Groß et al. 2006) and the VOF method (Greaves 2004; Popinet 2009). A disadvantage of tree-methods is that complex data structures are required.

Another possibility that has been realized in the LS method is the use of an auxiliary refined Cartesian grid to solve the LS and reinitialization equations in a narrow band around the interface, while maintaining a coarse grid to solve the mass and momentum conservation equations on a structured (Gomez et al. 2005) or unstructured grid (Herrmann 2008). An adaptively refined parallelized sharp interface LS based Cartesian grid method for 3D moving boundary problems is presented in Udaykumar et al. (2009), and a 3D anisotropic adaptive LS FE method on unstructured tetrahedral meshes in Compère et al. (2008). For PLIC-VOF methods, Rudman (1998) introduced the strategy to solve the volume fraction equation on a mesh which is twice-as-fine as the mesh used for solution of the NS equation. This procedure is also used in Hayashi et al. (2006) and Liovic and Lakehal (2007). A PLIC-VOF method with adaptive local grid refinement where the refinement criteria is based on the interface curvature is presented in Malik et al. (2007). A CF-VOF method based on the CICSAM scheme with adaptive local grid refinement around the interface can be found in Theodorakakos and Bergeles (2004). Farhat et al. (2010) presented a color-gradient multiphase LB method where a fine grid block engulfs the fluid-fluid interface and migrates with it. Yu and Fan (2009) developed an interaction potential-based LB method with adaptive mesh refinement for two-phase flow simulations. In order to keep the fluid viscosity independent of the grid size, the relaxation factor has to be adjusted with the grid spacing. For the PF method, the interface must be thin enough to attain the sharp-interface limit and yet be adequately resolved for the interfacial forces to be computed accurately. Therefore, to achieve a high numerical accuracy at moderate computational costs a mesh with dense grids covering the interfacial region and coarser grids in the bulk are required (Zhou et al. 2010). Thus, for the efficient computation of moving interfaces with the PF method adaptive meshing is of special relevance. FE based PF methods with adaptive meshing are presented in Villanueva and Amberg (2006), Yue et al. (2006) and Zhou et al. (2010), a stencil adaptive FD method in Ding et al. (2010) and a moving mesh spectral method in Shen and Yang (2009).

2.4.3 *Multiscale methods*

With current computer power, direct numerical simulations of multi-fluid flows offer the opportunity to capture scales whose ratio spans over two orders of magnitude (Tryggvason et al. 2010). While this is by far insufficient to resolve all scales in macroscopic multiphase flows, it may be sufficient for some microfluidic applications. However, also in microchannels multi-fluid flows can generate features much smaller than the channel size, consisting for example of very thin filaments (during droplet breakup), very thin liquid films (at walls or between colliding bubbles or droplets) and very thin concentration boundary layers (in case of high Schmidt numbers). While local adaptive grid refinement allows effectively resolving some of these small scale phenomena in certain regions of interest, it also increases the complexity of the computations significantly and usually results in greatly increased CPU time. An alternative are multiscale methods which allow for efficient computations by combining the description and modeling

of physical phenomena occurring at different scales by distinct approaches in a thorough or approximate manner.

Examples for such multiscale methods are the study of Davis et al. (1989) where a thin film model was coupled with a boundary integral computation to investigate the collision of drops and the micro-layer models for nucleate boiling of Son et al. (1999) and Kunkelmann and Stephan (2009), cf. Section 3.3. Recently Tomar et al. (2010) coupled a PLIC-VOF algorithm with a two-way coupling Lagrangian particle-tracking method and performed multiscale simulations of primary jet breakup and atomization. Thomas et al. (2010) introduced a multiscale method to account for thin films trapped between a drop and a solid wall in FT simulations. The evolution of the film is described by a semi-analytical model which is coupled with the solution of the fully resolved flow in the rest of the domain and allows capturing the evolution of films thinner than the grid spacing reasonably well. Alke et al. (2010) combined a PLIC-VOF-based approach for the numerical simulation of mass transfer across deformable fluidic interfaces with a subgrid-scale model for the concentration boundary layer at the interface. Building on a moving-frame-of-reference technique and a local mesh refinement around the bubble they were able to handle single bubbles under moderate Reynolds numbers and Schmidt numbers on the order of 100. In a broader sense, also the incorporation of microscale interactions in VOF-based continuum simulations by Hardt (2005), cf. Sect. 3.1.3.3, may be considered as a kind of multiscale approach.

2.4.4 *Discretization techniques*

For spatial discretization of the NS equation different methods can be used, which are based e.g. on finite differences (FD), finite volumes (FV), finite elements (FE) or spectral representations (Chung 2002). PLIC-VOF methods are traditionally solved by FV codes. The LS method is most often used in combination with a FD or FE discretization but is combined with a FV method in Chatzikyriakou et al. (2009). Marchandise et al. (2006) used a discontinuous Galerkin method for the LS equation. The FT method is traditionally used with a FD code but FV (Muradoglu and Kayaalp 2006) and FE (Chung et al. 2008) discretizations are also possible. For CF-VOF methods and the C-LS method FD, FV and FE schemes are equally suitable.

Also the LB method can be considered as a type of discretization scheme. With a Chapman–Enskog expansion the discrete LB system can be written in a continuous form. With the proper lattice topology and collision rules the partial differential equations emerging from the expansion can be shown to resemble the compressible continuity and NS equations. Actually, the LB equations are equivalent to an explicit finite difference scheme of the NS equations with second-order spatial accuracy and first-order temporal accuracy with a non-zero or zero compressibility depending on the scaling (convective or diffusive) used in the expansion (Luo and Girimaji 2003; Junk et al. 2005). In this sense the free energy LB method approximates the Cahn-Hilliard equation in combination with the incompressible NS equation and can be considered as a discretization of the PF method.

2.4.5 *Computer codes*

Various commercially available CFD and multiphysics code packages have been developed and can be used to compute single and multiphase flows in microfluidic devices. Codes widely used in the engineering community for the computation of general single and multiphase flows are FLUENT and CFX (both from ANSYS, http://www.ansys.com), STAR-CD (from CD-adapco, http://www.cd-adapco.com), and CFD-ACE+ (from ESI Group, http://www.esi-cfd.com). The CFD solver of all these software packages is based on a FV discretization on a structured/block-structured or unstructured grid. For interface resolving two-fluid simulations variants of the CF-VOF method are provided in CFX, FLUENT and STAR-CD. A PLIC-VOF method is offered by FLUENT, CFD-ACE+ and FLOW3D (from Flow Science Inc., http://www.flow3d.com). The latter is a commercial FD/FV CFD code on a structured grid whose roots date back to Hirt and Nichols (1981). Another commercial FV code with structured multi-block meshing is TransAT (from ASCOMP GmbH, http://www.ascomp.ch); for interfacial flows it provides a IR-VOF, a LS and a PF method. A commercial FE based package for various applications including CFD is COMSOL Multiphysics (from COMSOL, http://www.comsol.com) which was formerly known as FEMLAB. For computation of interfacial flows COMSOL provides both, a LS and a PF method. A commercial code based on the LB method which is, however, restricted to single phase flow applications so far is PowerFLOW (from Exa Corporation, http://www.exa.com). A very powerful suite of simulation tools (including a VOF method) that are primarily intended for biochip design is CoventorWare (from Coventor Inc., http://www.coventor.com). Beside these commercial codes there exist also freely available open source codes. Widely used is OpenFOAM (http://www.openfoam.com, see also http://www.extend-project.de). A freely available very advanced state-of the art adaptive 3D PLIC-VOF code is the Gerris flow solver (http://www.gfs.sourceforge.net) (Popinet 2009). Also a software package for front tracking is freely available from the web (http://frontier.ams.sunysb.edu/download).

From the various applications that will be discussed in the second part of this review, FLUENT is used in (Hardt 2005; Taha and Cui 2006a, b; Tanthapanichakoon et al. 2006; Abdallah et al. 2006; Hardt and Wondra 2008; Özkan et al. 2007; Zhu et al. 2008; Liu and Wang 2008; Urbant et al. 2008; Alke and Bothe 2009; Gupta et al. 2009b, 2010; Santos and Kawaji 2010), CFX in (Schönfeld and Rensink 2003; Ndinisa et al. 2005; Özkan et al. 2007; Shao et al. 2008; Shepel and Smith 2009; Xiong and Chung 2010), STAR-CD in (Özkan et al. 2007; Wegener et al. 2009), CFD-ACE+ in (Kobayashi et al. 2004; Rosengarten et al. 2006; Saha and Mitra 2009b; Lai et al. 2010), TransAT in (Naraynan and Lakehal 2006; Lakehal et al. 2008; Narayanan and Lakehal 2008; Chatzikyriakou et al. 2009; Gupta et al. 2010), COMSOL in (Zagnoni et al. 2010; Constantinou and Gavriilidis 2010; Chasanis et al. 2010; Kenig et al. 2011) and OpenFOAM in (Saha and Mitra 2009a; Kunkelmann and Stephan 2009). Further applications of various codes (mainly in the lab-on-a-chip context) can be found in the review of Erickson (2005).

2.4.6 Comparison of methods and codes

There exist a number of papers in which different methods or codes are compared for certain applications. The interested reader is referred to Gerlach et al. (2006) for a comparison of various VOF methods with the CLSVOF method and to Zacharioudaki et al. (2007) for a comparison of a VOF and FT method. Glatzel et al. (2008) evaluated the performance of four commercial FV CFD codes (CFD-ACE+, CFX, FLOW-3D and FLUENT) for typical microfluidic engineering problems and compared the results with experimental data. As examples for surface tension dominated flows, bubble dynamics in a microchannel and micro droplet generation were considered. While all four codes are based on variants of the VOF method, large differences in the interfacial shape computed by the different codes were observed, and only the CFD-ACE+ and FLUENT codes are recommended for simulations of interfacial flows involving capillary forces. Özkan et al. (2007) compared the performance of the VOF method in three commercial and one in-house code for bubble train flow in a square mini-channel. They found that the results of the two PLIC-VOF codes (FLUENT and the in-house code) were in good agreement and clearly superior to results obtained with CF-VOF methods (CFX and STAR-CD). Gupta et al. (2010) compared the PLIC-VOF method in FLUENT with the LS method in TransAT, see also Sect. 3.2.1.

Hysing et al. (2009) proposed two benchmark configurations with a 2D bubble rising in a liquid column for quantitative validation and comparison of interfacial flow codes. The results of three independent groups (two employing a FE LS and one an ALE moving grid method) were in good agreement up to the point of break-up, after which all three codes predicted different bubble shapes. The authors highlighted the need to establish reference benchmark solutions for interfacial flows with break-up and coalescence.

Cheng et al. (2010) performed 3D simulations of multiple bubbles rising under buoyancy in a quiescent viscous incompressible liquid. They extended the LB method of Zheng et al. (2006) to density ratios up to 1000 and evaluated the computational efficiency by comparison of single bubble computations with the VOF and FT method. For serial computing on a single CPU the LB method took about 4.5 and 6.2 times more CPU time than the FT and VOF method, respectively. Also Zheng et al. (2005) reported that their LB method required more CPU time than the LS and VOF methods. To reduce the computational effort, recently a 3D LB method has been proposed which uses only seven lattice velocities instead of the commonly adopted number of (at least) 15 (Zheng et al. 2008).

2.4.7 Recommendations and guidelines

Any numerical simulation inevitably involves some errors and uncertainties. An overview on the various error sources existing in CFD methods is given in Casey and Wintergerste (2000). Beside round-off and convergence errors, these are mainly related to numerical discretization techniques, to grid resolution and design, to boundary and inlet condition treatment, and last but not least to physical modeling. The ERCOFTAC "Best Practice Guidelines" provide a practical guide giving the best practice advice for achieving high-quality CFD simulations for single phase flow computations with the Reynolds averaged Navier–Stokes (RANS) equations (Casey and Wintergerste 2000) and for disperse two-phase flows (Sommerfeld et al. 2008) (with focus mainly on the Euler-Euler and Euler-Lagrange methods).

It is well-known that the numerical solution of interfacial flow is very much dependent on the quality of the grid. Orthogonality, skewness and aspect ratio of the grid directly affect the numerical accuracy of many methods. In general structured grids are favorable. Any numerical investigation should be accompanied by a grid refinement study in order to demonstrate that the results based on the final grid system are independent of the mesh size. Bothe and Warnecke (2007) strikingly illustrated the critical influence of grid resolution by considering the mixing of two streams of the same liquid (one of them carrying a passive tracer substance) in a T-junction microchannel, see also the book chapter of Bothe (2009) on evaluation and validation of CFD simulations in microchemical applications. Here, we cite and emphasize one important statement. Namely, while a CFD result is rather easy to obtain

(especially with commercial codes), it is the duty of the user to check whether this result gives an appropriate approximation of the physical solution.

This completes the first part of the present review, which gave an overview on various numerical methods and related models that are available for computation of interfacial two-fluid flows, including their mathematical foundation and physical assumptions. In this sense it may be helpful for selecting for a given application an appropriate method and model and thus to avoid errors related to physical modeling.

3 Two-phase microfluidic applications

In the second part of this article we review various applications where the different numerical methods and models discussed above are used for investigation of two-fluid flows in mini- and microchannels or microdevices and microreactors, respectively. We begin by studies devoted to hydrodynamic aspects (such as separated and segmented flow, bubble and drop formation, breakup and coalescence) and then turn to applications related to heat transfer, mixing and dispersion, mass transfer and chemical reactions, Marangoni flows and surfactants, and boiling.

3.1 Flow hydrodynamics

While there exist various possibilities for contacting of gas and liquid or immiscible liquids in micro-structured devices most often one of two principles is used (Hessel et al. 2005). The first principle is continuous phase contacting where both phases flow continuously but separately side by side. The flow can be gravity-driven such as in falling film microreactors or pressure-driven. In the latter case the flow may be annular, stratified or parallel (e.g. in overlapping channels). The second possibility is dispersed-phase contacting where one of the phases is immersed in a second continuous phase such as in micro bubble columns. The respective flow pattern is often denoted as segmented flow, slug flow, bubble train flow or Taylor flow.

3.1.1 Separated and parallel flow

A review of separated (or parallel) multiphase microflows with focus on fundamental physics, stabilization methods for the interface, and applications for liquid–liquid extraction is given by Aota et al. (2009). An advantage of parallel flow as compared with segmented flow is that it permits counter-current flow of the phases which is of interest for some applications. Essential for parallel multiphase microflows is the stabilization of the interface under varying flow rates. This can be achieved by partial modification of the solid surface. A pinned interface between immiscible liquids (e.g. an aqueous and an organic phase) can be created by selective surface patterning (hydrophilic and hydrophobic) of a microchannel (Atencia and Beebe 2005). However, it is difficult to form parallel multiphase microflows when the interfacial tension (and thus the Laplace pressure) is low or when the pressure loss along the channel is high (Aota et al. 2009). Options for stabilizing the interface under such conditions provide so-called mesh microreactors.

The description of separated interfacial flows poses no special difficulty for the continuum methods covered in this review. The same is, however, not true for LB methods. Rannou (2008) evaluated the effectiveness of various two-phase LB models in maintaining the continuity of shear stress and velocity at the interface for a fully developed two-phase Poiseuille flow in a 2D channel and found that the performance of each model strongly depended on the density and viscosity ratio, see also Aidun and Clausen (2010). When the fluids had different densities, none of the tested approaches satisfied the continuity of velocity at the interface. For fluids with different viscosity, all methods had problems when the viscosity ratio was larger than about 100.

3.1.2 Segmented flow

The flow of immiscible fluids in mini- and microchannels often occurs in the form of segmented flow, where a disperse phase flowing in the center of the channel segments a continuous liquid phase into distinct slugs. Often, the continuous phase is perfectly wetting so that the disperse elements are not in contact with the wall but fully surrounded by a liquid film. When the bubbles or drops are sufficiently large (typically several hydraulic diameters) they are of elongated bullet-type shape and almost fill the entire channel cross-section. This flow pattern is known as Taylor flow. Taylor flow is attractive for multiphase monolith reactors (Kreutzer et al. 2005b) and micro bubble columns (Haverkamp et al. 2006) because high gas/liquid and gas/liquid/solid mass transfer rates are combined with reduced axial dispersion.

In the following, we review only numerical investigations of segmented flow and Taylor flow in narrow channels where the bubble/drop shape is not prescribed but part of the solution and where the flow within both phases is resolved. For a more general review we refer to Angeli and Gavriilidis (2008). Even with this restriction, there exist a large number of numerical investigations of segmented flow in *circular* channels where usually axisymmetry is assumed. Various methods have been used, e.g. PLIC-VOF (Taha and Cui 2006a; Gupta et al. 2009b, 2010), LS (Fukagata et al. 2007; Lakehal et al. 2008; Narayanan and

Lakehal 2008), PF (He et al. 2010) and LB (Yu et al. 2007). Gupta et al. (2009b) give practical guidelines for modeling Taylor flow with FLUENT. Ndinisa et al. (2005) computed a single Taylor bubble in a tube (diameter 19 mm) with the CFX code, both with the CF-VOF and the Euler-Euler method. For the CL-VOF method, they found an excessive mixing due to numerical diffusion in the wake region of the Taylor bubble which leads to unrealistic results. For the E–E method, the results depended very much on the prescribed interfacial length scale which is required to model the drag force. A sufficiently sharp interface could only be obtained by an ad-hoc adaption of this length scale with different values close and far from the interface. Since these results were obtained for laminar flow, one may expect that the findings apply to Taylor flow in mini- and micro-channels as well.

There exist only a few numerical studies on segmented flow in *non-circular* channels. Taha and Cui (2006b) investigated the flow of a single Taylor bubble rising in a square vertical channel (side length 2 mm) for a wide range of capillary numbers using the PLIC-VOF method in FLUENT. Liu and Wang (2008) extended this study to vertical square and equilateral triangular channels with 1 mm hydraulic diameter. Wörner and coworkers performed comprehensive numerical simulations of concurrent upward and downward Taylor flow in millimeter sized square vertical channels with an in-house PLIC-VOF code (Ghidersa et al. 2004; Wörner et al. 2005; Wörner et al. 2007; Öztaskin et al. 2009; Keskin et al. 2010). The use of periodic boundary conditions in the axial direction allowed restriction of the computational domain to a single flow unit cell (which consists of one bubble and one liquid slug). The computed bubble shapes were compared with experimental flow visualizations and good agreement was obtained (Keskin et al. 2010). In Öztaskin et al. (2009) the interaction of equal sized Taylor bubbles separated by liquid slugs of different length was studied.

Sarrazin et al. (2006, 2008) performed simulations of water-in-oil droplet hydrodynamics in a 60×50 μm rectangular microchannel by a CF-VOF method and reported good agreement of the computed droplet shape and flow field with experiments. Liu et al. (2009a, b) investigated the motion of water droplet immersed in an oil flow through an array of microfluidic ratchets by a LS method, see Fig. 4, and found that the droplet moved faster in the diffuser direction than in the nozzle direction (in agreement with experiments).

3.1.3 Topological changes

3.1.3.1 Droplet formation and breakup Microfluidic drop formation is not only important for the generation of highly mono-disperse emulsions (e.g. to prepare highly functional

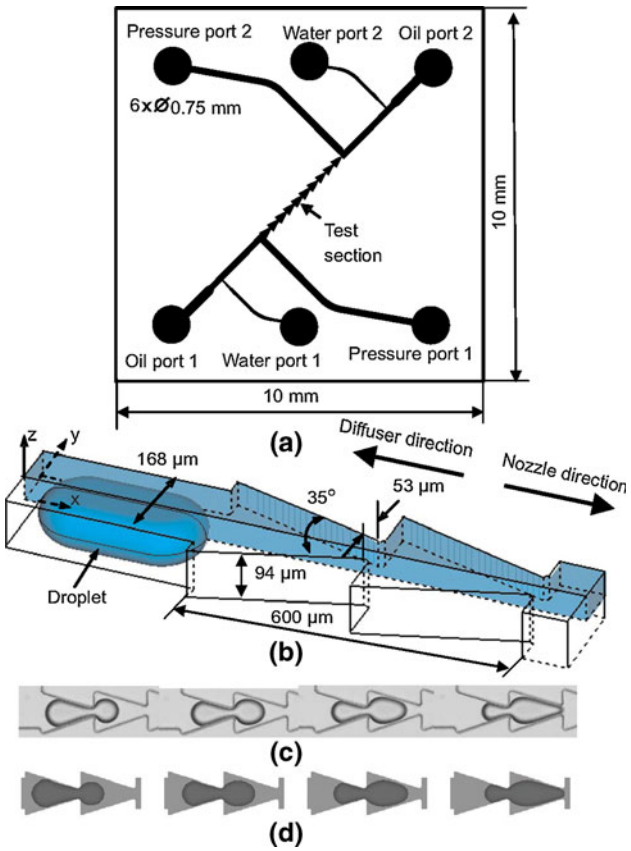

Fig. 4 Numerical simulation of the motion of a droplet through microfluidic ratchets by a level set method. **a** Device schematic for investigation of microdroplets in diffuser/nozzle structures. The test section contains ten diffuser/nozzle structures; **b** numerical model and dimensions of the ratchet; **c** deformation of a droplet passing through the ratchet; **d** simulated deformation of a droplet under the same conditions as of the experiment shown in (**c**). Reprinted with permission from Liu et al. (2009b). Copyright 2009 by the American Physical Society

particles), but micron-sized droplets can also be used to deliver substances in well-defined amounts, or as tiny chemical reactors involving only picoliters of reagents, where the kinetics can be monitored and controlled very precisely (Bringer et al. 2004). Such droplets are typically generated in continuous-flow systems using either T-junctions, Y-junctions, cross-junctions or flow focusing methods (Gu et al. 2011). In microfluidic T-junctions and Y-junctions the continuous and disperse phases are injected from two inlets, which are orthogonal or inclined. The formation of droplets or bubbles occurs as a result of shear and interfacial tension forces at the fluid-fluid interface (Garstecki et al. 2006). In cross-junctions and flow focusing methods three inlets are used; the fluid forming the continuous phase is introduced via two orthogonal channels while the fluid forming the disperse phase is injected through a central channel.

Simulations of microfluidic droplet formation with the LB method have been performed for flow-focusing devices

(Dupin et al. 2006), T-junctions (van der Graaf et al. 2006; Gupta et al. 2009a) and cross-junctions (Wu et al. 2008a, b). In Wu et al. (2008b), the computed 3D drop shapes and drop lengths were in very good agreement with experiments for various flow conditions. Hao and Cheng (2009) used the multiphase free-energy LB method to study the formation of a water droplet emerging through a micro-pore on the hydrophobic surface in a proton exchange membrane fuel cell (PEMFC) and its subsequent movement on the surface under the action of gas shear. Hagedorn et al. (2004) investigated the influence of geometrical confinement on the breakup of long fluid threads in the absence of imposed flow by a LB model. They found that confinement can substantially alter the thread breakup process as compared with the unconfined case.

The group of Davidson considered a cylinder containing a 4:1 contraction of diameter and investigated the axisymmetric drop formation by flow focusing (Davidson et al. 2005) and the drop deformation for Newtonian (Harvie et al. 2006a) and shear-thinning (Harvie et al. 2007) liquids in an immiscible liquid stream by a PLIC-VOF method. Harvie et al. (2008) performed 2D simulations of a viscoelastic drop passing through a microfluidic contraction in good agreement with experimental results. Kobayashi et al. (2004) performed 3D PLIC-VOF simulations of the droplet formation in microchannels with circular and elliptic cross-sections with CFD-ACE+. They verified the CFD results by experiments and concluded that the CFD approach can help to design suitable channel structures. Zhu et al. (2008) investigated the dynamic behavior of a water droplet emerging from a single lateral pore into a microchannel gas stream for typical PEMFC conditions by 2D VOF-PLIC simulations with the FLUENT code. Lai et al. (2010) studied the influence of liquid hydrophobicity and nozzle passage curvature in a drop ejection process with an oscillating nozzle plate with CFD-ACE+ and reported good agreement with experimental data. Fang et al. (2008) performed 3D PLIC-VOF simulations of liquid slugs which are formed by the inflow of water through a slit in the bottom of a rectangular microchannel (with a main air flow). They noted that for good agreement with the experiments it was essential to take into account contact line hysteresis, which is responsible for the slug elongation and the post-detachment instability.

Muradoglu's group used a FT method to study the buoyancy-driven motion, deformation and breakup in constricted sinusoidal channels, both for the 2D planar (Muradoglu and Gokaltun 2004) and axisymmetric case (Muradoglu and Kayaalp 2006; Olgac et al. 2006). Chung et al. (2008) investigated the effect of viscoelasticity on drop deformation and dynamics in a 5:1:5 contraction/expansion microchannel by a finite element FT method. The authors considered an Oldroyd-B model and studied a wide range of capillary and Deborah numbers; in a follow-up paper they extended the investigations to drop breakup (Chung et al. 2009).

Zhou et al. (2006) used a FE-based PF method with adaptive mesh refinement to simulate the breakup of simple and compound jets in flow focusing microfluidic devices and explored the flow regimes (dripping and jetting) that prevail in different parameter ranges. The authors addressed the influence of viscoelasticity and identified a narrow window of flow rate and viscosity ratio in which compound drops (double emulsions) can be achieved. De Menech (2006) used the PF method to investigate the droplet breakup in a microfluidic T-junction and reported that the critical value of the capillary number for droplet breakup depends on the viscosity ratio, see also De Menech et al. (2008) where the transition between different droplet formation mechanism was studied. Carlson et al. (2010) performed 3D PF simulations of droplet dynamics in a bifurcating channel and identified two distinct regimes (splitting and non-splitting) as the droplets interacted with the junction, see Fig. 5.

Zagnoni et al. (2010) showed experimentally and by 2D LS simulations with COMSOL that oil-water multiphase flow in a hydrophilic microfluidic T-junction has hysteresis. Namely, different flow patterns in the form of segmented flow and co-flowing phases could be obtained, depending on *Ca*, the volumetric flow rate ratio of the phases, and the history of the applied phase flow rates. Also, the transition mechanisms between the two states were analyzed. Yap et al. (2009) used the LS method and studied in 2D the influence of a temperature field (via

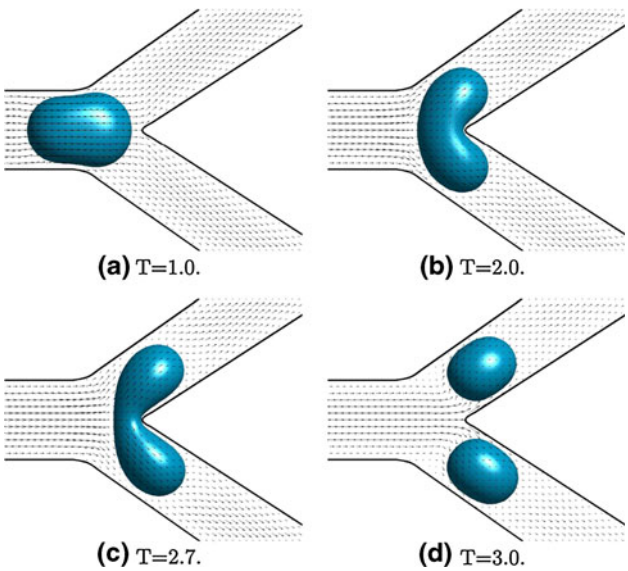

Fig. 5 Phase-field simulations of droplet dynamics in a square bifurcating channel in the splitting regime for four instants in time. Reprinted from Carlson et al. (2010) with permission from Elsevier

variable interfacial tension and phase viscosities) on droplet dynamics and breakup at a bifurcation.

3.1.3.2 Bubble formation Cubaud et al. (2005) investigated bubble formation by flow focusing in a 100 μm square channel experimentally and by 3D LS simulations. The numerical results for the bubble size were within the experimental scatter. Shao et al. (2008) studied the mechanism of Taylor bubble formation at the inlet of a 1 mm circular microchannel and the ensuing bubble size for very low superficial gas velocities using the CF-VOF method in CFX 4.3. They considered an axisymmetric co-flowing inlet configuration and investigated the influence of gas and liquid inlet velocities, liquid properties, contact angle, gas nozzle size and nozzle wall thickness. Simulated bubble sizes compared favorably with experimental data in a similar system. The authors reported that the geometry of the inlet had a significant influence on the size of the formed bubbles and slugs. A similar conclusion is drawn in Chen et al. (2009a), where the formation of Taylor bubbles in a nozzle/tube co-flow arrangement was investigated by a LS method. The authors reported that even under the same liquid and gas superficial velocities, the change of nozzle geometry alone could drastically change the size of Taylor bubbles and the pressure drop behavior inside the capillary.

For bubble formation in a T-junction, simulations with the VOF method in FLUENT became very popular since Qian and Lawal (2006) studied this problem for planar 2D minichannels, and are quite standard now both in 2D (Guo and Chen 2009) and in 3D (Dai et al. 2009). Also Santos and Kawaji (2010) used FLUENT to investigate the gas–liquid slug formation in a T-junction with nearly square microchannels of 113 μm hydraulic diameter. By comparison of the numerical results with experiments it is concluded that the code accurately captures the breakup physics while improvements need to be made in modeling the contact angle and contact line slip. These results, however, need a remark not made in that paper. The simulations are performed with a mesh spacing of 5.67 μm. For the range of capillary numbers simulated, this mesh size is much larger than the lateral thickness of the thin liquid film in Taylor flow, which is thus not resolved by the grid. Therefore, some mesh cells closest to the walls are not pure liquid cells but contain portions of both phases. As a consequence in these mesh cells a contact line was modeled numerically, whereas physically the wall is likely to be completely wetted. Chen et al. (2009a) used a LS method to investigate the formation of bubbles on an orifice plate with two kinds of moving contact line models. They found that the results obtained with a contact line velocity dependent model greatly depended on the prescribed maximum contact line velocity, whereas with the stick-slip model a parameter-independent prediction could be obtained provided the mesh was sufficiently fine.

In many of the applications mentioned so far, the computed bubble or drop shapes are in qualitative agreement with experiments. However, for many codes (especially commercial ones) a detailed quantitative validation by experimental data with respect to both the bubble/drop shape and the *local* flow field is still lacking. Recently, very detailed μPIV experiments on the bubble formation in a micro T-junction became available which show that the bubble pinch-off is triggered by a flow reversal (van Steijn et al. 2007, 2009). These data pose a good opportunity for detailed qualitative validation of numerical methods and computer codes.

3.1.3.3 Coalescence Topological changes such as breakup and coalescence are the result of the complex interplay of viscous, inertial, capillary, Marangoni, electrostatic and van der Waals forces (Cristini and Tan 2004). The timescales for coalescence and interface breakup are highly variable from fluid system to fluid system, depending not only on viscous drainage times but on both long-range (micro-scale) and short-range (nano-scale) electrostatic and molecular interactions. Coalescence is generally depicted as consisting of three consecutive steps: approach, drainage, and rupture. Coalescence of liquid droplets dispersed in an immiscible liquid matrix plays an important role in many industrial processes such as liquid–liquid extraction, emulsification, and polymer blending. Since coalescence involves droplet/bubble interactions, it is a more complex process than single droplet/bubble breakup, and hence more difficult to study both numerically and experimentally.

Both the standard PLIC-VOF and LS methods are not capable of representing multiple interfaces in a single computational mesh cell. When the interfaces of different drops/bubbles collide, they merge automatically, resulting in so-called numerical coalescence. In PLIC-VOF methods numerical coalescence occurs when the film thickness of approaching interfaces is smaller than the mesh size. Thus, there exists an artificial reconnection length (usually the mesh spacing) which is imposed by the grid. In methods where the interface has a small but finite thickness such as in the LB, CF-VOF, C-LS and PF method the interfaces of approaching drops overlap for a sufficient time during the collision so that the drops coalesce more easily than real drops. Jia et al. (2008) remarked that also LB simulations of drop collisions at low Reynolds numbers with the free energy and Shan–Chen model predicted coalescence at capillary numbers for which it has not been observed in experiments.

The front tracking method with its detailed control of the interface topology does not involve an artificial

reconnection length. Instead, it allows merging of the interfaces at prescribed film rupture time or film thickness (Nobari and Tryggvason 1996; Nobari et al. 1996). A transfer of this concept to the VOF method was presented by Nikolopoulos et al. (2009) who considered two VOF indicator functions in conjunction with adaptive local grid refinement in order to preserve the identity of each droplet until a prescribed coalescence time. Hardt (2005) implemented short-range interaction potentials between fluid interfaces in the VOF method in order to account for intermolecular forces. He considered two approaching micro droplets and demonstrated by 2D simulations with adaptive grid refinement that with this method quite different scenarios can be reproduced.

In order to prevent numerical coalescence without excessive local grid refinement, Coyajee and Boersma (2009) developed a multiple marker front-capturing CLSVOF method. In their method separate volumes of the same fluid are represented by a separate scalar marker function so that for the simulation of N drops, N different LS or VOF functions are used. Thus, the computational effort increases with the number of drops which actually limits the method to simulations of dispersions with a rather low number of fluid particles. While the results obtained with this method for test problems are very promising, the author is not aware of any detailed and experimentally validated numerical simulations of interfacial flows with colliding interfaces in microfluidic applications.

3.1.4 *Contact lines and geometrically or chemically patterned surfaces*

An attractive means to control the flow within microchannels is chemical or geometrical patterning of a surface (Zhao et al. 2001). Rapid developments in this area have led to a need to consider the capillary-driven flow of liquid within narrow channels or tubes that have varying cross sections or heterogeneous walls, which are chemically and/or topographically patterned. A chemically patterned wall not only leads to variations in the value of the static contact angle, but also changes the value of the slip coefficient in a slip boundary condition at the capillary wall. Experiments showed that the wetting properties of immiscible liquids crucially determine whether the flow pattern in the microchannel is regular or not and whether the drops move continuously with the main stream or intermittently adhere to the channel walls (Dreyfus et al. 2003).

Erickson et al. (2002) studied the wetting behavior of converging-diverging and diverging-converging capillaries numerically by an in-house FE code which uses an interface tracking procedure that is based on the predicted change in the total liquid volume to update the interface location. They found that the surface tension-driven flow is fastest in straight capillaries and any deviation in the capillary diameter along its length will slow down the wetting speed. Rosengarten et al. (2006) used the VOF method in CFD-ACE+ to study the effect of contact angle on droplet shape as it moves through a 4:1 contraction. They used a static contact angle in the range from 30° to 150° along with a method where the contact angle is treated within the surface tension model in the solver. The authors showed that under certain conditions contact forces will affect the shape and breakup of a droplet passing through a contraction. Low contact angles can induce droplet breakup while higher contact angles can form slugs with contact angle dependent shape.

Saha and Mitra (2009a) performed a 3D numerical (and experimental) study of the capillary filling of narrow microfluidics channel with integrated pillars. They used the VOF method in OpenFOAM and tested eight different models for the dynamic contact angle. While the dynamic contact angle models modified the transient response of the meniscus displacement, the different models had only a very small effect on the meniscus profile, so that the use of the static contact angle approach seems to be adequate for this application. In another paper, the same authors studied the capillary flow in a 100 μm high 2D microchannel with alternate hydrophilic-hydrophobic bottom wall using CFD-ACE+ (Saha and Mitra 2009b). Naraynan and Lakehal (2006) studied the filling of a microfluidic device with a LS method whereas Huang et al. (2006) used a PLIC-VOF method and considered capillary filling flows inside surface-patterned microchannels.

Villanueva and Amberg (2006) used the PF method of Jacqmin (2000) to investigate some basic wetting phenomena dominated by capillary forces. Kuksenok et al. (2003) studied the droplet formation in chemically patterned microchannels by a PF method. Di and Wang (2009) used the PF model in combination with a generalized Navier boundary conditions and a multi-mesh adaptive FE method and investigated wetting dynamics with focus on the development of the precursor film and the dissipation therein in the early stage of spreading.

There also exists a number of studies where the LB method is used to study wetting of droplets on a flat surface with heterogeneous wetting conditions (Dupuis and Yeomans 2004; Chang and Alexander 2006; Yan and Zu 2007; Huang et al. 2008) or the capillary rise between parallel plates (Wolf et al. 2010). In some references, the codes are validated by applying them to test problems with known analytical solution. Sbragaglia et al. (2006) investigated the wetting-dewetting transition of fluids in the presence of nanoscopic groves by a LB method. Mognetti and Yeomans (2009, 2010) used a free energy (diffuse interface) LB method to perform advanced simulations of the

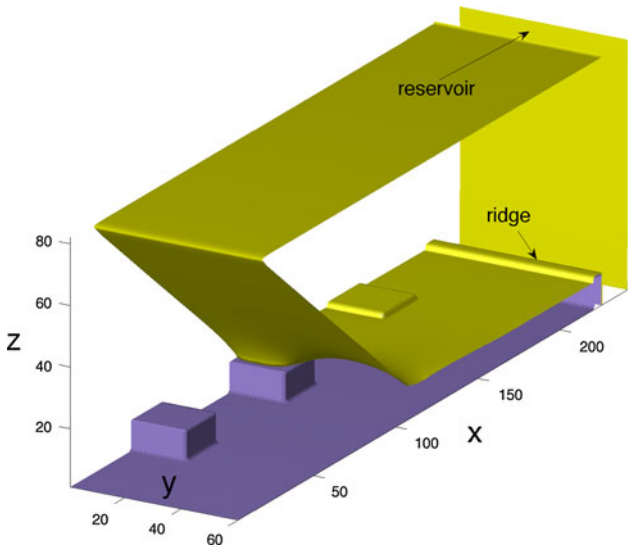

Fig. 6 Numerical simulation of the de-pinning of a receding contact line on a super-hydrophobic surface patterned by a regular array of posts with a free-energy LB method. Reprinted with permission from Mognetti and Yeomans (2010). Copyright 2010 by the American Chemical Society

capillary filling in microchannels patterned by square posts, and of receding contact lines on super-hydrophobic surfaces, see Fig. 6. It is shown that pinning on the edges of the posts can suppress and even halt capillary filling. As the contact angle of a fluid within a microchannel can rather easily be varied by applying an electrowetting potential, this opens the possibility of controlling fluid motion.

3.2 Heat and mass transfer and related issues

An obvious effect of shrinking a system to the millimeter scale and below is the large increase in surface area relative to volume, often by several orders of magnitude. For gas–liquid and liquid–liquid systems this allows for more efficient heat and mass transfer in microsystems since relatively more interfacial area is available for transfer to occur. Especially attractive is segmented two-phase flow because it enhances radial mixing in both phases while reducing axial dispersion in the continuous phase. Furthermore, multiphase microsystems enable highly exothermic gas–liquid or gas–liquid–solid reactions under well defined isothermal conditions.

3.2.1 Heat transfer without phase change

Gas–liquid two-phase flows without phase change are an interesting option for heat transfer enhancement in compact heat exchangers. The presence of gas bubbles separating neighboring liquid slugs causes a recirculation inside the liquid phase so that the overall wall heat transfer is enhanced with only moderate penalty of the pressure drop. Furthermore, such gas–liquid flows are rather stable due to an absence of explosive boiling.

Systematic numerical studies of the (axisymmetric) convective heat transfer of gas-liquid flows in circular micro tubes were performed by Kasagi and coworkers (Fukagata et al. 2007; He et al. 2010). Temperature was treated as passive scalar and a single flow unit cell with axially periodic boundary conditions was considered. In the first paper, the LS method was used to investigate the heat transfer in a 20 μm inner diameter pipe for constant wall heat flux boundary conditions, whereas in the second paper the PF method was used and the pipe diameter was 600 μm. The authors varied the Peclet number and the length of the liquid slug and found that the highest temperature was located at the rear of the gas bubble. The Nusselt number strongly depended on the flow pattern and was up to 2.4 times higher than that of a comparable single-phase laminar flow. The authors also investigated the influence of the number of grid nodes in the film region on the thickness of the liquid film. In the simulations the liquid film was resolved by at least six mesh cells and doubling the number of radial grid cells caused only a 2% change in the liquid film thickness.

Lakehal and coworkers (Lakehal et al. 2008; Narayanan and Lakehal 2008) studied the convective heat transfer in slug flow in 1 and 1.5 mm diameter pipes for a constant wall temperature boundary condition with a LS method. They found that the presence of gas bubbles increased the heat transfer three to four times above that for liquid flow only. Gupta et al. (2010) investigated the flow and heat transfer in gas–liquid Taylor flow within a 0.5 mm pipe by 2D axisymmetric simulations for constant wall heat flux and constant wall temperature boundary conditions. They compared results obtained with the PLIC-VOF method in FLUENT with those of LS computations with TransAT. Though the timing of break-off in the bubble formation process was slightly different, the final bubble sizes and shapes were similar. While the results of the TransAT code were considered to be more accurate, its simulations were also vastly more expensive. In agreement with other studies the computed Nusselt numbers were about 2.5 times higher than for liquid-only flow.

Urbant et al. (2008) used FLUENT to investigate droplet motion and forced heat transport in a droplet-laden laminar flow in a circular 1 mm pipe. In their 2D axisymmetric investigation they considered a train of equally spaced droplets of given size (diameter 400–700 μm) moving on the channel centerline. They found that the presence of drops considerably augmented the heat transfer and shortened the thermal entrance length as compared with single phase Poiseuille flow. This effect is attributed to the distortion of the uni-directional Poiseuille flow of the carrier

fluid (oil) by the translating water drops and the internal circulation within the drops.

3.2.2 Mixing and dispersion

For droplet based microfluidics and lab-on-chip systems in biological and chemical applications the efficiency of these devices to quickly achieve mixing within the drop is of great importance (Bringer et al. 2004). Also continuous phase mixing is of relevance for enhanced heat and mass transfer, homogenizations and chemical reactions. However, at small scales efficient mixing is more difficult to achieve because the familiar use of turbulence is unavailable. Aubin et al. (2010) presented a review of current experimental methods for characterizing mixing in single and two-phase flows in microchannels. It is stressed that the majority of the experimental techniques available for two-phase flows employ optical methods, which require that the micro device is transparent or has a transparent window. In the process industries, however, transparent construction materials may not be entirely adapted for the harsh environment of the chemical and physical processes encountered and these characterization methods may not be applicable, so that non-intrusive sensors that do not require optical access to the flow are required. While some development in this area has been started, as an alternative to experimental methods CFD simulations are attractive for characterizing mixing in two-phase flows in microdevices.

In order to numerically investigate the mixing inside disperse elements or the dispersion within the continuous phase, often the time evolution of passive Lagrangian tracer particles immersed within the respective phase is studied. Another possibility is to initialize a part of the phase by a passive tracer for which then an Eulerian convection equation or convection-diffusion equation is solved, see e.g. Sarrazin et al. (2006) and Tanthapanichakoon et al. (2006), respectively. Both approaches allow to quantify axial dispersion or to identify regions where mixing inside the disperse phase is poor. Schönfeld and Rensink (2003) used the Eulerian approach to investigate the internal flow pattern and fluid distribution during multi-fluid droplet formation of aqueous solutions at a mixing nozzle by the CF-VOF method in CFX 4.4. Depending on the geometry and flow rates, complex patterns inside the drop were found. In spite of the fine grids used, the authors remark that the results still suffer from numerical diffusion.

Several numerical investigations show that in straight circular channels recirculation regions may be present at the front and back of drops (Sarrazin et al. 2006; Blanchette 2009). These regions also exist inside bubbles in square channels for certain conditions (Ghidersa et al. 2004). Inside Taylor bubbles or drops these are the regions where mixing is poor and is mainly by diffusion (Sarrazin et al. 2006). Galusinski and Vigneaux (2008) used a LS method to study the mixing dynamics inside a confined bubble in a straight 2D channel by analyzing the streamline patterns in bubbles of various sizes. Tanthapanichakoon et al. (2006) investigated the mixing of reactants due to the recirculating flow inside an elongated drop of prescribed shape. They showed that axially arranged reactants give much faster mixing rates than radially arranged reactants, in agreement with experiments.

When a drop moves through a straight channel under laminar conditions, the flow within the drop is axisymmetric. To enhance mixing, meandering channels with constant cross-sectional area or channels with periodic variation of the cross-section area in the axial direction are often used so that the disperse element is subjected to a time-dependent shear. When the channel is curved, the symmetry is broken and the mixing within the droplet becomes chaotic. Muradoglu and Stone (2005) investigated the mixing in a drop moving through a serpentine channel by a 2D FT method. They found that the best mixing is obtained when the drop size is comparable with the channel width and when the viscosity of the drop phase fluid is small compared with that of the ambient phase. Blanchette (2009) showed by 2D planar simulations that in a sinusoidal channel cross-stream mixing in the drop is efficient, while streamwise mixing is hindered by the front and back recirculation regions. While such 2D studies can provide an insight in mixing phenomena, it is unclear in how far they reflect the mixing in real non-circular microchannels where the flow field is usually three-dimensional.

While mixing in the disperse phase is usually a desired effect, mixing in the continuous phase is sometimes unwanted since it can lead to axial dispersion. This is especially important for applications involving chemical reactions such as in tubular reactors where backmixing should be avoided. In segmented flow at low values of the capillary number a recirculation pattern exists in the liquid slug (Taylor 1961; Thulasidas et al. 1997; Abiev 2009) which results in good mixing, while axial dispersion is low because of the segmentation (Günther et al. 2004). Muradoglu et al. (2007) studied axial dispersion in the continuous phase in gas–liquid segmented flow within a straight narrow 2D channel by a FT method. The tracer was simulated by a large number of Lagrangian particles inserted in the liquid slug and molecular diffusion was modeled by the random walk of the tracer particles. The authors identified three characteristic dispersion regimes, depending on the Peclet number. In a follow-up paper, Muradoglu (2010) investigated the effects of alternating channel curvature and found that the axial dispersion in a serpentine channel is enhanced as compared with a straight one. Wörner et al. (2007) evaluated the diffusion-free liquid phase residence time distribution in Taylor flow through a square mini-

channel from 3D PLIC-VOF computations. The method relied on the uniform introduction of virtual tracer particles into the liquid phase, and the statistical evaluation of the time needed by any particle to travel a certain axial distance.

3.2.3 Mass transfer across the interface

Phases separated by a pinned interface and flowing either in concurrent or countercurrent laminar flow allow for highly efficient separation or solvent extraction (Aota et al. 2007). Also microfluidic droplet-based liquid–liquid extraction/purification processes are orders of magnitude faster than in non-miniaturized techniques (Mary et al. 2008). A literature survey on numerical investigations of mass transfer in two-fluid systems by interface resolving methods can be found in Onea et al. (2009). Here, we restrict ourselves to microfluidic applications. Constantinou and Gavriilidis (2010) investigated the CO_2 absorption in a microstructured mesh reactor with COMSOL. Their 2D reactor model was divided in three zones: the gas phase, the mesh, and the liquid phase. Chasanis et al. (2010) also used COMSOL but investigated the CO_2 absorption in a falling-film micro-contactor. In their 2D approach they proceeded in two steps. First, the steady position of the gas–liquid interface was identified by means of a LS method. Afterwards, the computational domain was subdivided into a gas-phase and a liquid-phase part, whereas the interface was fixed at the position determined previously. In each phase then the steady species transport equation was solved. At the interface, thermodynamical equilibrium and continuity of the component flux were assumed. Mary et al. (2008) solved the advection–diffusion equation within a circular droplet by a FE method for the case of a prescribed velocity field inside the drop (Hills vortex) and appropriate boundary conditions at the interface.

When both phases are in relative motion (such as in Taylor flow) concentration boundary layers develop close to the interface. In aqueous systems the Schmidt number $Sc \equiv \mu/\rho D$ has typically a value of 1000 or higher. Though the Reynolds number is low this results in very high values of the Peclet number. Then there is a narrow transition layer adjacent to the interface across which the species concentration varies rapidly. Without adaptive or very fine meshes near the moving interface, applications of numerical methods are limited to artificial small values of Sc in order to avoid the separation of spatial scales in the narrow transition layer and the need to accurately resolve them.

Raimondi et al. (2008) presented 2D simulations of mass transfer in liquid–liquid slug flow with a CF-VOF method. The Henry number was $H = 1$ and the values of Sc in the continuous and disperse phase were 1000 and 2000, respectively. The authors stated that even for the finest grid used in their study the numerical diffusion was in the same range as the molecular diffusion. This is an obvious consequence of the unresolved concentration boundary layers for these high values of Sc. Full 3D simulations of gas–liquid mass transfer in Taylor flow within square and rectangular microchannels with a PLIC-VOF method were presented in Onea et al. (2009) and Kececi et al. (2009), see Fig. 7. To adequately resolve the concentration boundary layer the authors used a value of $Sc = 0.8$ for the continuous phase and investigated the influence of the unit cell length, the liquid slug length, and the channel aspect ratio on mass transfer for two different values of H, namely 0.03 and 3.

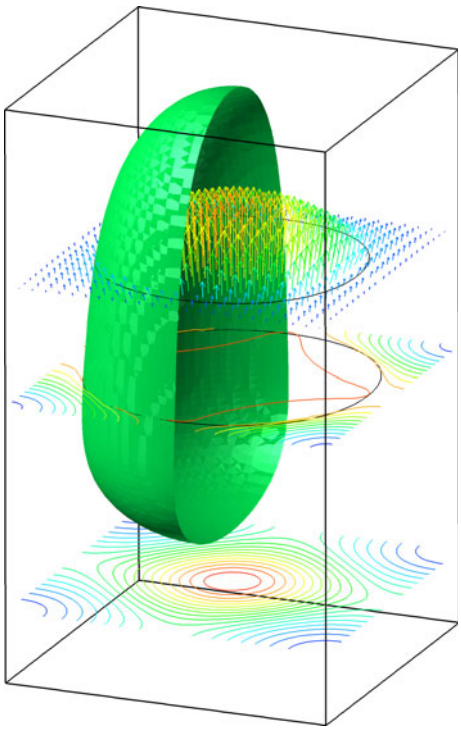

Fig. 7 PLIC-VOF computation of the gas–liquid mass transfer of a passive species in co-current upward Taylor flow within a square mini-channel. The figure shows the instantaneous velocity (vectors) and concentration (isolines) fields in certain axial cross-sections with half of bubble shape. Results from Onea et al. (2009)

3.2.4 Chemical reactions

For microfluidic applications, numerical investigations of multiphase mass transfer processes accompanied by chemical reactions are in general not very advanced and often rely on simplifying assumptions. When the interface is planar and its position in space is fixed the reaction-diffusion equations can be solved by standard single phase methods within each phase with appropriate coupling conditions at the interface. This approach has been adopted

e.g. for a T-shaped microreactor (Baroud et al. 2003) and for a membrane microreactor (Schuster et al. 2003). CFD computations of mass transfer accompanied by a very fast catalytic chemical reaction (hydrogenation of α-methylsterol) in a mesh microreactor were presented by Abdallah et al. (2006). Instead accounting for the mesh, which serves to stabilize the position of the gas–liquid interface, in the computation a continuous and flat interface was assumed. The species concentration at the interface was specified and only the concentration field in the liquid phase was computed. The numerical conversion rates were significantly lower than the measured ones. Haroun et al. (2010a, b) performed 2D CF-VOF simulations of non-reactive and reactive mass transfer in a falling film and of reactive absorption in gas–liquid flow on a structured zig-zag shaped packing. For the structured packing, mass transfer was increased as compared with that for a flat film.

Of special interest for certain chemical reactions is segmented gas–liquid flow. For synthesis of quantum dots, the reactants are dissolved in the continuous liquid phase and the gas bubbles serve to segment the liquid into plugs (Yen et al. 2005; Wang et al. 2010). Another example are multiphase monolithic reactors where the walls are coated by a catalytic washcoat (Kreutzer et al. 2005a). Such reactors operated in segmented flow are e.g. of interest for Fischer–Tropsch synthesis (Guettel et al. 2008). Onea et al. (2009) considered in their qualitative study on mass transfer in square channel Taylor flow (see above) also cases where the mass transfer is accompanied by a first-order homogeneous or heterogeneous chemical reaction. For a given gas holdup in the unit cell they found that short unit cells were more efficient for both, mass transfer with homogenous chemical reaction and without reaction. This is because for the conditions considered, the liquid film became quickly saturated so that the mass transfer occurred mainly through the bubble front and rear. For a fast heterogeneous reaction, it was instead found that long unit cells were more efficient since a sustained large concentration gradient persisted in the thin liquid film which separated the bubble and the catalytic wall.

3.2.5 *Marangoni effects and surfactants*

Surfactants influence the mobility of fluid interfaces and the magnitude of the hydrodynamic force that affects the probability of the film between the bubbles or drops to reach a critical thickness for rupture. They are therefore essential for the stabilization of emulsions produced e.g. by microfluidic devices. In the literature, there exist a large number of experimental, theoretical and numerical studies on drops covered by surfactants in extensional or shear flows, see e.g. Booty and Siegel (2010) and Feigl et al. (2007). However, only very few studies consider the effect of confinement, which is of relevance in microfluidics. Johnson and Borhan (2003) investigated the effects of surfactant solubility on pressure-driven drop motion through cylindrical capillaries in the Stokes flow regime by a BI method. Grotberg and coworkers solved the NS equations for the liquid phase with free-surface boundary conditions and the surfactant transport equation using a FV scheme in combination with a moving mesh, and performed detailed numerical studies of the steady propagation of a surfactant-laden liquid plug in a 2D narrow channel (Fujioka and Grotberg 2005; Zheng et al. 2007).

Zhang et al. (2006) investigated a deformable intravascular bubble in a tube with a soluble or insoluble surfactant. It is shown that the bubble motion in Poiseuille flow may be significantly slowed down due to the presence of a soluble surfactant in the bulk medium. For identical initial surface concentrations of the surfactant, the bubble motion was more retarded in the presence of a soluble than an insoluble surfactant. In the former case, the Marangoni induced motion was in a direction opposite to that driven by the bulk pressure. Lee and Pozrikidis (2006) studied the effects on insoluble surfactants on the deformation of drops and bubbles in a 2D channel and demonstrated the possibility of interface immobilization due to Marangoni tractions even for mild variations in the surfactant concentration (cf. the studies of Alke and Bothe (2009) and Lakshmanan and Ehrhard (2010) for freely rising bubbles).

Blanchette (2010) used a FT like front marker algorithm to perform numerical simulations of drops surrounded by a fluid of equal density and viscosity in an axisymmetric cylindrical tube. He investigated the mixing within drops due to surface tension variations and found that these may result in faster mixing than mixing due to geometric confinement. Though not directly related to microfluidics we refer to an interesting numerical study by Wegener et al. (2009) with STAR-CD, where full 3D simulations of interfacial mass transfer accompanied by Marangoni convection were performed for a single spherical droplet rising in a quiescent liquid. The computed time-dependent solute concentration in the drop compared well with experiments. The numerical results suggest that even for very low initial concentrations Marangoni convection generates complex convective flow patterns which enhance mass transfer significantly. The simulations furthermore revealed a sophisticated nonlinear interaction of concentration and velocity field due to Marangoni convection.

A major issue in direct methanol fuel cells is the removal of CO_2 bubbles at the anode side, which are generated there on oxidation of methanol. Together with the liquid methanol–water solution a two-phase flow forms which exhibits a slug/intermittent flow pattern for most current densities of interest. Fei et al. (2006) and Fei and Hong (2007) investigated the bubble transport in a micron-

sized channel by a 2D LB method. In a follow-up paper, they studied heat transfer including Marangoni effects due to a temperature dependent surface tension and found that bubbles moved more rapidly in a divergent microchannel than in a straight or convergent channel (Fei et al. 2008).

3.3 Phase change (boiling)

For flow boiling in microchannels significant experimental and theoretical progress has been made in recent years (Thome 2004; Kandlikar 2010). From the numerical side, however, there exist only a small number of interfacial simulation studies devoted to phase change phenomena in microchannels. All these concern boiling and the author is not aware of any such study concerning condensation. Mukherjee and Kandlikar (2005, 2009) studied the growth of a single vapor bubble during flow boiling of water in a square 200 μm wide channel by a LS method. The numerical bubble growth patterns were similar to experimental observations. However, the bubble growth rate (which increases with the incoming liquid superheat but decreases with Reynolds number) was quite different from the experimental data. In a more recent paper, Mukherjee (2009) investigated the influence of the dynamic contact angle for this configuration. Lee and Son (2008) employed the LS method of Son et al. (1999) and studied the effects of channel size, contact angle and wall superheat on the bubble growth and heat transfer from a bottom-heated rectangular microchannel. The wall heat flux was found to be negligible in the dry regions and maximum near the contact line, where the microlayer forms.

Kunkelmann and Stephan (2009) implemented the phase change model of Hardt and Wondra (2008) in the CF-VOF solver of OpenFOAM and simulated the growth and detachment of a single vapor bubble from a heated steel foil. The macroscopic CFD simulation was coupled with a microscopic model for the contact line evaporation via two variables, the local wall superheat (which is the input for the micro region model and is taken from the CFD simulations) and the heat transferred in the near contact line region (which is a boundary condition for the CFD simulation and is taken from the micro region model).

3.4 Beyond single channels

Applications of droplet-based microfluidics (digital microfluidics, Fair (2007)) involve the generation of sequences of mono-disperse droplets flowing in complex hydrodynamic networks, which consist of junctions connected by capillaries. The viscous dissipation introduced by the droplets alters the distribution of pressure in the capillary network and the path undertaken by any droplet depends on the positions of all other droplets in the network. As this process is nonlinear, even a simple system consisting of a channel that splits in two arms and subsequently recombines exhibits complex patterns of flow (Jousse et al. 2006). For applications such as lab-on-a-chip and high-throughput screening it is essential to predict and control the path of each droplet. This is the motivation for experimental, numerical, and theoretical investigations with the ultimate goal to develop simplified models to describe the "traffic" in the entire hydrodynamic network (Sessoms et al. 2009). In this context, Gleichmann et al. (2008) developed a toolkit for computational fluidic simulation and interactive parameterization of fluid networks with segmented flow. The computational toolkit is based on a network of fluidic nodes, which are interconnected by virtual fluid pipes for the transfer of segment streams. The particular behavior of a functional node may be given by user definable rules, which may be derived from experimental data and parameter studies of CFD simulations of the functional element.

A conceptually quite different approach for simulation of flow and heat transfer in complex microdevices is to consider the entire structure as a porous body. As the individual channels are not resolved by the grid, computations for devices consisting of hundreds or thousands of channels become feasible with limited amount of CPU time. However, the porous body approach fully relies on suitable empirical correlations to describe fluid friction and heat transfer. Imke (2004) used conventional pipe flow closure relations and investigated single and two-phase flow (boiling) in cross-flow and counter-flow micro heat exchangers. The predicted outlet temperatures and pressure drops were in rather good agreement with measurements for a wide range of flow rates.

4 Conclusions

From the various numerical methods presented in the first part of this review each has its own advantages and disadvantages. The volume-of-fluid method with interface reconstruction is attractive because of its ability to strictly conserve mass. However, piecewise linear interface calculation algorithms and geometric flux advection schemes are quite complex in three dimensions. Level set methods avoid explicit interface reconstruction but require special measures to reduce mass conservation errors to an acceptable value. Also level set methods are very flexible in treating topological changes without requiring manual or algorithmic intervention, an advantage that is shared to some extend by volume-of-fluid methods as well. However, both methods are at least in their standard versions not able to describe multiple interfaces within one mesh cell and thus impose an artificial reconnection length (with

size of one mesh cell). Front-tracking methods accurately describe the motion of multiple interfaces without imposing artificial coalescence but involve special complexity in its handling and that of breakup. In contrast to the aforementioned sharp interface methods, the interface thickness in the color function volume-of-fluid method and the conservative level set method is finite for numerical reasons. Special measures are required to maintain the interface thickness constant and uniform throughout the simulation. On the other hand these methods are attractive because they are rather easy to implement. Phase-field methods introduce a physically motivated amount of diffusion and allow for effective control of the interface thickness. Unlike the other methods mentioned above, the interface evolution is not governed by an advection equation but by the Cahn–Hilliard equation. This allows the simulation of flows with moving contact lines without difficulty. However, for accurate results the diffuse interface region must be well resolved. Lattice Boltzmann methods are mesoscopic in nature but can be considered as simple explicit discretization schemes for the Navier–Stokes equations. In recent years, various hybrid approached have been proposed. Widely used among them are only methods which combine the level set method with the interface reconstructing volume-of-fluid method.

Modeling of surface tension has reached a mature status in many methods. Spurious currents are, however, still an issue in many codes and methods though it is clear now, how numerical discretization schemes have to be designed to avoid them in combination with accurate curvature estimation algorithms. There, the trend is toward height function based methods, at least in the volume-of-fluid context. For modeling, the motion of moving contact lines no consensus is reached in many methods. This statement applies especially to sharp interface methods, where many ad-hoc solutions are proposed but none of them is generally accepted and widely used. The only exceptions are the phase-field and lattice Boltzmann approach which allow in a natural way for the inclusion of microscopic interactions. Both approaches have proved to be well suited for capillary-driven flow on chemically or geometrically patterned heterogeneous surfaces.

The formation of bubbles and drops can be described rather well by many methods. Since the underlying processes depend to large extend on the geometrical configuration of the inlet, CFD simulations constitute already a valuable and reliable tool to perform engineering design studies. Modeling of coalescence is much more subtle. In the Navier–Stokes equations the discontinuous density and viscosity fields are usually smoothed close to the interface over a distance of 2–3 mesh cells. Hence, local phenomena are not handled accurately when the interfaces come closer than 1–2 mesh cells and numerical coalescence often occurs.

Segmented flow with a perfectly wetting continuous phase can well be described by many methods. A considerable number of axisymmetric studies are already performed for channels with circular cross-section; many of them include convective heat transfer (without phase change). However, in microfluidic devices channels have often a square or rectangular cross-section so that three-dimensional computations are required. Though these are very CPU time intense some studies have already been performed and further are under way.

The modeling of surfactants and related Marangoni flows is an actual field of research and the status of numerical methods is advancing. Computations of soluble surfactants suffer from a separation of scales, as for realistic Schmidt and Peclet numbers the concentration boundary layer at a moving interface is much thinner than the viscous one. The same holds for species mass transfer across moving interfaces. There, the conjugate problem is even more complicated since the equilibrium distribution coefficient is often far from unity. The treatment of the discontinuous concentration field is a numerical challenge though promising modeling concepts are now emerging in the literature. Mixing and dispersion phenomena within one phase can well be studied numerically by inserting virtual tracers in a Lagrangian or Eulerian manner. Applications of interface resolving methods for two-fluid flows involving chemical reactions in microchannels or microreactors are in their infancy. The same holds for numerical studies on boiling in small channels, which are mostly qualitative in nature.

Overall, considerable progress has been made in the last decade in the development and improvement of different numerical methods for interfacial flow simulations. As an example we mention the PLIC-VOF method with balanced-force surface tension and quad/octree adaptive mesh refinement which makes the open source code Gerris (http://gfs.sourceforge.net) a powerful tool for numerical investigation of two-phase flows even when it undergoes large topological changes. It is very likely that the development of ever improved numerical methods will continue. While the proposal and testing of various variants and modifications of methods may be fruitful from an academic point of view, it partly hinders the advancement of engineering applications. These often rely on commercial computer codes where only widely accepted quasi-standard methods and models are implemented with a considerable lag in time. As a consequence many groups from academia use very advanced numerical methods and codes to study very fundamental applications, while engineering computations for complex technical problems are attacked by far less advanced and appropriate methods and codes. Also, it became a standard in academia to demonstrate the performance of any new method for artificial test problems

such as Zalesak's circle or similar exercises. While these numerical tests are of certain academic value, actually reference solutions to problems involving break-up and coalescence are required and there is a strong need for additional more *physical* test cases. Suitable detailed experimental data bases which allow for a sound physical validation of methods and models are missing and would be highly welcome.

A special focus should also be put on the development of multiscale methods which combine models valid at different length scales and account for the interaction between them. Here, the challenge lies in the development of methods that involve an appropriate level of detail, are computationally efficient and are at the same time robust in the sense that varying the mesh size (at least in a certain range) yields the same and correct grid-independent asymptotic solution. Such multiscale methods are especially required to account for very thin filaments, films and concentration boundary layers, moving contact lines and phenomena associated with the transport of surfactants on fluid interfaces.

In conclusion, understanding transport phenomena is essential for the successful development of microfluidic devices and microreactors. Various numerical methods for detailed simulations of interfacial two-phase flows are available and yield already valuable contributions. As their capabilities will be extended in the future, their role will further increase and may lead to highly integrated advanced multiphysics simulation tools for virtual development and prototyping of microfluidic devices and microreactors.

Acknowledgments The author acknowledges the support of Deutsche Forschungsgemeinschaft by grant WO 1682/1-1 within priority programme "Transport Processes at Fluidic Interfaces" (SPP 1506). He also thanks Prof. R. Sh. Abiev for initiating this review article.

References

Abdallah R, Magnico P, Fumey B, de Bellefon C (2006) CFD and kinetic methods for mass transfer determination in a mesh microreactor. AIChE J 52(6):2230–2237

Abiev RS (2009) Circulation and bypass modes of the slug flow of a gas–liquid mixture in capillaries. Theor Found Chem Eng 43(3):298–306

Abou-Hassan A, Sandre O, Cabuil V (2010) Microfluidics in inorganic chemistry. Angew Chem Int Edit 49(36):6268–6286

Adalsteinsson D, Sethian JA (1995) A fast level set method for propagating interfaces. J Comput Phys 118(2):269–277

Afkhami S, Bussmann M (2009) Height functions for applying contact angles to 3D VOF simulations. Int J Numer Methods Fluids 61(8):827–847

Afkhami S, Zaleski S, Bussmann M (2009) A mesh-dependent model for applying dynamic contact angles to VOF simulations. J Comput Phys 228(15):5370–5389

Ahn HT, Shashkov M (2007) Multi-material interface reconstruction on generalized polyhedral meshes. J Comput Phys 226(2):2096–2132

Ahn HT, Shashkov M (2009) Adaptive moment-of-fluid method. J Comput Phys 228(8):2792–2821

Aidun CK, Clausen JR (2010) Lattice-Boltzmann method for complex flows. Annu Rev Fluid Mech 42:439–472

Alke A, Bothe D (2009) 3D Numerical modeling of soluble surfactant at fluidic interfaces based on the volume-of-fluid method. FDMP 5(4):345–372

Alke A, Bothe D, Kröger M, Weigand B, Weirich D, Weking H (2010) Direct numerical simulation of high Schmidt number mass transfer from air bubbles rising in liquids using the volume-of-fluid-method. Ercoftac Bull 82:5–10

Amaya-Bower L, Lee T (2010) Single bubble rising dynamics for moderate Reynolds number using lattice Boltzmann method. Comput Fluids 39(7):1191–1207

Anderson DM, McFadden GB, Wheeler AA (1998) Diffuse-interface methods in fluid mechanics. Annu Rev Fluid Mech 30:139–165

Angeli P, Gavriilidis A (2008) Hydrodynamics of Taylor flow in small channels: a review. P I Mech Eng C-J Mec 222(5):737–751

Aota A, Nonaka M, Hibara A, Kitamori T (2007) Countercurrent laminar microflow for highly efficient solvent extraction. Angew Chem Int Edit 46(6):878–880

Aota A, Mawatari K, Kitamori T (2009) Parallel multiphase microflows: fundamental physics, stabilization methods and applications. Lab Chip 9(17):2470–2476

Atencia J, Beebe DJ (2005) Controlled microfluidic interfaces. Nature 437(7059):648–655

Aubin J, Ferrando M, Jiricny V (2010) Current methods for characterising mixing and flow in microchannels. Chem Eng Sci 65(6):2065–2093

Aulisa E, Manservisi S, Scardovelli R (2003) A mixed markers and volume-of-fluid method for the reconstruction and advection of interfaces in two-phase and free-boundary flows. J Comput Phys 188(2):611–639

Aulisa E, ManserviSi S, Scardovelli R (2006) A novel representation of the surface tension force for two-phase flow with reduced spurious currents. Comput Method Appl M 195(44–47):6239–6257

Aulisa E, Manservisi S, Scardovelli R, Zaleski S (2007) Interface reconstruction with least-squares fit and split advection in three-dimensional Cartesian geometry. J Comput Phys 225(2):2301–2319

Ausas RF, Dari EA, Buscaglia GC (2011) A geometric mass-preserving redistancing scheme for the level set function. Int J Numer Methods Fluids 65(8):989–1010

Badalassi VE, Ceniceros HD, Banerjee S (2003) Computation of multiphase systems with phase field models. J Comput Phys 190(2):371–397

Bänsch E (2001) Finite element discretization of the Navier–Stokes equations with a free capillary surface. Numer Math 88(2):203–235

Bao J, Yuan P, Schaefer L (2008) A mass conserving boundary condition for the lattice Boltzmann equation method. J Comput Phys 227(18):8472–8487

Baroud CN, Okkels F, Menetrier L, Tabeling P (2003) Reaction–diffusion dynamics: confrontation between theory and experiment in a microfluidic reactor. Phys Rev E 67(6):060104

Benson DJ (2002) Volume of fluid interface reconstruction methods for multi-material problems. Appl Mech Rev 55(2):151–165

Bhatnagar PL, Gross EP, Krook M (1954) A model for collision processes in gases 1. Small amplitude processes in charged and neutral one-component systems. Phys Rev 94(3):511–525

Bird RB, Stewart WE, Lightfoot EN (2007) Transport phenomena. 2nd rev. edn. Wiley, New York

Blanchette F (2009) Flow lines and mixing within drops in microcapillaries. Phys Rev E 80(6):066316

Blanchette F (2010) Simulation of mixing within drops due to surface tension variations. Phys Rev Lett 105(7):074501

Bonn D, Eggers J, Indekeu J, Meunier J, Rolley E (2009) Wetting and spreading. Rev Mod Phys 81(2):739–805

Bonometti T, Magnaudet J (2007) An interface-capturing method for incompressible two-phase flows. Validation and application to bubble dynamics. Int J Multiph Flow 33 (2):109–133

Booty MR, Siegel M (2010) A hybrid numerical method for interfacial fluid flow with soluble surfactant. J Comput Phys 229(10):3864–3883

Bothe D (2009) Calculations and simulations. In: Dietrich TR (ed) Microchemical engineering in practice. Wiley, Oxford, pp 165–184

Bothe D, Warnecke HJ (2007) Berechnung und Beurteilung strömungsbasierter komplex-laminarer Mischprozesse. Chem-Ing-Tech 79(7):1001–1014

Bothe D, Koebe M, Wielage K, Prüss J, Warnecke HJ (2004) Direct numerical simulation of mass transfer between rising gas bubbles and water. In: Sommerfeld M (ed) Bubbly flows. Analysis, modelling and calculation. Springer, Berlin, pp 159–174

Bothe D, Kröger M, Alke A, Warnecke H-J (2009a) VOF-based simulation of conjugate mass transfer from freely moving fluid particles. In: Mammoli AA, Brebbia CA (eds) Computational methods in multiphase flow V. WIT Press, Southampton, pp 157–168

Bothe D, Kröger M, Alke A, Warnecke HJ (2009b) VOF-based simulation of reactive mass transfer across deformable interfaces. Prog Comput Fluid Dyn 9(6–7):325–331

Bothe D, Kröger M, Warnecke HJ (2011) A VOF-based conservative method for the simulation of reactive mass transfer from rising bubbles. FDMP 7(3):303–316

Boyer F (2002) A theoretical and numerical model for the study of incompressible mixture flows. Comput Fluids 31(1):41–68

Brackbill JU, Kothe DB, Zemach C (1992) A continuum method for modeling surface tension. J Comput Phys 100(2):335–354

Bringer MR, Gerdts CJ, Song H, Tice JD, Ismagilov RF (2004) Microfluidic systems for chemical kinetics that rely on chaotic mixing in droplets. Philos T Roy Soc A 362(1818):1087–1104

Bruus H (2008) Theoretical microfluidics. Oxford master series in physics, vol 18. Oxford University Press, Oxford

Carlson A, Do-Quang M, Amberg G (2010) Droplet dynamics in a bifurcating channel. Int J Multiph Flow 36(5):397–405

Casey M, Wintergerste T (2000) Best practice guidelines for industrial computational fluid dynamics of single-phase flows. ERCOFTAC

Ceniceros HD (2003) The effects of surfactants on the formation and evolution of capillary waves. Phys Fluids 15(1):245–256

Ceniceros HD, Roma AM (2007) A nonstiff, adaptive mesh refinement-based method for the Cahn–Hilliard equation. J Comput Phys 225(2):1849–1862

Ceniceros HD, Roma AM, Silveira-Neto A, Villar MM (2010) A robust, fully adaptive hybrid level-set/front-tracking method for two-phase flows with an accurate surface tension computation. Commun Comput Phys 8(1):51–94

Cervone A, Manservisi S, Scardovelli R, Zaleski S (2009) A geometrical predictor–corrector advection scheme and its application to the volume fraction function. J Comput Phys 228(2):406–419

Chang QM, Alexander JID (2006) Analysis of single droplet dynamics on striped surface domains using a lattice Boltzmann method. Microfluid Nanofluid 2(4):309–326

Chang YC, Hou TY, Merriman B, Osher S (1996) A level set formulation of Eulerian interface capturing methods for incompressible fluid flows. J Comput Phys 124(2):449–464

Chao J, Mei R, Singh R, Shyy W (2011) A filter-based, mass-conserving lattice Boltzmann method for immiscible multiphase flows. Int J Numer Methods Fluids 66(5):622–647

Chasanis P, Lautenschleger A, Kenig EY (2010) Numerical investigation of carbon dioxide absorption in a falling-film microcontactor. Chem Eng Sci 65(3):1125–1133

Chatzikyriakou D, Walker SP, Hewitt GF, Narayanan C, Lakehal D (2009) Comparison of measured and modelled droplet-hot wall interactions. Appl Therm Eng 29(7):1398–1405

Chen S, Doolen GD (1998) Lattice Boltzmann method for fluid flows. Annu Rev Fluid Mech 30:329–364

Chen Y, Kulenovic R, Mertz R (2009a) Numerical study on the formation of Taylor bubbles in capillary tubes. Int J Therm Sci 48(2):234–242

Chen YP, Zhang CB, Shi MH, Peterson GP (2009b) Role of surface roughness characterized by fractal geometry on laminar flow in microchannels. Phys Rev E 80(2):026301

Cheng M, Hua J, Lou J (2010) Simulation of bubble–bubble interaction using a lattice Boltzmann method. Comput Fluids 39(2):260–270

Chung TJ (2002) Computational fluid dynamics. Cambridge University Press, Cambridge

Chung C, Hulsen MA, Kim JM, Ahn KH, Lee SJ (2008) Numerical study on the effect of viscoelasticity on drop deformation in simple shear and 5:1:5 planar contraction/expansion microchannel. J Non-Newton Fluid Mech 155(1–2):80–93

Chung C, Kim JM, Hulsen MA, Ahn KH, Lee SJ (2009) Effect of viscoelasticity on drop dynamics in 5:1:5 contraction/expansion microchannel flow. Chem Eng Sci 64(22):4515–4524

Compère G, Marchandise E, Remacle J-F (2008) Transient adaptivity applied to two-phase incompressible flows. J Comput Phys 227(3):1923–1942

Constantinou A, Gavriilidis A (2010) CO_2 absorption in a micro-structured mesh reactor. Ind Eng Chem Res 49(3):1041–1049

Cox RG (1986) The dynamics of the spreading of liquids on a solid-surface. 1. Viscous-flow. J Fluid Mech 168:169–194

Coyajee E, Boersma BJ (2009) Numerical simulation of drop impact on a liquid–liquid interface with a multiple marker front-capturing method. J Comput Phys 228(12):4444–4467

Cristini V, Tan Y-C (2004) Theory and numerical simulation of droplet dynamics in complex flows-a review. Lab Chip 4(4):257–264

Croce G, D'Agaro P (2005) Numerical simulation of roughness effect on microchannel heat transfer and pressure drop in laminar flow. J Phys D Appl Phys 38(10):1518–1530

Crowe CT, Sommerfeld M, Tsuji Y (1998) Multiphase flows with droplets and particles. CRC Press, Boca Raton

Cubaud T, Tatineni M, Zhong XL, Ho CM (2005) Bubble dispenser in microfluidic devices. Phys Rev E 72(3):037302

Cummins SJ, Francois MM, Kothe DB (2005) Estimating curvature from volume fractions. Comput Struct 83(6–7):425–434

Dai L, Cai WF, Xin F (2009) Numerical study on bubble formation of a gas–liquid flow in a T-junction microchannel. Chem Eng Technol 32(12):1984–1991

Davidson MR, Harvie DJE (2007) Predicting the effect of interfacial flow of insoluble surfactant on the deformation of drops rising in a liquid. ANZIAM J 48:C661–C676

Davidson MR, Rudman M (2002) Volume-of-fluid calculation of heat or mass transfer across deforming interfaces in two-fluid flow. Numer Heat Tr B-Fund 41(3–4):291–308

Davidson MR, Harvie DJE, Cooper-White JJ (2005) Flow focusing in microchannels. ANZIAM J 46 (E):C47–C58

Davis RH, Schonberg JA, Rallison JM (1989) The lubrication force between two viscous drops. Phys Fluids A 1(1):77–81
De Menech M (2006) Modeling of droplet breakup in a microfluidic T-shaped junction with a phase-field model. Phys Rev E 73(3):031505
De Menech M, Garstecki P, Jousse F, Stone HA (2008) Transition from squeezing to dripping in a microfluidic T-shaped junction. J Fluid Mech 595:141–161
de Sousa FS, Mangiavacchi N, Nonato LG, Castelo A, Tomé MF, Ferreira VG, Cuminato JA, McKee S (2004) A front-tracking/front-capturing method for the simulation of 3D multi-fluid flows with free surfaces. J Comput Phys 198(2):469–499
Di Carlo D (2009) Inertial microfluidics. Lab Chip 9(21):3038–3046
Di Carlo D, Irimia D, Tompkins RG, Toner M (2007) Continuous inertial focusing, ordering, and separation of particles in microchannels. P Natl Acad Sci USA 104(48):18892–18897
Di Y, Wang X-P (2009) Precursor simulations in spreading using a multi-mesh adaptive finite element method. J Comput Phys 228(5):1380–1390
Dietrich TR (2009) Microchemical engineering in practice. Wiley, Oxford
Dijkhuizen W, Roghair I, Annaland MVS, Kuipers JAM (2010) DNS of gas bubbles behaviour using an improved 3D front tracking model—model development. Chem Eng Sci 65(4):1427–1437
Ding H, Spelt PDM (2007) Inertial effects in droplet spreading: a comparison between diffuse-interface and level-set simulations. J Fluid Mech 576:287–296
Ding H, Spelt PDM, Shu C (2007) Diffuse interface model for incompressible two-phase flows with large density ratios. J Comput Phys 226(2):2078–2095
Ding L, Shu C, Ding H, Zhao N (2010) Stencil adaptive diffuse interface method for simulation of two-dimensional incompressible multiphase flows. Comput Fluids 39(6):936–944
Diwakar SV, Das SK, Sundararajan T (2009) A quadratic spline based interface (QUASI) reconstruction algorithm for accurate tracking of two-phase flows. J Comput Phys 228(24):9107–9130
Doku GN, Verboom W, Reinhoudt DN, van den Berg A (2005) On-microchip multiphase chemistry—a review of microreactor design principles and reagent contacting modes. Tetrahedron 61(11):2733–2742
Drew DA (1983) Mathematical-modeling of two-phase flow. Annu Rev Fluid Mech 15:261–291
Drew DA, Passman SL (1999) Theory of multicomponent fluids. Springer, New York
Dreyfus R, Tabeling P, Willaime H (2003) Ordered and disordered patterns in two-phase flows in microchannels. Phys Rev Lett 90(14):144505
Drumright-Clarke MA, Renardy Y (2004) The effect of insoluble surfactant at dilute concentration on drop breakup under shear with inertia. Phys Fluids 16(1):14–21
Dupin MM, Halliday I, Care CM (2006) Simulation of a microfluidic flow-focusing device. Phys Rev E 73(5):055701
Dupont J-B, Legendre D (2010) Numerical simulation of static and sliding drop with contact angle hysteresis. J Comput Phys 229(7):2453–2478
Dupuis A, Yeomans JM (2004) Lattice Boltzmann modelling of droplets on chemically heterogeneous surfaces. Future Gener Comp Syst 20(6):993–1001
Dussan EB (1979) Spreading of liquids on solid-surfaces—static and dynamic contact lines. Annu Rev Fluid Mech 11:371–400
Dziuk G (1991) An algorithm for evolutionary surfaces. Numer Math 58(6):603–611
Ehrfeld W, Hessel V, Löwe H (2000) Microreactors: new technology for modern chemistry. Wiley, Chichester
Enright D, Fedkiw R, Ferziger J, Mitchell I (2002) A hybrid particle level set method for improved interface capturing. J Comput Phys 183(1):83–116
Enright D, Losasso F, Fedkiw R (2005) A fast and accurate semi-Lagrangian particle level set method. Comput Struct 83(6–7):479–490
Erickson D (2005) Towards numerical prototyping of labs-on-chip: modeling for integrated microfluidic devices. Microfluid Nanofluid 1(4):301–318
Erickson D, Li D, Park CB (2002) Numerical simulations of capillary-driven flows in nonuniform cross-sectional capillaries. J Colloid Interf Sci 250(2):422–430
Fair RB (2007) Digital microfluidics: is a true lab-on-a-chip possible? Microfluid Nanofluid 3(3):245–281
Fang C, Hidrovo C, Wang F-M, Eaton J, Goodson K (2008) 3-D numerical simulation of contact angle hysteresis for microscale two phase flow. Int J Multiph Flow 34(7):690–705
Farhat H, Choi W, Lee JS (2010) Migrating multi-block lattice Boltzmann model for immiscible mixtures: 3D algorithm development and validation. Comput Fluids 39(8):1284–1295
Fedkiw RP, Aslam T, Merriman B, Osher S (1999) A non-oscillatory Eulerian approach to interfaces in multimaterial flows (the ghost fluid method). J Comput Phys 152(2):457–492
Fei K, Hong CW (2007) All-angle removal of CO2 bubbles from the anode microchannels of a micro fuel cell by lattice-Boltzmann simulation. Microfluid Nanofluid 3(1):77–88
Fei K, Cheng CH, Hong CW (2006) Lattice Boltzmann simulations of CO2 bubble dynamics at the anode of a μDMFC. J Fuel Cell Sci Tech 3(2):180–187
Fei K, Chen WH, Hong CW (2008) Microfluidic analysis of CO_2 bubble dynamics using thermal lattice-Boltzmann method. Microfluid Nanofluid 5(1):119–129
Feigl K, Megias-Alguacil D, Fischer P, Windhab EJ (2007) Simulation and experiments of droplet deformation and orientation in simple shear flow with surfactants. Chem Eng Sci 62(12):3242–3258
Ferziger JH, Peric M (2002) Computational methods for fluid dynamics, 3rd edn. Springer, Berlin
Fletcher DF, Haynes BS, Aubin J, Xuereb C (2009) Modelling of microfluidic devices. In: Hessel V, Renken A, Schouten JC, Yoshida J (eds) Micro process engineering, vol 1., Fundamentals, operations and catalysts. Wiley, Weinheim, pp 117–144
Francois M, Shyy W (2003) Computations of drop dynamics with the immersed boundary method, Part 2: drop impact and heat transfer. Numer Heat Tr B-Fund 44(2):119–143
Francois MM, Swartz BK (2010) Interface curvature via volume fractions, heights, and mean values on nonuniform rectangular grids. J Comput Phys 229(3):527–540
Francois MM, Cummins SJ, Dendy ED, Kothe DB, Sicilian JM, Williams MW (2006) A balanced-force algorithm for continuous and sharp interfacial surface tension models within a volume tracking framework. J Comput Phys 213(1):141–173
Fujioka H, Grotberg JB (2005) The steady propagation of a surfactant-laden liquid plug in a two-dimensional channel. Phys Fluids 17(8):082102
Fukagata K, Kasagi N, Ua-arayaporn P, Himeno T (2007) Numerical simulation of gas–liquid two-phase flow and convective heat transfer in a micro tube. Int J Heat Fluid Flow 28(1):72–82
Fukai J, Shiiba Y, Yamamoto T, Miyatake O, Poulikakos D, Megaridis CM, Zhao Z (1995) Wetting effects on the spreading of a liquid droplet colliding with a flat surface—experiment and modeling. Phys Fluids 7(2):236–247
Fuster D, Agbaglah G, Josserand C, Popinet S, Zaleski S (2009) Numerical simulation of droplets, bubbles and waves: state of the art. Fluid Dyn Res 41(6):065001

Gada VH, Sharma A (2009) On derivation and physical interpretation of level set method-based equations for two-phase flow simulations. Numer Heat Tr B-Fund 56(4):307–322

Gad-el-Hak M (1999) The fluid mechanics of microdevices—the Freeman scholar lecture. J Fluids Eng 121(1):5–33

Galusinski C, Vigneaux P (2008) On stability condition for bifluid flows with surface tension: Application to microfluidics. J Comput Phys 227(12):6140–6164

Ganesan S, Tobiska L (2008) An accurate finite element scheme with moving meshes for computing 3D-axisymmetric interface flows. Int J Numer Methods Fluids 57(2):119–138

Ganesan S, Tobiska L (2009a) A coupled arbitrary Lagrangian–Eulerian and Lagrangian method for computation of free surface flows with insoluble surfactants. J Comput Phys 228(8):2859–2873

Ganesan S, Tobiska L (2009b) Modelling and simulation of moving contact line problems with wetting effects. Comput Visual Sci 12(7):329–336

Garstecki P, Fuerstman MJ, Stone HA, Whitesides GM (2006) Formation of droplets and bubbles in a microfluidic T-junction-scaling and mechanism of break-up. Lab Chip 6(3):437–446

Gerlach D, Tomar G, Biswas G, Durst F (2006) Comparison of volume-of-fluid methods for surface tension-dominant two-phase flows. Int J Heat Mass Transfer 49(3–4):740–754

Germann TC, Kadau K (2008) Trillion-atom molecular dynamics becomes a reality. Int J Mod Phys C 19(9):1315–1319

Geschke O, Klank H, Telleman P (2008) Microsystem engineering of lab-on-a-chip devices, 2nd edn. Wiley, Weinheim

Ghidersa BE, Wörner M, Cacuci DG (2004) Exploring the flow of immiscible fluids in a square vertical mini-channel by direct numerical simulation. Chem Eng J 101(1–3):285–294

Gibou F, Chen L, Nguyen D, Banerjee S (2007) A level set based sharp interface method for the multiphase incompressible Navier–Stokes equations with phase change. J Comput Phys 222(2):536–555

Ginzburg I, Wittum G (2001) Two-phase flows on interface refined grids modeled with VOF, staggered finite volumes, and spline interpolants. J Comput Phys 166(2):302–335

Glatzel T, Litterst C, Cupelli C, Lindemann T, Moosmann C, Niekrawietz R, Streule W, Zengerle R, Koltay P (2008) Computational fluid dynamics (CFD) software tools for microfluidic applications—a case study. Comput Fluids 37(3):218–235

Gleichmann N, Malsch D, Kielpinski M, Rossak W, Mayer G, Henkel T (2008) Toolkit for computational fluidic simulation and interactive parametrization of segmented flow based fluidic networks. Chem Eng J 135:S210–S218

Gomez FA (2008) Biological applications of microfluidics. Wiley, Hoboken

Gomez P, Hernandez J, Lopez J (2005) On the reinitialization procedure in a narrow-band locally refined level set method for interfacial flows. Int J Numer Methods Eng 63(10):1478–1512

Greaves D (2004) A quadtree adaptive method for simulating fluid flows with moving interfaces. J Comput Phys 194(1):35–56

Groß S, Reusken A (2007) An extended pressure finite element space for two-phase incompressible flows with surface tension. J Comput Phys 224(1):40–58

Groß S, Reusken A (2011) Numerical methods for two-phase incompressible flows. Springer, Heidelberg

Groß S, Reichelt V, Reusken A (2006) A finite element based level set method for two-phase incompressible flows. Comput Visual Sci 9(4):239–257

Gu H, Duits MHG, Mugele F (2011) Droplets formation and merging in two-phase flow microfluidics. Int J Mol Sci 12(4):2572–2597

Gubbins KE, Moore JD (2010) Molecular modeling of matter: impact and prospects in engineering. Ind Eng Chem Res 49(7):3026–3046

Guettel R, Knochen J, Kunz U, Kassing M, Turek T (2008) Preparation and catalytic evaluation of cobalt-based monolithic and powder catalysts for Fischer–Tropsch synthesis. Ind Eng Chem Res 47(17):6589–6597

Gueyffier D, Li J, Nadim A, Scardovelli R, Zaleski S (1999) Volume-of-fluid interface tracking with smoothed surface stress methods for three-dimensional flows. J Comput Phys 152(2):423–456

Gunstensen AK, Rothman DH, Zaleski S, Zanetti G (1991) Lattice Boltzmann model of immiscible fluids. Phys Rev A 43(8):4320–4327

Günther A, Jensen KF (2006) Multiphase microfluidics: from flow characteristics to chemical and materials synthesis. Lab Chip 6(12):1487–1503

Günther A, Kreutzer MT (2009) Multiphase flow. In: Hessel V, Renken A, Schouten JC, Yoshida J (eds) Micro process engineering, vol 1., Fundamentals, operations and catalystsWiley, Weinheim, pp 3–40

Günther A, Khan SA, Thalmann M, Trachsel F, Jensen KF (2004) Transport and reaction in microscale segmented gas–liquid flow. Lab Chip 4(4):278–286

Guo F, Chen B (2009) Numerical study on Taylor bubble formation in a micro-channel T-junction using VOF method. Microgravity Sci Technol 21:51–58

Gupta A, Murshed SMS, Kumar R (2009a) Droplet formation and stability of flows in a microfluidic T-junction. Appl Phys Lett 94(16):164107

Gupta R, Fletcher DF, Haynes BS (2009b) On the CFD modelling of Taylor flow in microchannels. Chem Eng Sci 64(12):2941–2950

Gupta R, Fletcher DF, Haynes BS (2010) CFD modelling of flow and heat transfer in the Taylor flow regime. Chem Eng Sci 65(6):2094–2107

Hagedorn JG, Martys NS, Douglas JF (2004) Breakup of a fluid thread in a confined geometry: droplet-plug transition, perturbation sensitivity, and kinetic stabilization with confinement. Phys Rev E 69(5):056312

Haj-Hariri H, Shi Q, Borhan A (1997) Thermocapillary motion of deformable drops at finite Reynolds and Marangoni numbers. Phys Fluids 9(4):845–855

Hao L, Cheng P (2009) Lattice Boltzmann simulations of liquid droplet dynamic behavior on a hydrophobic surface of a gas flow channel. J Power Sources 190(2):435–446

Hao Y, Prosperetti A (2004) A numerical method for three-dimensional gas–liquid flow computations. J Comput Phys 196(1):126–144

Hardt S (2005) An extended volume-of-fluid method for micro flows with short-range interactions between fluid interfaces. Phys Fluids 17(10):100601

Hardt S, Wondra F (2008) Evaporation model for interfacial flows based on a continuum-field representation of the source terms. J Comput Phys 227(11):5871–5895

Harlow FH, Welch JE (1965) Numerical calculation of time-dependent viscous incompressible flow of fluid with free surface. Phys Fluids 8(12):2182–2189

Haroun Y, Legendre D, Raynal L (2010a) Direct numerical simulation of reactive absorption in gas–liquid flow on structured packing using interface capturing method. Chem Eng Sci 65(1):351–356

Haroun Y, Legendre D, Raynal L (2010b) Volume of fluid method for interfacial reactive mass transfer: application to stable liquid film. Chem Eng Sci 65(10):2896–2909

Hartman RL, Jensen KF (2009) Microchemical systems for continuous-flow synthesis. Lab Chip 9(17):2495–2507

Hartmann D, Meinke M, Schröder W (2008) Differential equation based constrained reinitialization for level set methods. J Comput Phys 227(14):6821–6845

Hartmann D, Meinke M, Schröder W (2010a) The constrained reinitialization equation for level set methods. J Comput Phys 229(5):1514–1535

Hartmann D, Meinke M, Schröder W (2010b) On accuracy and efficiency of constrained reinitialization. Int J Numer Methods Fluids 63(11):1347–1358

Harvie DJE, Fletcher DF (2000) A new volume of fluid advection algorithm: the stream scheme. J Comput Phys 162(1):1–32

Harvie DJE, Fletcher DF (2001) A new volume of fluid advection algorithm: the defined donating region scheme. Int J Numer Methods Fluids 35(2):151–172

Harvie DJE, Davidson MR, Cooper-White JJ, Rudman M (2006a) A parametric study of droplet deformation through a microfluidic contraction: Low viscosity Newtonian droplets. Chem Eng Sci 61(15):5149–5158

Harvie DJE, Davidson MR, Rudman M (2006b) An analysis of parasitic current generation in volume of fluid simulations. Appl Math Model 30(10):1056–1066

Harvie DJE, Davidson MR, Cooper-White JJ, Rudman M (2007) A parametric study of droplet deformation through a microfluidic contraction: shear thinning liquids. Int J Multiph Flow 33(5):545–556

Harvie DJE, Cooper-White JJ, Davidson MR (2008) Deformation of a viscoelastic droplet passing through a microfluidic contraction. J Non-Newton Fluid Mech 155(1–2):67–79

Haverkamp V, Hessel V, Löwe H, Menges G, Warnier MJF, Rebrov EV, de Croon MHJM, Schouten JC, Liauw MA (2006) Hydrodynamics and mixer-induced bubble formation in micro bubble columns with single and multiple-channels. Chem Eng Technol 29(9):1015–1026

Hayashi K, Sou A, Tomiyama A (2006) A volume tracking method based on non-uniform subcells and continuum surface force model using a local level set function. Comput Fluid Dyn J 15(2):225–232

He QW, Kasagi N (2008) Phase-Field simulation of small capillary-number two-phase flow in a microtube. Fluid Dyn Res 40(7–8):497–509

He QW, Hasegawa Y, Kasagi N (2010) Heat transfer modelling of gas–liquid slug flow without phase change in a micro tube. Int J Heat Fluid Flow 31(1):126–136

Herrmann M (2008) A balanced force refined level set grid method for two-phase flows on unstructured flow solver grids. J Comput Phys 227(4):2674–2706

Herwig H, Gloss D, Wenterodt T (2010) Flow in channels with rough walls—old and new concepts. Heat Transfer Eng 31(8):658–665

Hessel V, Hardt S, Löwe H (2004) Chemical micro process engineering: fundamentals, modelling and reactions. Wiley, Weinheim

Hessel V, Angeli P, Gavriilidis A, Löwe H (2005) Gas–liquid and gas–liquid–solid microstructured reactors: contacting principles and applications. Ind Eng Chem Res 44(25):9750–9769

Hessel V, Renken A, Schouten JC, Yoshida J (2009) Micro process engineering: a comprehensive handbook. Wiley, Weinheim

Heyes DM, Baxter J, Tuzun U, Qin RS (2004) Discrete-element method simulations: from micro to macro scales. Philos T Roy Soc A 362(1822):1853–1865

Hirsch C (2007) Numerical computation of internal and external flows: fundamentals of computational fluid dynamics, 2nd edn. Butterworth-Heinemann, Amsterdam

Hirt CW, Nichols BD (1981) Volume of fluid (VOF) method for the dynamics of free boundaries. J Comput Phys 39(1):201–225

Hirt CW, Amsden AA, Cook JL (1974) Arbitrary Lagrangian–Eulerian computing method for all flow speeds. J Comput Phys 14(3):227–253

Hu HH, Patankar NA, Zhu MY (2001) Direct numerical simulations of fluid–solid systems using the arbitrary Lagrangian–Eulerian technique. J Comput Phys 169(2):427–462

Huang W, Russell RD (2011) Adaptive moving mesh methods. Springer, New York

Huang H, Liang D, Wetton B (2004) Computation of a moving drop/bubble on a solid surface using a front-tracking method. Commun Math Sci 2(4):535–552

Huang WF, Liu QS, Li Y (2006) Capillary filling flows inside patterned-surface microchannels. Chem Eng Technol 29(6):716–723

Huang JJ, Shu C, Chew YT (2008) Numerical investigation of transporting droplets by spatiotemporally controlling substrate wettability. J Colloid Interf Sci 328(1):124–133

Huebner A, Sharma S, Srisa-Art M, Hollfelder F, Edel JB, deMello AJ (2008) Microdroplets: a sea of applications? Lab Chip 8(8):1244–1254

Huh C, Scriven LE (1971) Hydrodynamic model of steady movement of a solid/liquid/fluid contact line. J Colloid Interf Sci 35(1):85–101

Hysing S (2006) A new implicit surface tension implementation for interfacial flows. Int J Numer Methods Fluids 51(6):659–672

Hysing S, Turek S, Kuzmin D, Parolini N, Burman E, Ganesan S, Tobiska L (2009) Quantitative benchmark computations of two-dimensional bubble dynamics. Int J Numer Methods Fluids 60(11):1259–1288

Imke U (2004) Porous media simplified simulation of single- and two-phase flow heat transfer in micro-channel heat exchangers. Chem Eng J 101(1–3):295–302

Inamuro T, Ogata T, Tajima S, Konishi N (2004) A lattice Boltzmann method for incompressible two-phase flows with large density differences. J Comput Phys 198(2):628–644

Ishii M (1975) Thermo-fluid dynamic theory of two-phase flow. Eyrolles, Paris

Ishii M, Hibiki T (2006) Thermo-fluid dynamics of two-phase flow. Springer, New York

Jacqmin D (1999) Calculation of two-phase Navier–Stokes flows using phase-field modeling. J Comput Phys 155(1):96–127

Jacqmin D (2000) Contact-line dynamics of a diffuse fluid interface. J Fluid Mech 402:57–88

James AJ, Lowengrub J (2004) A surfactant-conserving volume-of-fluid method for interfacial flows with insoluble surfactant. J Comput Phys 201(2):685–722

Jamet D, Lebaigue O, Coutris N, Delhaye JM (2001) The second gradient method for the direct numerical simulation of liquid–vapor flows with phase change. J Comput Phys 169(2):624–651

Jamet D, Torres D, Brackbill JU (2002) On the theory and computation of surface tension: the elimination of parasitic currents through energy conservation in the second-gradient method. J Comput Phys 182(1):262–276

Jang W, Jilesen J, Lien FS, Ji H (2008) A study on the extension of a VOF/PLIC based method to a curvilinear co-ordinate system. Int J Comput Fluid Dyn 22(4):241–257

Jia XL, McLaughlin JB, Kontomaris K (2008) Lattice Boltzmann simulations of flows with fluid–fluid interfaces. Asia-Pac J Chem Eng 3(2):124–143

Johnson RA, Borhan A (2003) Pressure-driven motion of surfactant-laden drops through cylindrical capillaries: effect of surfactant solubility. J Colloid Interf Sci 261(2):529–541

Jousse F, Farr R, Link DR, Fuerstman MJ, Garstecki P (2006) Bifurcation of droplet flows within capillaries. Phys Rev E 74(3):036311

Junk M, Klar A, Luo L-S (2005) Asymptotic analysis of the lattice Boltzmann equation. J Comput Phys 210(2):676–704

Juric D, Tryggvason G (1998) Computations of boiling flows. Int J Multiph Flow 24(3):387–410

Kadau K, Barber JL, Germann TC, Holian BL, Alder BJ (2010) Atomistic methods in fluid simulation. Philos T R Soc A 368(1916):1547–1560

Kadioglu SY, Sussman M (2008) Adaptive solution techniques for simulating underwater explosions and implosions. J Comput Phys 227(3):2083–2104

Kandlikar SG (2008) Exploring roughness effect on laminar internal flow-are we ready for change? Nanosc Microsc Therm Eng 12(1):61–82

Kandlikar SG (2010) Scale effects on flow boiling heat transfer in microchannels: a fundamental perspective. Int J Therm Sci 49(7):1073–1085

Kang M, Fedkiw RP, Liu X-D (2000) A boundary condition capturing method for multiphase incompressible flow. J Sci Comput 15(3):323–360

Karniadakis G, Beskok A, Aluru NR (2005) Microflows and nanoflows: fundamentals and simulation. Springer, New York

Kashid MN, Kiwi-Minsker L (2009) Microstructured reactors for multiphase reactions: state of the art. Ind Eng Chem Res 48(14):6465–6485

Kececi S, Wörner M, Onea A, Soyhan HS (2009) Recirculation time and liquid slug mass transfer in co-current upward and downward Taylor flow. Catal Today 147(Supplement 1):S125–S131

Kenig EY, Ganguli AA, Atmakidis T, Chasanis P (2011) A novel method to capture mass transfer phenomena at free fluid–fluid interfaces. Chem Eng Process 50(1):68–76

Keskin O, Wörner M, Soyhan HS, Bauer T, Deutschmann O, Lange R (2010) Viscous co-current downward Taylor flow in a square mini-channel. AIChE J 56(7):1693–1702

Khenner M (2004) Computation of the material indicator function near the contact line (in Tryggvason's method). J Comput Phys 200(1):1–7

Kim J (2005) A continuous surface tension force formulation for diffuse-interface models. J Comput Phys 204(2):784–804

Kim J, Lowengrub J (2005) Phase field modeling and simulation of three-phase flows. Interface Free Bound 7(4):435–466

Kobayashi I, Mukataka S, Nakajima M (2004) CFD simulation and analysis of emulsion droplet formation from straight-through microchannels. Langmuir 20(22):9868–9877

Kockmann N (2008) Transport phenomena in micro process engineering. Springer, Berlin

Kreutzer MT, Bakker JJW, Kapteijn F, Moulijn JA, Verheijen PJT (2005a) Scaling-up multiphase monolith reactors: linking residence time distribution and feed maldistribution. Ind Eng Chem Res 44(14):4898–4913

Kreutzer MT, Kapteijn F, Moulijn JA, Heiszwolf JJ (2005b) Multiphase monolith reactors: chemical reaction engineering of segmented flow in microchannels. Chem Eng Sci 60(22):5895–5916

Kuksenok O, Jasnow D, Yeomans J, Balazs AC (2003) Periodic droplet formation in chemically patterned microchannels. Phys Rev Lett 91(10):108303

Kunkelmann C, Stephan P (2009) CFD simulation of boiling flows using the volume-of-fluid method within OpenFOAM. Numer Heat Tr A-Appl 56(8):631–646

Lafaurie B, Nardone C, Scardovelli R, Zaleski S, Zanetti G (1994) Modelling merging and fragmentation in multiphase flows with SURFER. J Comput Phys 113(1):134–147

Lai JM, Huang CY, Chen CH, Kung LL, Lin JD (2010) Influence of liquid hydrophobicity and nozzle passage curvature on microfluidic dynamics in a drop ejection process. J Micromech Microeng 20(1):015033

Lakehal D (2002) On the modelling of multiphase turbulent flows for environmental and hydrodynamic applications. Int J Multiphase Flow 28(5):823–863

Lakehal D, Labois M (2011) A new modelling strategy for phase-change heat transfer in turbulent interfacial two-phase flow. Int J Multiphase Flow 37(6):627–639

Lakehal D, Meier M, Fulgosi M (2002) Interface tracking towards the direct simulation of heat and mass transfer in multiphase flows. Int J Heat Fluid Flow 23(3):242–257

Lakehal D, Larrignon G, Narayanan C (2008) Computational heat transfer and two-phase flow topology in miniature tubes. Microfluid Nanofluid 4(4):261–271

Lakshmanan P, Ehrhard P (2010) Marangoni effects caused by contaminants adsorbed on bubble surfaces. J Fluid Mech 647:143–161

Lallemand P, Luo L-S, Peng Y (2007) A lattice Boltzmann front-tracking method for interface dynamics with surface tension in two dimensions. J Comput Phys 226(2):1367–1384

Lauga E, Brenner MP, Stone HA (2007) Microfluidics: the no-slip boundary condition. In: Tropea C, Yarin A, Foss JF (eds) Handbook of experimental fluid dynamics. Springer, New York, pp 1219–1240

Lee T (2009) Effects of incompressibility on the elimination of parasitic currents in the lattice Boltzmann equation method for binary fluids. Comput Math Appl 58(5):987–994

Lee T, Lin C-L (2005) A stable discretization of the lattice Boltzmann equation for simulation of incompressible two-phase flows at high density ratio. J Comput Phys 206(1):16–47

Lee J, Pozrikidis C (2006) Effect of surfactants on the deformation of drops and bubbles in Navier–Stokes flow. Comput Fluids 35(1):43–60

Lee W, Son G (2008) Bubble dynamics and heat transfer during nucleate boiling in a microchannel. Numer Heat Tr A-Appl 53(10):1074–1090

Lion N, Rossier JS, Girault HH (2006) Microfluidic applications in biology: from technologies to systems biology. Wiley, Weinheim

Liovic P, Lakehal D (2007) Multi-physics treatment in the vicinity of arbitrarily deformable gas–liquid interfaces. J Comput Phys 222(2):504–535

Liovic P, Rudman M, Liow JL, Lakehal D, Kothe D (2006) A 3D unsplit-advection volume tracking algorithm with planarity-preserving interface reconstruction. Comput Fluids 35(10):1011–1032

Lishchuk SV, Care CM, Halliday I (2003) Lattice Boltzmann algorithm for surface tension with greatly reduced microcurrents. Phys Rev E 67(3):036701

Liu DS, Wang SD (2008) Hydrodynamics of Taylor flow in noncircular capillaries. Chem Eng Process 47(12):2098–2106

Liu X-D, Fedkiw RP, Kang M (2000) A boundary condition capturing method for Poisson's equation on irregular domains. J Comput Phys 160(1):151–178

Liu H, Krishnan S, Marella S, Udaykumar HS (2005) Sharp interface Cartesian grid method II: a technique for simulating droplet interactions with surfaces of arbitrary shape. J Comput Phys 210(1):32–54

Liu J, Yap YF, Nguyen NT (2009a) Behavior of microdroplets in diffuser/nozzle structures. Microfluid Nanofluid 6(6):835–846

Liu J, Yap YF, Nguyen NT (2009b) Motion of a droplet through microfluidic ratchets. Phys Rev E 80(4):046319

Lopez J, Hernandez J (2010) On reducing interface curvature computation errors in the height function technique. J Comput Phys 229(13):4855–4868

López J, Hernández J, Gómez P, Faura F (2004) A volume of fluid method based on multidimensional advection and spline interface reconstruction. J Comput Phys 195(2):718–742

López J, Hernández J, Gómez P, Faura F (2005) An improved PLIC-VOF method for tracking thin fluid structures in incompressible two-phase flows. J Comput Phys 208(1):51–74

Losasso F, Fedkiw R, Osher S (2006) Spatially adaptive techniques for level set methods and incompressible flow. Comput Fluids 35(10):995–1010

Lowengrub J, Truskinovsky L (1998) Quasi-incompressible Cahn–Hilliard fluids and topological transitions. P R Soc Lond a Mat 454(1978):2617–2654

Luo LS, Girimaji SS (2003) Theory of the lattice Boltzmann method: two-fluid model for binary mixtures. Phys Rev E 67(3):036302

Lv X, Zou QP, Zhao Y, Reeve D (2010) A novel coupled level set and volume of fluid method for sharp interface capturing on 3D tetrahedral grids. J Comput Phys 229(7):2573–2604

Lyklema J (1991) Fundamentals of interface and colloid science, vol III: liquid–fluid interfaces. Academic Press, London

Ma C, Bothe D (2011) Direct numerical simulation of thermocapillary flow based on the volume of fluid method. Int J Multiphase Flow 37(9):1045–1058

Macklin P, Lowengrub J (2006) An improved geometry-aware curvature discretization for level set methods: application to tumor growth. J Comput Phys 215(2):392–401

Malik M, Fan ES-C, Bussmann M (2007) Adaptive VOF with curvature-based refinement. Int J Numer Methods Fluids 55(7):693–712

Marchandise E, Remacle J-F (2006) A stabilized finite element method using a discontinuous level set approach for solving two phase incompressible flows. J Comput Phys 219(2):780–800

Marchandise E, Remacle J-F, Chevaugeon N (2006) A quadrature-free discontinuous Galerkin method for the level set equation. J Comput Phys 212(1):338–357

Mary P, Studer V, Tabeling P (2008) Microfluidic droplet-based liquid–liquid extraction. Anal Chem 80(8):2680–2687

Mehravaran M, Hannani SK (2008) Simulation of incompressible two-phase flows with large density differences employing lattice Boltzmann and level set methods. Comput Method Appl M 198(2):223–233

Min C (2010) On reinitializing level set functions. J Comput Phys 229(8):2764–2772

Min C, Gibou F (2007) A second order accurate level set method on non-graded adaptive Cartesian grids. J Comput Phys 225(1):300–321

Mognetti BM, Yeomans JM (2009) Capillary filling in microchannels patterned by posts. Phys Rev E 80(5):056309

Mognetti BM, Yeomans JM (2010) Modeling receding contact lines on superhydrophobic surfaces. Langmuir 26(23):18162–18168

Mohammadi A, Floryan JM, Kaloni PN (2011) Spectrally accurate method for analysis of stationary flows of second-order fluids in rough micro-channels. Int J Numer Methods Fluids 66(4):509–536

Mukherjee A (2009) Contribution of thin-film evaporation during flow boiling inside microchannels. Int J Therm Sci 48(11): 2025–2035

Mukherjee A, Dhir VK (2004) Study of lateral merger of vapor bubbles during nucleate pool boiling. J Heat Transfer 126(6):1023–1039

Mukherjee A, Kandlikar SG (2005) Numerical simulation of growth of a vapor bubble during flow boiling of water in a microchannel. Microfluid Nanofluid 1(2):137–145

Mukherjee A, Kandlikar SG (2009) The effect of inlet constriction on bubble growth during flow boiling in microchannels. Int J Heat Mass Transf 52(21–22):5204–5212

Muradoglu M (2010) Axial dispersion in segmented gas–liquid flow: effects of alternating channel curvature. Phys Fluids 22(12):122106

Muradoglu M, Gokaltun S (2004) Implicit multigrid computations of buoyant drops through sinusoidal constrictions. J Appl Mech 71(6):857–865

Muradoglu M, Kayaalp AD (2006) An auxiliary grid method for computations of multiphase flows in complex geometries. J Comput Phys 214(2):858–877

Muradoglu M, Stone HA (2005) Mixing in a drop moving through a serpentine channel: a computational study. Phys Fluids 17(7):073305

Muradoglu M, Tasoglu S (2010) A front-tracking method for computational modeling of impact and spreading of viscous droplets on solid walls. Comput Fluids 39(4):615–625

Muradoglu M, Tryggvason G (2008) A front-tracking method for computation of interfacial flows with soluble surfactants. J Comput Phys 227(4):2238–2262

Muradoglu M, Günther A, Stone HA (2007) A computational study of axial dispersion in segmented gas–liquid flow. Phys Fluids 19(7):072109

Muzaferija S, Peric M (1999) Computation of flows using interface-tracking and interface-capturing methods. In: Mahrenholtz O, Markiewicz M (eds) Nonlinear water wave interaction. WIT Press, Southampton, pp 59–100

Narayanan C, Lakehal D (2008) Two-phase convective heat transfer in miniature pipes under normal and microgravity conditions. J Heat Transf 130(7):074502

Naraynan C, Lakehal D (2006) Simulation of filling of microfluidic devices using a coarse-grained continuum contact angle model. In: Paper presented at the NSTI Nanotechnology Conference and Trade Show, Boston, May 7–11

Nas S, Tryggvason G (2003) Thermocapillary interaction of two bubbles or drops. Int J Multiphase Flow 29(7):1117–1135

Ndinisa NV, Wiley DE, Fletcher DF (2005) Computational fluid dynamics simulations of Taylor bubbles in tubular membranes—model validation and application to laminar flow systems. Chem Eng Res Des 83 (A1):40–49

Nguyen N-T, Wereley ST (2006) Fundamentals and applications of microfluidics, 2nd edn. Artech House, Boston

Nie XB, Chen SY, Weinan E, Robbins MO (2004) A continuum and molecular dynamics hybrid method for micro- and nano-fluid flow. J Fluid Mech 500:55–64

Nikolopoulos N, Nikas KS, Bergeles G (2009) A numerical investigation of central binary collision of droplets. Comput Fluids 38(6):1191–1202

Nobari M, Tryggvason G (1996) Numerical simulations of three-dimensional drop collisions. AIAA J 34(4):750–755

Nobari MR, Jan Y-J, Tryggvason G (1996) Head-on collision of drops—a numerical investigation. Phys Fluids 8(1):29–42

Noh WF, Woodward P (1976) SLIC (simple line interface calculation). In: Lecture notes in physics, vol 59. Springer, New York, pp 330–340

Nourgaliev RR, Dinh TN, Theofanous TG, Joseph D (2003) The lattice Boltzmann equation method: theoretical interpretation, numerics and implications. Int J Multiphase Flow 29(1):117–169

Ohta M, Suzuki M (1996) Numerical analysis of mass transfer from a free motion drop in a solvent extraction process. Solvent Extr Res Dev 3:138–149

Olgac U, Kayaalp AD, Muradoglu M (2006) Buoyancy-driven motion and breakup of viscous drops in constricted capillaries. Int J Multiphase Flow 32(9):1055–1071

Olsson E, Kreiss G (2005) A conservative level set method for two phase flow. J Comput Phys 210(1):225–246

Olsson E, Kreiss G, Zahedi S (2007) A conservative level set method for two phase flow II. J Comput Phys 225(1):785–807

Onea A, Wörner M, Cacuci DG (2009) A qualitative computational study of mass transfer in upward bubble train flow through square and rectangular mini-channels. Chem Eng Sci 64(7):1416–1435

Osher S, Fedkiw RP (2003) Level set methods and dynamic implicit surfaces. Springer, Berlin

Osher S, Sethian JA (1988) Fronts propagating with curvature-dependent speed: algorithms based on Hamilton–Jacobi formulations. J Comput Phys 79(1):12–49

Özkan F, Wörner M, Wenka A, Soyhan HS (2007) Critical evaluation of CFD codes for interfacial simulation of bubble-train flow in a narrow channel. Int J Numer Methods Fluids 55(6):537–564

Öztaskin MC, Wörner M, Soyhan HS (2009) Numerical investigation of the stability of bubble train flow in a square minichannel. Phys Fluids 21(4):042108

Peskin CS (1977) Numerical analysis of blood flow in the heart. J Comput Phys 25(3):220–252

Peskin CS (2002) The immersed boundary method. Acta Numerica 11:479–517

Petera J, Weatherley LR (2001) Modelling of mass transfer from falling droplets. Chem Eng Sci 56(16):4929–4947

Pilliod JE, Puckett EG (2004) Second-order accurate volume-of-fluid algorithms for tracking material interfaces. J Comput Phys 199(2):465–502

Pooley CM, Furtado K (2008) Eliminating spurious velocities in the free-energy lattice Boltzmann method. Phys Rev E 77(4):046702

Pooley CM, Kusumaatmaja H, Yeomans JM (2008) Contact line dynamics in binary lattice Boltzmann simulations. Phys Rev E 78(5):056709

Popinet S (2009) An accurate adaptive solver for surface-tension-driven interfacial flows. J Comput Phys 228(16):5838–5866

Popinet S, Zaleski S (1999) A front-tracking algorithm for accurate representation of surface tension. Int J Numer Methods Fluids 30(6):775–793

Pozrikidis C (2001) Interfacial dynamics for stokes flow. J Comput Phys 169(2):250–301

Price G, Reader G, Rowe R, Bugg J (1998) A piecewise parabolic interface calculation for volume-tracking. In: Paper presented at the 6th Annual conference of the computational fluid dynamics society of Canada, Quebec, June 7–9 2001

Prosperetti A, Tryggvason G (2007) Computational methods for multiphase flow. Cambridge University Press, Cambridge

Qian DY, Lawal A (2006) Numerical study on gas and liquid slugs for Taylor flow in a T-junction microchannel. Chem Eng Sci 61(23):7609–7625

Qian TZ, Wang XP, Sheng P (2006) A variational approach to moving contact line hydrodynamics. J Fluid Mech 564:333–360

Quan S, Schmidt DP (2007) A moving mesh interface tracking method for 3D incompressible two-phase flows. J Comput Phys 221(2):761–780

Quan S, Lou J, Schmidt DP (2009) Modeling merging and breakup in the moving mesh interface tracking method for multiphase flow simulations. J Comput Phys 228(7):2660–2675

Raessi M, Mostaghimi J, Bussmann M (2007) Advecting normal vectors: a new method for calculating interface normals and curvatures when modeling two-phase flows. J Comput Phys 226(1):774–797

Raessi M, Bussmann M, Mostaghimi J (2009) A semi-implicit finite volume implementation of the CSF method for treating surface tension in interfacial flows. Int J Numer Methods Fluids 59(10):1093–1110

Raessi M, Mostaghimi J, Bussmann M (2010) A volume-of-fluid interfacial flow solver with advected normals. Comput Fluids 39(8):1401–1410

Raimondi ND, Prat L, Gourdon C, Cognet P (2008) Direct numerical simulations of mass transfer in square microchannels for liquid–liquid slug flow. Chem Eng Sci 63(22):5522–5530

Ralston J, Popescu M, Sedev R (2008) Dynamics of wetting from an experimental point of view. Annu Rev Mater Res 38:23–43

Rannou G (2008) Lattice-Boltzmann method and immiscible two-phase flow, Master Thesis. Georgia Institute of Technology, Atlanta

Renardy Y, Renardy M (2002) PROST: a parabolic reconstruction of surface tension for the volume-of-fluid method. J Comput Phys 183(2):400–421

Renardy M, Renardy Y, Li J (2001) Numerical simulation of moving contact line problems using a volume-of-fluid method. J Comput Phys 171(1):243–263

Renardy YY, Renardy M, Cristini V (2002) A new volume-of-fluid formulation for surfactants and simulations of drop deformation under shear at a low viscosity ratio. Eur J Mech B-Fluid 21(1):49–59

Rider WJ, Kothe DB (1998) Reconstructing volume tracking. J Comput Phys 141(2):112–152

Rohde M, Kandhai D, Derksen JJ, van den Akker HEA (2006) A generic, mass conservative local grid refinement technique for lattice-Boltzmann schemes. Int J Numer Methods Fluids 51(4):439–468

Rosengarten G, Harvie DJE, Cooper-White J (2006) Contact angle effects on microdroplet deformation using CFD. Appl Math Model 30(10):1033–1042

Rudman M (1997) Volume-tracking methods for interfacial flow calculations. Int J Numer Methods Fluids 24(7):671–691

Rudman M (1998) A volume-tracking method for incompressible multifluid flows with large density variations. Int J Numer Methods Fluids 28(2):357–378

Russo G, Smereka P (2000) A remark on computing distance functions. J Comput Phys 163(1):51–67

Sabisch W (2000) Dreidimensionale numerische Simulation der Dynamik von aufsteigenden Einzelblasen und Blasenschwärmen mit einer Volume-of-Fluid-Methode. Forschungszentrum Karlsruhe Wissenschaftliche Berichte, FZKA 6478

Sabisch W, Wörner M, Grötzbach G, Cacuci DG (2001) Dreidimensionale numerische Simulation von aufsteigenden Einzelblasen und Blasenschwärmen mit einer Volume-of-Fluid Methode. Chem-Ing-Tech 73(4):368–373

Saha AA, Mitra SK (2009a) Effect of dynamic contact angle in a volume of fluid (VOF) model for a microfluidic capillary flow. J Colloid Interf Sci 339(2):461–480

Saha AA, Mitra SK (2009b) Numerical study of capillary flow in microchannels with alternate hydrophilic–hydrophobic bottom wall. J Fluids Eng 131(6):061202

Saliterman S (2006) Fundamentals of bioMEMS and medical microdevices. SPIE, Bellingham

Santos RM, Kawaji M (2010) Numerical modeling and experimental investigation of gas–liquid slug formation in a microchannel T-junction. Int J Multiphase Flow 36(4):314–323

Sarrazin F, Loubiere K, Prat L, Gourdon C, Bonometti T, Magnaudet J (2006) Experimental and numerical study of droplets hydrodynamics in microchannels. AIChE J 52(12):4061–4070

Sarrazin F, Bonometti T, Prat L, Gourdon C, Magnaudet J (2008) Hydrodynamic structures of droplets engineered in rectangular micro-channels. Microfluid Nanofluid 5(1):131–137

Sbragaglia M, Benzi R, Biferale L, Succi S, Toschi F (2006) Surface roughness-hydrophobicity coupling in microchannel and nanochannel flows. Phys Rev Lett 97(20):204503

Scardovelli R, Zaleski S (1999) Direct numerical simulation of free-surface and interfacial flow. Annu Rev Fluid Mech 31:567–603

Scardovelli R, Zaleski S (2000) Analytical relations connecting linear interfaces and volume fractions in rectangular grids. J Comput Phys 164(1):228–237

Schlottke J, Weigand B (2008) Direct numerical simulation of evaporating droplets. J Comput Phys 227(10):5215–5237

Schönfeld F, Hardt S (2009) Dynamic contact angles in CFD simulations. Comput Fluids 38(4):757–764

Schönfeld F, Rensink D (2003) Simulation of droplet generation by mixing nozzles. Chem Eng Technol 26(5):585–591

Schubert K, Brandner J, Fichtner M, Linder G, Schygulla U, Wenka A (2001) Microstructure devices for applications in thermal and chemical process engineering. Microscale Therm Eng 5(1):17–39

Schuster A, Lakshmanan R, Ponton J, Sefiane K (2003) Simulation and design of a non-adiabatic multiphase microreactor. Int J Chem React Eng 1:A45

Seppecher P (1996) Moving contact lines in the Cahn–Hilliard theory. Int J Eng Sci 34(9):977–992

Sessoms DA, Belloul M, Engl W, Roche M, Courbin L, Panizza P (2009) Droplet motion in microfluidic networks: Hydrodynamic interactions and pressure-drop measurements. Phys Rev E 80(1):016317

Sethian JA (1996) A fast marching level set method for monotonically advancing fronts. P Natl Acad Sci USA 93(4):1591–1595

Sethian JA (1999a) Fast marching methods. Siam Rev 41(2):199–235

Sethian JA (1999b) Level set methods and fast marching methods: evolving interfaces in computational geometry, fluid mechanics, computer vision, and materials science, 2nd edn. Cambridge University Press, New York

Sethian JA, Smereka P (2003) Level set methods for fluid interfaces. Annu Rev Fluid Mech 35:341–372

Shan XW, Chen HD (1993) Lattice Boltzmann model for simulating flows with multiple phases and components. Phys Rev E 47(3):1815–1819

Shao N, Salman W, Gavriilidis A, Angeli P (2008) CFD simulations of the effect of inlet conditions on Taylor flow formation. Int J Heat Fluid Flow 29(6):1603–1611

Shen J, Yang X (2009) An efficient moving mesh spectral method for the phase-field model of two-phase flows. J Comput Phys 228(8):2978–2992

Shepel SV, Smith BL (2009) On surface tension modelling using the level set method. Int J Numer Methods Fluids 59(2):147–171

Shin S, Juric D (2002) Modeling three-dimensional multiphase flow using a level contour reconstruction method for front tracking without connectivity. J Comput Phys 180(2):427–470

Shin S, Juric D (2009) A hybrid interface method for three-dimensional multiphase flows based on front tracking and level set techniques. Int J Numer Methods Fluids 60(7):753–778

Shirani E, Ashgriz N, Mostaghimi J (2005) Interface pressure calculation based on conservation of momentum for front capturing methods. J Comput Phys 203(1):154–175

Shui LL, Eijkel JCT, van den Berg A (2007) Multiphase flow in micro- and nanochannels. Sensor Actuat B Chem 121(1):263–276

Sikalo S, Wilhelm HD, Roisman IV, Jakirlic S, Tropea C (2005) Dynamic contact angle of spreading droplets: experiments and simulations. Phys Fluids 17(6):062103

Silva G, Leal N, Semiao V (2008) Micro-PIV and CFD characterization of flows in a microchannel: velocity profiles, surface roughness and Poiseuille numbers. Int J Heat Fluid Flow 29(4):1211–1220

Smith KA, Ottino JM, Warren PB (2005) Simple representation of contact-line dynamics in a level-set model of an immiscible fluid interface. Ind Eng Chem Res 44(5):1194–1198

Smolianski A (2005) Finite-element/level-set/operator-splitting (FELSOS) approach for computing two-fluid unsteady flows with free moving interfaces. Int J Numer Methods Fluids 48(3):231–269

Sommerfeld M, van Wachem B, Oliemans R (2008) Best practice guidelines for computational fluid dynamics of dispersed multiphase flows. ERCOFTAC, SIAMUF Swedish Industrial Association for Multiphase Flows

Son G, Dhir VK (1998) Numerical simulation of film boiling near critical pressures with a level set method. J Heat Transf 120(1):183–192

Son G, Dhir VK (2007) A level set method for analysis of film boiling on an immersed solid surface. Numer Heat Tr B-Fund 52(2):153–177

Son G, Hur N (2002) A coupled level set and volume-of-fluid method for the buoyancy-driven motion of fluid particles. Numer Heat Tr B-Fund 42(6):523–542

Son G, Dhir VK, Ramanujapu N (1999) Dynamics and heat transfer associated with a single bubble during nucleate boiling on a horizontal surface. J Heat Transfer 121(3):623–631

Spelt PDM (2005) A level-set approach for simulations of flows with multiple moving contact lines with hysteresis. J Comput Phys 207(2):389–404

Squires TM, Quake SR (2005) Microfluidics: fluid physics at the nanoliter scale. Rev Mod Phys 77(3):977–1026

Stone HA (1990) A simple derivation of the time-dependent convective-diffusion equation for surfactant transport along a deforming interface. Phys Fluids A 2(1):111–112

Stone HA, Kim S (2001) Microfluidics: basic issues, applications, and challenges. AIChE J 47(6):1250–1254

Stone HA, Stroock AD, Ajdari A (2004) Engineering flows in small devices. Annu Rev Fluid Mech 36(1):381–411

Strain J (1999) Tree methods for moving interfaces. J Comput Phys 151(2):616–648

Strubelj L, Tiselj I, Mavko B (2009) Simulations of free surface flows with implementation of surface tension and interface sharpening in the two-fluid model. Int J Heat Fluid Flow 30(4):741–750

Succi S (2001) The Lattice Boltzmann equation for fluid dynamics and beyond. Clarendon, Oxford

Sun Y, Beckermann C (2007) Sharp interface tracking using the phase-field equation. J Comput Phys 220(2):626–653

Sun DL, Tao WQ (2010) A coupled volume-of-fluid and level set (VOSET) method for computing incompressible two-phase flows. Int J Heat Mass Transf 53(4):645–655

Sussman M (2003) A second order coupled level set and volume-of-fluid method for computing growth and collapse of vapor bubbles. J Comput Phys 187(1):110–136

Sussman M, Fatemi E (1999) An efficient, interface-preserving level set redistancing algorithm and its application to interfacial incompressible fluid flow. Siam J Sci Comput 20(4):1165–1191

Sussman M, Puckett EG (2000) A coupled level set and volume-of-fluid method for computing 3D and axisymmetric incompressible two-phase flows. J Comput Phys 162(2):301–337

Sussman M, Smereka P, Osher S (1994) A level set approach for computing solutions to incompressible two-phase flow. J Comput Phys 114(1):146–159

Sussman M, Almgren AS, Bell JB, Colella P, Howell LH, Welcome ML (1999) An adaptive level set approach for incompressible two-phase flows. J Comput Phys 148(1):81–124

Sussman M, Smith KM, Hussaini MY, Ohta M, Zhi-Wei R (2007) A sharp interface method for incompressible two-phase flows. J Comput Phys 221(2):469–505

Swift MR, Orlandini E, Osborn WR, Yeomans JM (1996) Lattice Boltzmann simulations of liquid–gas and binary fluid systems. Phys Rev E 54(5):5041–5052

Tabeling P (2005) Introduction to microfluidics. Oxford University Press, New York

Tabeling P (2009) A brief introduction to slippage, droplets and mixing in microfluidic systems. Lab Chip 9(17):2428–2436

Tabeling P (2010) Investigating slippage, droplet breakup, and synthesizing microcapsules in microfluidic systems. Phys Fluids 22(2):021302

Taha T, Cui ZF (2006a) CFD modelling of slug flow in vertical tubes. Chem Eng Sci 61(2):676–687

Taha T, Cui ZF (2006b) CFD modelling of slug flow inside square capillaries. Chem Eng Sci 61(2):665–675

Takada N, Misawa M, Tomiyama A (2006) A phase-field method for interface-tracking simulation of two-phase flows. Math Comput Simulat 72(2–6):220–226

Tanguy S, Ménard T, Berlemont A (2007) A level set method for vaporizing two-phase flows. J Comput Phys 221(2):837–853

Tanthapanichakoon W, Aoki N, Matsuyama K, Mae K (2006) Design of mixing in microfluidic liquid slugs based on a new dimensionless number for precise reaction and mixing operations. Chem Eng Sci 61(13):4220–4232

Taylor GI (1961) Deposition of a viscous fluid on the wall of a tube. J Fluid Mech 10(2):161–165

Terashima H, Tryggvason G (2009) A front-tracking/ghost-fluid method for fluid interfaces in compressible flows. J Comput Phys 228(11):4012–4037

Theberge AB, Courtois F, Schaerli Y, Fischlechner M, Abell C, Hollfelder F, Huck WTS (2010) Microdroplets in microfluidics: an evolving platform for discoveries in chemistry and biology. Angew Chem Int Edit 49(34):5846–5868

Theodorakakos A, Bergeles G (2004) Simulation of sharp gas–liquid interface using VOF method and adaptive grid local refinement around the interface. Int J Numer Methods Fluids 45(4):421–439

Thomas S, Esmaeeli A, Tryggvason G (2010) Multiscale computations of thin films in multiphase flows. Int J Multiph Flow 36(1):71–77

Thome JR (2004) Boiling in microchannels: a review of experiment and theory. Int J Heat Fluid Flow 25(2):128–139

Thömmes G, Becker J, Junk M, Vaikuntam AK, Kehrwald D, Klar A, Steiner K, Wiegmann A (2009) A lattice Boltzmann method for immiscible multiphase flow simulations using the level set method. J Comput Phys 228(4):1139–1156

Thulasidas TC, Abraham MA, Cerro RL (1997) Flow patterns in liquid slugs during bubble-train flow inside capillaries. Chem Eng Sci 52(17):2947–2962

Tomar G, Biswas G, Sharma A, Agrawal A (2005) Numerical simulation of bubble growth in film boiling using a coupled level-set and volume-of-fluid method. Phys Fluids 17(11):112103

Tomar G, Fuster D, Zaleski S, Popinet S (2010) Multiscale simulations of primary atomization. Comput Fluids 39(10):1864–1874

Tong AY, Wang Z (2007) A numerical method for capillarity-dominant free surface flows. J Comput Phys 221(2):506–523

Tornberg A-K, Engquist B (2000) A finite element based level-set method for multiphase flow applications. Comput Visual Sci 3(1):93–101

Torres DJ, Brackbill JU (2000) The point-set method: front-tracking without connectivity. J Comput Phys 165(2):620–644

Tryggvason G, Bunner B, Esmaeeli A, Juric D, Al-Rawahi N, Tauber W, Han J, Nas S, Jan YJ (2001) A front-tracking method for the computations of multiphase flow. J Comput Phys 169(2):708–759

Tryggvason G, Thomas S, Lu J, Aboulhasanzadeh B (2010) Multiscale issues in DNS of multiphase flows. Acta Math Sci 30(2):551–562

Tryggvason G, Scardovelli R, Zaleski S (2011) Direct numerical simulations of gas–liquid multiphase flows. Cambridge University Press, Cambridge

Ubbink O, Issa RI (1999) A method for capturing sharp fluid interfaces on arbitrary meshes. J Comput Phys 153(1):26–50

Udaykumar HS, Krishnan S, Marella S (2009) Adaptively refined, parallelised sharp interface Cartesian grid method for three-dimensional moving boundary problems. Int J Comput Fluid Dyn 23(1):1–24

Unverdi SO, Tryggvason G (1992) A front-tracking method for viscous, incompressible, multi-fluid flows. J Comput Phys 100(1):25–37

Urbant P, Leshansky A, Halupovich Y (2008) On the forced convective heat transport in a droplet-laden flow in microchannels. Microfluid Nanofluid 4(6):533–542

van der Graaf S, Nisisako T, Schroen CGPH, van der Sman RGM, Boom RM (2006) Lattice Boltzmann simulations of droplet formation in a T-shaped microchannel. Langmuir 22(9):4144–4152

van der Pijl SP, Segal A, Vuik C, Wesseling P (2005) A mass-conserving level-set method for modelling of multi-phase flows. Int J Numer Methods Fluids 47(4):339–361

van der Sman R, van der Graaf S (2006) Diffuse interface model of surfactant adsorption onto flat and droplet interfaces. Rheol Acta 46(1):3–11

van Steijn V, Kreutzer MT, Kleijn CR (2007) μ-PIV study of the formation of segmented flow in microfluidic T-junctions. Chem Eng Sci 62(24):7505–7514

van Steijn V, Kleijn CR, Kreutzer MT (2009) Flows around confined bubbles and their importance in triggering pinch-off. Phys Rev Lett 103(21):214501

Verhaeghe F, Luo L-S, Blanpain B (2009) Lattice Boltzmann modeling of microchannel flow in slip flow regime. J Comput Phys 228(1):147–157

Villanueva W, Amberg G (2006) Some generic capillary-driven flows. Int J Multiphase Flow 32(9):1072–1086

Wang ZY, Tong AY (2010) A sharp surface tension modeling method for two-phase incompressible interfacial flows. Int J Numer Methods Fluids 64(7):709–732

Wang Z, Yang J, Koo B, Stern F (2009a) A coupled level set and volume-of-fluid method for sharp interface simulation of plunging breaking waves. Int J Multiphase Flow 35(3):227–246

Wang Z, Yang J, Stern F (2009b) An improved particle correction procedure for the particle level set method. J Comput Phys 228(16):5819–5837

Wang CW, Oskooei A, Sinton D, Moffitt MG (2010) Controlled self-assembly of quantum dot-block copolymer colloids in multiphase microfluidic reactors. Langmuir 26(2):716–723

Wegener M, Eppinger T, Bäumler K, Kraume M, Paschedag AR, Bänsch E (2009) Transient rise velocity and mass transfer of a single drop with interfacial instabilities—Numerical investigations. Chem Eng Sci 64(23):4835–4845

Welch SWJ (1995) Local simulation of two-phase flows including interface tracking with mass transfer. J Comput Phys 121(1):142–154

Welch SWJ, Wilson J (2000) A volume of fluid based method for fluid flows with phase change. J Comput Phys 160(2):662–682

Weller HG (2006) A new approach to VOF-based interface capturing methods for incompressible and compressible flow. Tech. Rep. TR/HGW/07, OpenCFD Ltd.

Werder T, Walther JH, Koumoutsakos P (2005) Hybrid atomistic–continuum method for the simulation of dense fluid flows. J Comput Phys 205(1):373–390

Weymouth GD, Yue DKP (2010) Conservative volume-of-fluid method for free-surface simulations on Cartesian-grids. J Comput Phys 229(8):2853–2865

Whitesides GM (2006) The origins and the future of microfluidics. Nature 442(7101):368–373

Wolf FG, dos Santos LOE, Philippi PC (2010) Capillary rise between parallel plates under dynamic conditions. J Colloid Interf Sci 344(1):171–179

Wörner M, Sabisch W, Grötzbach G, Cacuci DG (2001) Volume-averaged conservation equations for volume-of-fluid interface tracking. In: Proceedings of the 4th International Conference on Multiphase Flow, New Orleans, Louisiana, USA, May 27–June 1 2001

Wörner M, Ghidersa BE, Ilic M, Cacuci DG (2005) Volume-of-fluid method based numerical simulations of gas–liquid two-phase flow in confined geometries. Houille Blanche 6:91–104

Wörner M, Ghidersa B, Onea A (2007) A model for the residence time distribution of bubble-train flow in a square mini-channel based on direct numerical simulation results. Int J Heat Fluid Flow 28(1):83–94

Wu L, Tsutahara M, Kim L, Ha M (2008a) Numerical simulations of droplet formation in a cross-junction microchannel by the lattice Boltzmann method. Int J Numer Methods Fluids 57(6):793–810

Wu L, Tsutahara M, Kim LS, Ha M (2008b) Three-dimensional lattice Boltzmann simulations of droplet formation in a cross-junction microchannel. Int J Multiphase Flow 34(9):852–864

Xiao F, Honma Y, Kono T (2005) A simple algebraic interface capturing scheme using hyperbolic tangent function. Int J Numer Methods Fluids 48(9):1023–1040

Xiong RQ, Chung JN (2010) A new model for three-dimensional random roughness effect on friction factor and heat transfer in microtubes. Int J Heat Mass Transfer 53(15–16):3284–3291

Xu J-J, Li Z, Lowengrub J, Zhao H (2006) A level-set method for interfacial flows with surfactant. J Comput Phys 212(2):590–616

Yabe T, Xiao F, Utsumi T (2001) The constrained interpolation profile method for multiphase analysis. J Comput Phys 169(2):556–593

Yan YY, Zu YQ (2007) A lattice Boltzmann method for incompressible two-phase flows on partial wetting surface with large density ratio. J Comput Phys 227(1):763–775

Yang C, Li DQ (1996) A method of determining the thickness of liquid–liquid interfaces. Colloid Surf A 113(1–2):51–59

Yang C, Mao Z-S (2005) Numerical simulation of interphase mass transfer with the level set approach. Chem Eng Sci 60(10):2643–2660

Yang X, James AJ, Lowengrub J, Zheng X, Cristini V (2006) An adaptive coupled level-set/volume-of-fluid interface capturing method for unstructured triangular grids. J Comput Phys 217(2):364–394

Yap YF, Chai JC, Wong TN, Toh KC, Zhang HY (2006) A global mass correction scheme for the level-set method. Numer Heat Tr B-Fund 50(5):455–472

Yap YF, Tan SH, Nguyen NT, Murshed SMS, Wong TN, Yobas L (2009) Thermally mediated control of liquid microdroplets at a bifurcation. J Phys D Appl Phys 42(6):065503

Yen BKH, Günther A, Schmidt MA, Jensen KF, Bawendi MG (2005) A microfabricated gas–liquid segmented flow reactor for high-temperature synthesis: the case of CdSe quantum dots. Angew Chem Int Edit 44(34):5447–5451

Yokoi K (2007) Efficient implementation of THINC scheme: a simple and practical smoothed VOF algorithm. J Comput Phys 226(2):1985–2002

Youngs DL (1982) Time-dependent multi-material flow with large fluid distortion. In: Morton KW, Baines MJ (eds) Numerical methods for fluid dynamics, vol 24. Academic Press, New York, pp 273–285

Yu Z, Fan L-S (2009) An interaction potential based lattice Boltzmann method with adaptive mesh refinement (AMR) for two-phase flow simulation. J Comput Phys 228(17):6456–6478

Yu Z, Hemminger O, Fan L-S (2007) Experiment and lattice Boltzmann simulation of two-phase gas–liquid flows in microchannels. Chem Eng Sci 62(24):7172–7183

Yue PT, Feng JJ, Liu C, Shen J (2004) A diffuse-interface method for simulating two-phase flows of complex fluids. J Fluid Mech 515:293–317

Yue P, Zhou C, Feng JJ, Ollivier-Gooch CF, Hu HH (2006) Phase-field simulations of interfacial dynamics in viscoelastic fluids using finite elements with adaptive meshing. J Comput Phys 219(1):47–67

Yue P, Zhou C, Feng JJ (2007) Spontaneous shrinkage of drops and mass conservation in phase-field simulations. J Comput Phys 223(1):1–9

Zacharioudaki M, Kouris C, Dimakopoulos Y, Tsamopoulos J (2007) A direct comparison between volume and surface tracking methods with a boundary-fitted coordinate transformation and third-order upwinding. J Comput Phys 227(2):1428–1469

Zagnoni M, Anderson J, Cooper JM (2010) Hysteresis in multiphase microfluidics at a T-Junction. Langmuir 26(12):9416–9422

Zahedi S, Gustavsson K, Kreiss G (2009) A conservative level set method for contact line dynamics. J Comput Phys 228(17):6361–6375

Zalesak ST (1979) Fully multidimensional flux-corrected transport algorithms for fluids. J Comput Phys 31(3):335–362

Zhang J, Eckmann DM, Ayyaswamy PS (2006) A front tracking method for a deformable intravascular bubble in a tube with soluble surfactant transport. J Comput Phys 214(1):366–396

Zhang YL, Zou QP, Greaves D (2010) Numerical simulation of free-surface flow using the level-set method with global mass correction. Int J Numer Methods Fluids 63(6):651–680

Zhao CX, Middelberg APJ (2011) Two-phase microfluidic flows. Chem Eng Sci 66(7):1394–1411

Zhao B, Moore JS, Beebe DJ (2001) Surface-directed liquid flow inside microchannels. Science 291(5506):1023–1026

Zhao J-F, Li Z-D, Li H-X, Li J (2010) Thermocapillary migration of deformable bubbles at moderate to large Marangoni number in microgravity. Microgravity Sci Tec 22(3):295–303

Zheng HW, Shu C, Chew YT (2005) Lattice Boltzmann interface capturing method for incompressible flows. Phys Rev E 72(5):056705

Zheng HW, Shu C, Chew YT (2006) A lattice Boltzmann model for multiphase flows with large density ratio. J Comput Phys 218(1):353–371

Zheng Y, Fujioka H, Grotberg JB (2007) Effects of gravity, inertia, and surfactant on steady plug propagation in a two-dimensional channel. Phys Fluids 19(8):082107

Zheng HW, Shu C, Chew YT, Sun JH (2008) Three-dimensional lattice Boltzmann interface capturing method for incompressible flows. Int J Numer Methods Fluids 56(9):1653–1671

Zhou CF, Yue PT, Feng JJ (2006) Formation of simple and compound drops in microfluidic devices. Phys Fluids 18(9):092105

Zhou C, Yue P, Feng JJ, Ollivier-Gooch CF, Hu HH (2010) 3D phase-field simulations of interfacial dynamics in Newtonian and viscoelastic fluids. J Comput Phys 229(2):498–511

Zhu X, Sui PC, Djilali N (2008) Numerical simulation of emergence of a water droplet from a pore into a microchannel gas stream. Microfluid Nanofluid 4(6):543–555